EVALUATION OF REUTILIZING SINGLE-USE SURGICAL FACE MASK IN CONCRETE

JULIUS MALOBA WATAKO

MASTER OF SCIENCE

(Construction Engineering and Management)

JOMO KENYATTA UNIVERSITY

OF

AGRICULTURE AND TECHNOLOGY

2023

Evaluation of Reutilizing Single-Use Surgical Face Mask in Concrete

Julius Maloba Watako

A Thesis Submitted in Partial Fulfillment of the Requirements for the Degree of Master of Science in Construction Engineering and Management of the Jomo Kenyatta University of Agriculture and Technology

2023

DECLARATION

This thesis is my original work and has not been presented for a degree in any other University.

Signature: …………………………………… Date: …………………………

Julius Maloba Watako

This thesis has been submitted for examination with our approval as University Supervisors.

Signature: …………………………………… Date: …………………………

Dr. Eng. James Maina Kiambigi, PhD

JKUAT, Kenya.

Signature: …………………………………… Date: …………………………

Dr. Eng. Charles Karimi Kabubo, PhD

JKUAT, Kenya.

DEDICATION

This work is dedicated to my dear family, friends, professional, and academic colleagues.

ACKNOWLEDGEMENT

I wish to thank God for the gift of life and health while undertaking my studies. Secondly, I wish to thank and appreciate my able supervisors, Dr. (Eng) James Kiambigi and Dr. (Eng) Charles Kabubo, all of JKUAT, for being kind to me and for their valuable suggestions and guidance throughout this research study. I would also like to thank and appreciate the staff in the Ministry of Transport and Infrastructure, Materials Research and Testing Division, the Department of Science and Technology at Kibabii University, and the Department of Civil Engineering at the Jomo Kenyatta University of Agriculture and Technology for their great assistance. Finally, I wish to thank my dear wife and children for their support and prayers.

TABLE OF CONTENTS

LIST OF TABLES

LIST OF FIGURES

LIST OF PLATES

LIST OF APPENDICES

ABBREVIATIONS AND ACRONYMS

BS-	British Standards
CM-	Cubic Metre
COVID-19-	Coronavirus Diseases 2019
JKUAT-	Jomo Kenyatta University of Agriculture and Technology
KG-	Kilograms
MM-	Millimeters
NEMA-	National Environmental Management Authority
PET-	Polyethylene Terephthalate
PP-	Polypropylene
PPE-	Personal Protective Equipment
RA-	Recycled Aggregates
RCA-	Recycled Concrete Aggregate
SSD-	Saturated Surface Dry
SUSFM-	Single-Use Surgical Face Masks
UPV-	Ultrasonic Pulse Velocity
UTM-	Universal Testing Machine

ABSTRACT

The outbreak of coronavirus disease (COVID-19) caused a sharp increase in the utilization of Single Use Surgical Face Masks (SUSFM) around the world as personal protective equipment. These eventually ended up in waste disposal facilities, causing environmental pollution. Incineration of the SUSFM produces greenhouse gases that eventually contribute to global warming. Those that ended up in the water bodies fragments into microplastics that affect marine life and find their way into the human food chain. SUSFM materials are made from polypropylene, a thermoplastic polymer material that takes a long time to degrade. It was therefore, important to develop low carbon mitigation measures to remove these wastes from the environment. Concrete, as construction material, is strong in compression but brittle and weak in tensile strength. Hence need for reinforcement to improve on its qualities. Therefore, the main aim of the study was to evaluate the feasibility of re-utilizing single-use surgical face masks in concrete. In the study, SUSFM were shredded into 5 mm widths and 20 mm, 30 mm, and 40 mm lengths. The SUSFM were blended with C30 grade concrete in various percentages by mass of cement content, ranging from 0% (control mix) with incremental of 0.5% to 3.0%. The effect on workability, water absorption, and density were tested to BS standards for concrete blend with 20 mm long SUSFM material. Compressive strength, ultrasonic pulse velocity, and splitting tensile strength were tested to BS standards on varied contents and lengths of SUSFM in concrete. Acid attack and abrasion resistance were tested for durability of blend concrete. The addition of SUSFM material to concrete reduced its density by between 1.5% and 7.7% while water absorption increased from 16.9% to 70.8%. The addition of SUSFM materials decreased the workability of fresh concrete. Compressive strength decreased with minimum loss registered at 0.5% dosage of 30 mm length of SUSFM material. Splitting tensile strength improved to an optimum of 15.2% at 0.5% dosage of 30 mm SUSFM material. Further, the overall concrete quality remained at more than 4000 m/s UPV values. There was a notable decrease in acid attack resistance when exposed to hydrochloric acid conditions, but the abrasion resistance of concrete improved up to optimum dosage of 1.5% SUSFM fiber material, beyond which it decreased. The results underscored the crack bridging effect of SUSFM material in concrete. The composite concrete with 0.5% of 30 mm SUSFM fiber material can be used by design engineers to design structures that require improved tensile strength and abrasion resistance as compared to plain concrete. This is a low-carbon strategy for improvement of concrete strength at the same time safely disposing the SUSFM material to reduce the environmental pollution and global warming. Further studies are recommended on the effect of SUSFM materials at smaller widths and lengths on concrete

CHAPTER ONE

INTRODUCTION

1.1 Background of Study

Concrete is a versatile material strong in compression but brittle with low tensile strength (Pakravan & Ozbakkaloglu, 2019). To avoid concrete brittle failure, dispersed reinforcement in form of fibers are added to concrete (Blazy & Blazy, (2021). Cracks in concrete reduces serviceability and durability, hence need to reinforcement. Addition of fibers in concrete makes it isotropic and therefore transforming it to quasi-ductile material (Meddah & Bencheikh, 2009). Salunke (2017) deduced that adding uniformly dispersed, small, and closely spaced dispersed fibers to concrete would not only control plastic and dry shrinkage cracking but also enhance the tensile strength, fatigue resistance, and ductility of the concrete. Therefore, addition of short fibers to concrete limit initiation and propagation of cracks. Steel fibers are mostly used but increases concrete weight and therefore costs. Polypropylene fibers are adopted as they reduce weight of concrete and at the same time increase its strength (Madhavi et al., 2014). Reduction in dead weight of concrete reduces structural seismic risk because earthquake forces are directly proportional to dead weight (Yasar et al., 2003). Manufacture of virgin polypropylene fibers involves chain flow polymerization of propylene under high temperatures and pressure. This processes are high energy consumption and carbon emission. Therefore, there was need to adopt sustainable low carbon materials, preferably recycled, to improve concrete ductility at the same time removing waste materials from environment.

On the other hand, the outbreak of coronavirus disease (COVID-19) sharply increased the use of Single Use Surgical Face Masks (SUSFM) in the world (Prata et al., 2020). In June 2020, it was estimated that 129 billion SUSFM were discharged into the environment each month (Prata et al., 2020). Nzediegwu and Chang (2020) developed a model to predict SUSFM usage as a function of population, percentage urban population, percentage facemask acceptance rate, and average daily facemasks per capita. According to the model, 6.9 billion pieces, or the equivalent of 0.2 million tons of SUSFM, are generated globally per day, while Africa uses 700 million pieces.

The Government of Kenya made it mandatory to wear face masks as personal protective equipment in public spaces. As a result, there has been widespread use of surgical face masks, resulting in massive waste generation, which has raised concern from environmentalists. Despite the government putting in place systems, especially in health facilities, to ensure the safe disposal of hand gloves, surgical gowns, SUSFM, and other personal protective equipment, (NEMA, 2020), some are finding themselves in our environment. At the household level, there is haphazard disposal of surgical face masks among other household disposables, which end up in landfills. Also, they are flushed through toilets into the sewer system, which ends up blocking the sewer systems and causing overflows from manholes, thereby polluting the environment. In addition, these SUSFM are often dumped directly into open fields, roadsides, and or walkways, which eventually are washed away into our water bodies. The SUSFMs are mainly made from polypropylene, a thermoplastic polymer that remains in the environment for over 25 years, (Prata et al., 2020). Those that end up in our water bodies fragment into microplastics that are consumed, causing problems for our wildlife, marine life, and other animals, (Abbasi et al., 2020; Prata et al., 2020). This may probably end up in our food sources as humans consume some of these marine animals.

Despite COVID-19 reducing its severity, Ali et al., (2017) stated that in developing countries, 0.2 kg of medical waste per hospital bed per day is generated compared to 0.5 kg for developed countries. Kilmartin-Lynch et al., (2021) deduced that the effects of this environmental pollution will continue to impact human life even after the COVID-19 pandemic has ended. Currently in Kenya, incineration is the most commonly used method of disposal of SUSFM, which uses high temperatures to destroy the virus. However, this method generates greenhouse gases that harm the environment and also contribute to global warming.

It is for this reason that a more sustainable and low-carbon strategy to safely dispose of this medical waste by incorporating them in concrete instead of the virgin PP materials, may go a long way of improving the concrete quality and at the same time reduce on environmental pollution.

Several studies are being undertaken to re-utilize waste materials in concrete and related materials in the construction of infrastructure. This goes a long way to not only reduce pollution effects from these wastes but also offer a greener solution for sustainable development (Bheel et al., 2020). The commonly used SUSFM has polypropylene material enclosed in between non-woven materials (Sebarian et al., 2021). Because of these properties of SUSFM, several studies are being conducted to evaluate the feasibility of incorporating them into construction materials as a way of removing them from the landfill cycle in a more sustainable way.

Saberian et al., (2021) have shown that used single-use face masks can be added to reused concrete aggregate to produce a blended material that can be used as a base or subbase road construction material. Through his experiments, he concluded that recycled concrete aggregate mixed with shredded SUSFM material satisfied the requirements of road pavement base or sub-base blend material in terms of strength and stiffness. The greatest unconfined compressive strength and resilient modulus were achieved when 1% of SUSFM fiber material was combined with recycled concrete aggregate, while content levels above 2% decreased strength and stiffness. According to Zhu et al., (2022), the addition of 1.5% shredded COVID-19 nitrile gloves improves the unconfined compressive strength of expansive clay soil for use as a road pavement subgrade material by 23.6%. A preliminary strategy was reported by Kilmartin-Lynch et al., (2021) for the use of polypropylene extracted from medical single use surgical masks in the production of concrete. Preliminary results indicated increase in the tensile and compression capacity of concrete. Kilmartin-Lynch et al., (2022) in their studies on repurposing the plastic based COVID-19 isolation gowns in structural concrete, concluded that the shredded plastic based medical isolation gowns added to concrete improves its compressive strength by 15.5%. Further testing showed that the modulus of elasticity and flexural strength of concrete increased by 11.73% and 20.6%, respectively. This demonstrated the potential of using shredded isolation gowns as reinforcement material in concrete.

1.2 Problem Statement

The use of SUSFMs as personal protective equipment (PPE) to reduce the spread of the coronavirus disease had sharply increased since it first emerged. It was also estimated that 6.88 billion SUSFMs, or the equivalent of approximately 206,470 tons, were consumed around the world each day. In 2020, it was estimated that 700 million SUSFMs was used daily in Africa (Prata et al., 2020). Even before the pandemic, SUSFM were used in hospitals, pharmaceutical production facilities, and food production establishments, among other premises. As a result of the widespread use of SUSFMs, there has been massive waste generation, which has raised concern from environmentalists.

Despite the Kenyan Government putting in place systems to ensure the safe disposal of SUSFMs, hand gloves, and other personal protective equipment, some are finding themselves in our environment (Boroujeni et al., 2021). At the household level, there was haphazard disposal with other household disposables, which ended up in landfills. Further, some were flushed through toilets into the sewer system, which ended up blocking the systems and causing overflows through manholes, thereby polluting the environment. In addition, these surgical face masks were dumped directly into open fields, roadsides, and walkways, which eventually were washed away into our water bodies (Wang et al., 2022). The SUSFMs are mainly made from polypropylene, a thermoplastic polymer that remains in the environment for over 100 years to breakdown (Dhawan et al., 2019). Those SUSFMs ending up in our water bodies break up into microplastics that are ingested by our wildlife, marine life, and other animals, causing internal organ damage. This consumed microplastics will probably end up in our food sources as humans consume some of these marine animals. This may cause oxidative damage to humans. Therefore, these effects of environmental pollution will continue to impact human life even after the COVID-19 pandemic.

Currently, in Kenya, incineration is the most commonly used method of disposal of SUSFM, which uses high temperatures to destroy the virus. However, this method generates greenhouse gases that contribute to global warming (Silva et al., 2021). To mitigate these problems, a more sustainable and low-carbon strategy is required to safely dispose of this medical waste.

On the other hand, concrete is a versatile material that is strong in compression but brittle with low tensile strength (Pakravan & Ozbakkaloglu, 2019). Cracks in concrete reduce serviceability and durability. Hence, the addition of short fibers to concrete limits the initiation and propagation of cracks. Steel fibers are mostly used, but they increase concrete weight and, therefore, costs. Polypropylene fibers are adopted because they reduce the weight of concrete and, at the same time, increase its strength (Madhavi et al., 2014). A reduction in the dead weight of concrete reduces structural seismic risk because earthquake forces are directly proportional to the dead weight (Yasar et al., 2003). The manufacture of virgin polypropylene fibers increases carbon emissions, hence the need to adopt low-carbon materials that can improve concrete ductility. The use of recycled materials substitutes for the use of virgin construction materials, reducing the use of and depleting natural resources.

The problem of SUSFM polluting the environment, coupled with the need to improve the ductility of concrete using low-carbon materials, informed the need to investigate the probable re-utilization of SUSFMs in production of green concrete.

1.3 Research Objectives

1.3.1 Main Objective

The main aim of the study is to evaluate the feasibility of re-utilizing single-use surgical face masks in concrete.

1.3.2 Specific Objectives

i. To characterize fine aggregate, coarse aggregate and single use surgical face masks for use in concrete.
ii. To evaluate the effect of re-utilizing single-use surgical face masks on the physical characteristics of concrete.
iii. To assess the effect of re-utilizing single-use surgical face masks on the mechanical characteristics of concrete.

iv. To determine the influence of reutilized single-use surgical face mask material on concrete durability.

1.4 Research Questions

i. What are the physical characteristics of fine aggregates, coarse aggregates and single use surgical masks?
ii. How are the physical properties of concrete affected when shredded single-use surgical face masks are added to concrete?
iii. What is the effect on concrete mechanical characteristics if shredded single-use surgical face masks are added to concrete?
iv. What is the influence of the re-utilization of single-use surgical face mask material on concrete durability?

1.5 Justification of Study

The study developed a sustainable strategy for the disposal of SUSFM in our environment by incorporating them into concrete. Concrete is strong in compression but brittle with low tensile strength. Cracks in concrete reduce serviceability and durability. Hence, the addition of short fibers to concrete limits the initiation and propagation of cracks. The addition of SUSFM fiber material will substitute commonly used virgin polypropylene fiber material to enhance the qualities of plain concrete. Therefore, investigating the probable re-utilization of SUSFMs in concrete in these studies will provide a solution for improving the strength of concrete using low-carbon materials while at the same time mitigating the impact of pollution on our environment.

1.6 Scope and Limitation

1.6.1 Scope

The study used fine and coarse aggregates sourced from the Malakisi River in Bungoma County and Turbo Kakamega County, respectively. Promo-Kings 3-ply SUSFMs were sourced from a pharmaceutical shop in Bungoma Town, Bungoma

County. Cement was sourced from an authorized cement distributor in Bungoma town.

The SUSFMs were shredded manually using scissors at the Materials Testing & Research Division Regional laboratories of the Ministry of Transport, Infrastructure, Housing, and Urban Developments, Bungoma County.

The research was undertaken in the Materials Testing and Research Division Bungoma regional laboratories of the Ministry of Transport, Infrastructure, Housing, and Urban Development, Science and Technology laboratories at Kibabii University, and Civil Engineering Laboratories at JKUAT, Main Campus.

1.6.2 Limitations

The main limitation to this research was;

i. New SUSFMs were adopted instead of used SUSFMs to prevent potential COVID-19 disease infections and adhere to laboratory rules that did not allow use of COVID-19 materials.
ii. Because of lack of machine, the shredding of SUSFM was done manually with scissors.

CHAPTER TWO

LITERATURE REVIEW

2.1 Introduction

In this research study, theoretical literature and empirical literature have been reviewed. In the theoretical literature, a detailed review of ordinary concrete, fiber-reinforced concrete, concrete reinforced with recycled materials, as well as SUSFMs as concrete reinforcement material, has been conducted. In the empirical literature, several reviews on the current usage of recycled waste materials from our environment as concrete reinforcement materials to not only improve the quality of concrete but also help remove the waste from the environment have been conducted. Among the recycled waste materials reviewed as reinforcement materials are surgical face masks, medical plastic aprons, medical gloves, PET bottles, medical syringe needles, and human hair, among other industrial wastes.

2.2 Ordinary Concrete

Concrete is a composite construction material made from a mix of cement, water, fine aggregates, and coarse aggregates. Water in concrete combines with cementitious materials by hydration to form a paste that fills voids, glues aggregates together, and enables the mix to flow. It is an important material used in the construction of buildings, bridges, roads, dams, and pipes, among other applications. Admixtures are at times added to concrete to modify the rate of curing or properties of the concrete material, (Merin et al., 2014). Concrete is strong when subjected to compressive forces but weak under tensional forces, (Malagavelli & Paturu, 2011). Poor tensile strength is a result of the presence of internal micro-cracks in concrete. These micro-cracks propagate and eventually lead to brittle fractures as a result of the development of certain displacement discontinuity surfaces within the concrete solid. Normal tensile cracks are a result of displacement developing perpendicularly to the surface of displacement. Shear cracks cause displacement to develop tangentially to the surface of displacement. Structural cracks and micro-cracks develop even before loading is applied, particularly due to volumetric changes and the drying shrinkage of concrete.

When the concrete element is loaded, the micro-cracks propagate, opening up, and cracks developing in places where there are minor defects due to the effect of stress concentration. These micro-cracks cause inelastic deformations in concrete. According to Salunke (2017), when concrete blended with small, closely spaced, and uniformly dispersed fibers it becomes an isotropic and homogenous material. The additional fibers in concrete arrests the formation and propagation of cracks, hence improving the strength and ductility of the concrete composite. Therefore, fibers will not only control plastic, dry shrinkage cracking, and lower permeability but also enhance ductility, tensile strength, and resistance to fatigue, (Malagavelli & Paturu, 2011). Concrete reinforced with fibers offers a more practical, convenient, and economical method of overcoming the development of micro-cracks and also offers an effective construction method for seismic-resistant lightweight structures.

2.2.1 Physical Properties of Concrete.

2.2.1.1 Workability of Fresh Concrete.

Workability is the ability of the concrete mix, flow and properly fill the formwork with the desired work of pouring, spreading, and compacting without reducing the quality of the concrete. The workability of concrete depends on the amount of water in the mix, the shape, size, aggregate surface texture, temperature, the content of cementitious material, the level of hydration, and the contents of fiber materials. Concrete workability increases with an increase in water content or the addition of chemical admixtures, (Merin et al., 2014). However, more water than required will lead to the segregation of aggregates and/or increased bleeding. Using aggregates with undesirable grading can result in harsh concrete with a very low slump. The workability of fresh concrete reduces with the addition of fibers (Li et al., 2021). This reduced workability is a result of the shear resistance to flow that occurs when fibers are introduced into fresh concrete. Reduced workability affects how the fibers are distributed in concrete and makes compaction difficult, limiting its application in building construction. Malagavelli and Paturu (2011) found that maximum compaction of high-density polyethylene fiber-reinforced concrete is attained at 2% fiber content. However, if the workability is reduced beyond a certain limit, depending on the use of concrete, admixtures can be used to improve the workability of fiber-reinforced concrete (Gupta & Sharma, 2018). During clinker grinding, electrical charges are created on the surface particles. When cement is mixed with water, cement bonds together, trapping water, and therefore, plasticizer breaks these cement bonds, freeing water to be available for workability. This also makes available more cement surface area for hydration. The effect on workability depends on the type, size, and content of fibers used. Workability is measured by the compaction factor, slump test, flow table, or Vee-Bee test. The slump test is a simple method commonly used, especially in the field, to measure the plasticity of fresh concrete.

Cracking in concrete occurs when concrete is fresh or hardened. In fresh concrete, cracks are mainly plastic shrinkage cracks developing in straight lines, commonly in hot and windy environments. Plastic settlement cracks develop due to unstable formworks and others developing along the reinforcement lines. Other cracks appear after the concrete has hardened due to structural defects, settlement, and drying shrinkage. This requires structural analysis and the necessary retrofitting. Cracking of concrete affects the visual appearance, structural strength, and durability of the concrete element, (Kashinath & Gupta, 2015). In addition, cracking allows the possibility of air and moisture penetration, which may eventually damage the concrete, (Kim et al., 2017). Fibers are also used in concrete to reduce shrinkage and cracking.

2.2.1.2 Density of Hardened Concrete

The density of a material is its mass per unit volume. Normal-weight concrete ranges from 2,200 to 2,600 kg/m^3, (Neville, 2000). Lightweight concrete is adopted to reduce the dead weight of a concrete structure and also improve the buoyancy of the structure, (Iffat, 2015). But introducing lightweight aggregates in concrete often results in poor strength and low concrete durability performance if quality control protocols are not maintained. Therefore, instead of using lightweight aggregates, polypropylene fibers are added to concrete to reduce the overall weight of the material.

2.2.1.3 Water Absorption of Hardened Concrete

Water absorption is dependent on concrete cracking, which may be induced by shrinkage, loading, or a thermal effect on the concrete. This crack provides pathways for water and other aggressive agents like chlorides to penetrate the concrete. The serviceability of concrete depends on its durability, which depends on fluid penetration through its microstructure, (Zhang & Zong, 2014).

2.2.2 Mechanical Properties of Concrete

2.2.2.1 Ultrasonic Pulse Velocity of Hardened Concrete

The Ultrasonic Pulse Velocity (UPV) test is a nondestructive test to check concrete quality. The test is used to assess homogeneity and the relative quality of concrete by indicating the presence of voids and cracks. Concrete properties determine the velocity of the pulse of compressional waves passing through the concrete matrix. Ultrasonic pulse velocity speed of concrete greater than 4500m/s are regarded as excellent quality, (Kurup & Kumar, 2017).

2.2.2.2 Compressive Strength of Hardened Concrete

The concrete's compressive strength is its resistance to crushing. Concrete has lower tensile strength but relatively high compressive strength. Therefore, concrete is usually reinforced with materials that have higher tensile strength. The compressive strength depends upon concrete ingredients such as the type and amount of cement used; the amount and type of reinforcement fibers; the size, shape, and grading of aggregates; the quality and water-cement ratio; the degree of compaction; and curing. The strength of concrete is usually specified using standard test procedures as the lower-bound compressive strength of either the cubic or cylindrical samples. According to Xu et al., (2020), concrete’s compression strength increases when fibers are added up to a certain limiting content, after which it decreases. Compression strength increases because fibers restrict the propagation of cracks, (Nili & Afroughsabet, 2010). However, compressive strength decreases because of not only the presence of weak interfacial bonds between the binder material and fibers but also because of the presence of voids in the matrix, (Mohammadhosseini et al., 2017).

2.2.2.3 Splitting Tensile Strength of Hardened Concrete

The splitting tensile strength test is a measure of the shear resistance of concrete. The test is conducted on the universal testing machine. Concrete has poor tensile strength because of the presence of internal micro cracks. These micro cracks propagate and eventually lead to brittle fractures in the concrete. According to Salunke (2017), incorporating fibers improves the crack control and ductility of concrete. Malagavelli and Paturu (2011) concluded that increasing the waste high-density polyethylene (HDPE) fibers in concrete increases the tensile strength at an optimum fiber content of 3.5% and that it decreases when the fiber content increases further.

2.2.3 Durability Properties of Concrete

Concrete durability is its resistance to deterioration, depending on the environment in which it is placed. The deterioration is in the form of corrosion of steel in concrete, frost attack, chemical attack, and others. Abrasion of concrete is the loss of mass of concrete progressively due to degradation as a result of friction, wearing down and grinding, and others. It depends on the concrete constituents and the hardness of the concrete. Semanda et al., (2014) concluded that the presence of plastic fibers increases the abrasion resistance of the tiles. The depth of wear of concrete with rubber fibers decreases with increased rubber fibers (Gupta et al., 2015). Pineapple fibers increase the abrasion resistance of concrete by up to 3% fiber content and subsequently reduce it, (Vodounon et al., 2018). Plastic fibers have fibrous characteristics that greatly influence the cohesion of concrete particles.

Chemical attack through acid penetration provokes the degradation of concrete. According to Reju and Jacob (2012), ultra-high-performance fiber-reinforced concrete mass decreases when under acid attack with a concentration of more than

1%. However, a concentration of 0.5% didn’t show a remarkable decrease in the mass of concrete.

2.3 Fiber Reinforced Concrete

Plain concrete does not resist cracking as it is a brittle material with limited ductility, (Qasim et al., 2021). When tensile stresses are applied to concrete, the internal micro-cracks propagate, resulting in brittle fracture of the concrete as a result of insufficient energy absorption capacity. To mitigate these micro cracking, fibers are added to the concrete. Therefore, fiber-reinforced concrete is concrete that has fibrous material added to it. The fiber materials are added into the concrete blend in a uniformly dispersed and close-spaced manner to influence the properties of concrete, (Ravinkumar & Manjunath, 2015). These properties depend on the friction, physical, and chemical bonds, and interaction between the concrete matrix and fibers. The concrete properties also depend on the anchorage of fibers induced by their geometry.

Fibers are small pieces of reinforcement material that possess certain characteristic properties which can be flat or circular. They are described by their aspect ratio, which is the ratio of their length to their diameter. Typically, the fiber aspect ratio ranges between 30 and 150. Plastic fibers are grouped into discontinuous fibers or short fibers, whose aspect ratio ranges between 20 and 60, while long fibers or continuous fibers have an aspect ratio of more than 200, (Saberian et al., 2021). According to Naaman (2003), circular fibers have an aspect ratio given by Equation 2.1;

$$\text{Aspect ratio} = \frac{L}{A} \qquad (2.1)$$

Where,

L is the length of the fiber, and

A is the fiber's cross-sectional area.

However, the aspect ratio for the non-circular cross-sectional fiber is calculated by Equation 2.2;

Aspect ratio = $\frac{L}{\text{Dfiber}}$ (2.2)

Where,

L is the fiber length, and

D_{fibre} is an equivalent diameter.

The equivalent diameter, D_{fibre} is calculated by Equation 2.3;

$D_{fibre} = 4 * A/\psi$ (2.3)

Where,

A is fiber cross-sectional area, and

ψ is the fiber cross-sectional perimeter.

According to Mohod (2015), the length of fibers such as polypropylene is tied to the maximum nominal aggregate size. These fibers in the concrete matrix form a strong bond together and effectively act as a single structural element to withstand a variety of applied forces, such as compression and tension. The isotropic properties of plain concrete are enhanced by the uniform dispersion of fibers in the concrete, thereby increasing the static and dynamic tensile strengths, energy absorbing properties, and fatigue strength development. Concrete properties depend upon the bonding of fibers and the concrete matrix, which enables efficient stress transfer between fibers and the matrix, (Mohod, 2015). This transfer of stresses also depends on fiber volume, relative fiber matrix stiffness, orientation and aspect ratio of the fiber, concrete workability and compaction, and the size of coarse aggregate.

Some of the fibers used in the production of concrete are carbon, steel, nylon, polypropylene, coir, asbestos, and glass. The tensile strength of these fibers is developed as a result of the molecular orientation that is obtained during extrusion, (Mohod, 2015). Hard intrusion fibers have a higher elastic modulus of elasticity than the concrete mix, such as carbon steel and stainless steel, which improves the resistance against impact and the flexural strength of concrete, while soft intrusion fibers have a lower elastic modulus of elasticity than the concrete mix, such as polypropylene and vegetable fibers, which improve the resistance against impact of concrete. Organic fibers are cheaper, environmentally friendly, and sustainable fibers with encouraging mechanical characteristics that have found use in concrete production in recent times. Primarily, fiber-reinforced concrete is used for rigid pavement construction, (Malagavelli & Paturu, 2011). In addition, fiber-reinforced concrete is applicable in lining tunnels, rock stabilization, repair works, and hydraulic structures for erosion and cavitation control, (Gupta & Sharma, 2018).

2.4 Recycled Fiber Reinforcement Materials

The use of virgin materials as fiber reinforcement uses natural resources that are fast depleting. Sharma and Jha (2017) alluded to the use of waste materials as fiber material in concrete as an emerging green solution to waste pollution. This is because used materials are dumped in our environment and are therefore readily available at a lower cost, while also helping in environmental conservation and the promotion of sustainable development. Several types of waste material fibers have recently attracted the increasing interest of engineers and other scientists, as evidenced by studies done on the use of waste materials like single-use surgical masks, medical needles, human hair, synthetic hair, chicken feathers, and PET plastics, among others, as fiber reinforcement materials. To reduce the impact of waste on our environment, it is necessary to use recycled materials in construction activities.

2.5 Single Use Surgical Face Masks as Fiber Material in Concrete

Because of the COVID-19 pandemic, there has been a steady increase in the use of SUSFMs as a protective measure against contracting the infectious virus. These surgical masks are single-use protective equipment and hence are replaced frequently, at least once daily. These high-use turnovers generate waste that eventually ends up in waste facilities, our water bodies, and landfills. This necessitated research on the probable use of these wastes in concrete production to not only remove these wastes from the environment but also improve the quality of concrete used in construction activities. SUSFMs consist of a three-layer material that is made up of non-woven fabric with a polypropylene melt-blown polymer placed in between. The middle layer of melt-blown material is a filter, stopping microbes from entering or exiting the surgical mask. The commonly used single-use surgical mask has melt-blown polypropylene material enclosed in between non-woven spun-bond materials, (Akshayaa et al., 2020). Polypropylene is a thermoplastic polymer that is produced through a chain-growth polymerization process from the monomer propylene. It belongs to the polyolefin group that is non-polar and partially crystalline. It's a white, heat-resistant, chemically resistant, and mechanically rugged material, (Mohod, 2015). Nonwoven fabric materials, on the other hand, are web structures or sheets that are mechanically, chemically, or thermally bonded together. Non-woven are either flat or tufted porous sheets made directly from separate molten plastic, fibers, or plastic film, (Balogh et al., 2015).

The polypropylene in SUSFMs remains in the environment for a long time, (Prata et al., 2020). Those that are incinerated at high temperatures generate greenhouse gases that contribute to global warming. Those that end up in our water bodies fragment into microplastics, causing problems for our wildlife, animals, and marine life and probably ending up in our food sources, (Fadare & Okoff, 2020). Therefore, the effects of this environmental pollution will continue to impact human life days after the pandemic. In Kenya, despite the government putting in place systems to ensure the safe disposal of SUSFMs and other PPEs, (NEMA, 2020), some are finding themselves in our environment. Utilization of these waste materials into concrete and related materials in the construction of infrastructure helps not only reduce the pollution effects of these wastes but also offers a greener solution for sustainable development, (Bheel et al., 2020).

For commercial consumption of recycled SUSFMs, there must be an elaborate disinfection process. This is to avoid cross infection of the coronavirus diseases and or other contagious diseases such as influenza. Several methods of cleaning surgical face masks have been proposed for use, such as ultraviolet germicidal irradiation as suggested by Hamzavi et al., (2020) to inactivate the corona virus from the used SUSFM. It was also reported that the COVID-19 virus can be destroyed on surgical face masks by heating them at 70^{o}C for 60 minutes, (Xiang et al., 2020). After disinfection, surgical face masks are kept exposed to the sun in an open, enclosed space away from the general public for at least one week before commercial use, (Saberian et al., 2021). This process eliminates the risk of spreading the COVID-19 virus while transporting and using it in construction. Saberian et al., (2021) found out that heating SUSFMs at 75^{o}C minimally lowers the elongation from 118.96% to 118.91% and the tensile strength from 3.97MPa to 3.63MPa. Therefore the effect of disinfection by heating minimally affects the proprieties of single-use surgical masks for use in construction activities.

2.6 Empirical Review and the Research Gap

2.6.1 Empirical Literature Review

Several studies have been documented on the use of plastic-based waste materials in construction materials. Saberian et al. (2021) used shredded SUSFMs blended with recycled concrete aggregate to produce a blended material that is suitable for use as a road base or road subbase. The results indicated that recycled concrete aggregate mixed with surgical face masks at an optimum blend of 1% satisfied the pavement base strength, stiffness, and ductility requirements by giving the highest compressive strength and resilient modulus.

Studies were carried out by Malek et al. (2020) using green and white recycled polypropylene fibers in concrete at different contents. The study showed that at 1% green polypropylene fiber content, there was an increase of 69.7% in compression strength, 276.0% in flexural strength, and 269.4% in split tensile strength. The same content of 1% white polypropylene fibers indicated an increase of 39.4% compressive strength, 162.4% flexural strength, and 254.2% split tensile strength.

Al-Hadithi and Hilal (2016) evaluated the use of fibers from shredded plastic beverage bottles in concrete at different volumes. The study indicated an increase in compressive strength of 43.4% at 1.5% fiber content and a notable increase in flexural strength of 82.2% at 1.75% fiber content. Additionally, the plastic fibers improved the ultrasonic pulse velocity of concrete by 44.4% at a 0.25% fiber dosage.

Islam and Gupta (2016), while evaluating the permeability and plastic shrinkage of polypropylene fiber-reinforced concrete, concluded that increasing the polypropylene fiber content in concrete showed a marginal decrease in compressive strength from 2% at 0.1% fiber content to a 10% decrease at 0.3% fiber content. However, there was a noticeable increase in the tensile strength, with the highest increase of 39% noticed at 0.1% polypropylene fiber content. It was also concluded that plastic fibers reduce shrinkage cracking by more than half compared to cracking in plain concrete.

Kilmartin-Lynch et al. (2021) gave preliminary results showing that polypropylene fibers added to concrete increased the tensile from a control of 3.27 N/mm^2 to the highest of 3.67 N/mm^2 representing 12.2%. The compressive strengths of the concrete increased to the highest of 17.1% from the control of 50.34 N/mm^2 to 58.93 N/mm^2. However, the modulus of elasticity marginally increased by 3.3% with the inclusion of polypropylene in surgical face masks.

Further, Memon et al., (2018) deduced that an increase in the length of polypropylene fibers increased the flexural strength of concrete and decreased its compressive strength.

Meddah and Bencheikh (2009), while investigating the effect of industrial waste plastic fiber addition on concrete, concluded that the highest concrete compressive strength was registered at 0.5% fiber content of 50 mm long fibers. The highest concrete flexural strength was recorded at 1.0% fiber content of 50 mm-long fibers. The optimum dosage of the waste plastic fibers was 0.75% at 50 mm lengths, providing the optimum quality of physical and mechanical properties in concrete.

Pandya and Purochit (2014) concluded in their studies that concrete workability decreased with an increase in added PET fiber material. The compressive and flexural strengths of concrete improved up to 1.5% PET fiber content, after which they decreased.

Hidaya et al., (2017) in their investigation on concrete with PET fibers, deduced that workability was reduced when PET fibers were introduced in concrete by 33.0%, 48.9%, and 62.2% at 1%, 2%, and 3% PET fiber contents. Water absorption, density, and compression strength were reduced with the addition of PET fibers to concrete. However, split tensile increased by 10% and 5.2% at 1% and 2% dosages, respectively, and was reduced with increased PET fibers beyond 2%.

Mohod (2015), in his research on the performance of polypropylene fiber reinforced concrete, found that at a 0.5% PP fiber dosage, the tensile strength and compressive strength increased but reduced when the dosage was increased beyond 1.0%. A similar trend was reported for the flexural strength of the blended concrete. It was reported that beyond 1% PP fiber dosage, the workability was difficult to compact.

Konin (2011) studied the effect of plastic waste content on physico-mechanical properties of flexible pavement. The researcher used PE, PET and PP at 20%, 30% and 40% as pavement binder material. He reported that the plastic fibers improved abrasion resistance and slip resistance by 20% and less than 5% porosity. These plastic wastes improves splitting tensile strength of flexible pavement.

Nibudey et al., (2019) investigated the use of PET fibers on compressive and sorptivity for normal concrete and PET fiber reinforced concrete using M20 and M30 concrete. PET fibers with aspect ratios of 35 and 50 were used at 0%, and 3.0%. At an optimum fiber volume of 1%, the compressive strength increased and sorptivity decreased.

Zhu et al., (2022) utilized shredded nitrile medical gloves in expansive clay soil to evaluate the impact on mechanical characteristics. They reported that compressive strength of the expansive clay increased at an optimum dosage 1.5% to 315.5 kPa together with its resilient modulus and CBR improved.

Chandan and Sharma, (2023) used SUSFM material to stabilize clay soils for pavement construction. With the addition of SUSM fiber material in clay soils, the Unconfined Compressive Strength (UCS), increased by 64% at 1% dosage, while the

California Bearing Ratio (CBR) increased from 1.96% to 6.72%. There was a notable increase in consistency limits and compaction characteristics.

2.6.2 Summary of Literature Review and Research Gap

Looking at the previous studies above Malek et al., (2020); Islam and Gupta (2016); Mohod (2015); Meddah and Bencheikh (2009), reveals that detailed effect of waste fiber materials on performance of concrete composites were provided. However, none discussed the influence of blend waste PP and non-woven material on the physical and mechanical performance of concrete. Additionally, (Saberian et al., (2021); Zhu et al., (2022); Kilmartin-Lynch et al., (2021); Chandan and Sharma, (2023)), studied use of COVID-19 waste materials in flexible pavement base materials and on mechanical characteristics of concrete. However, there no candid and conclusive studies on the influence of reutilized waste SUSFM on the durability performance of concrete. This research gap coupled with the massive generation of SUSFM waste in our environment, informed the aim of the study to evaluation their probable reutilization of SUSFM in concrete. This study focused on determining the effect of the shredded SUSFM fiber material on the physical characteristics of concrete. The contents and aspect ratio of the SUSFM material were varied, and their influence on the mechanical strengths of concrete were evaluated. Further, the effect of adding SUSFM material at a fixed aspect ratio but varying the contents in concrete against the abrasion resistance and acid attack resistance of the hardened concrete blend was determined.

2.7 Conceptual Framework

In the research study, the independent variables are the content and length of shredded SUSFM material. The dependent variables were classified as physical properties: concrete workability, density, and water absorption; mechanical properties: concrete splitting tensile strength, compressive strength, and concrete ultrasonic pulse velocity; and durability characteristics: concrete chemical attack resistance and abrasion resistance.

The research study was conceptualized as shown in Figure 2.1.

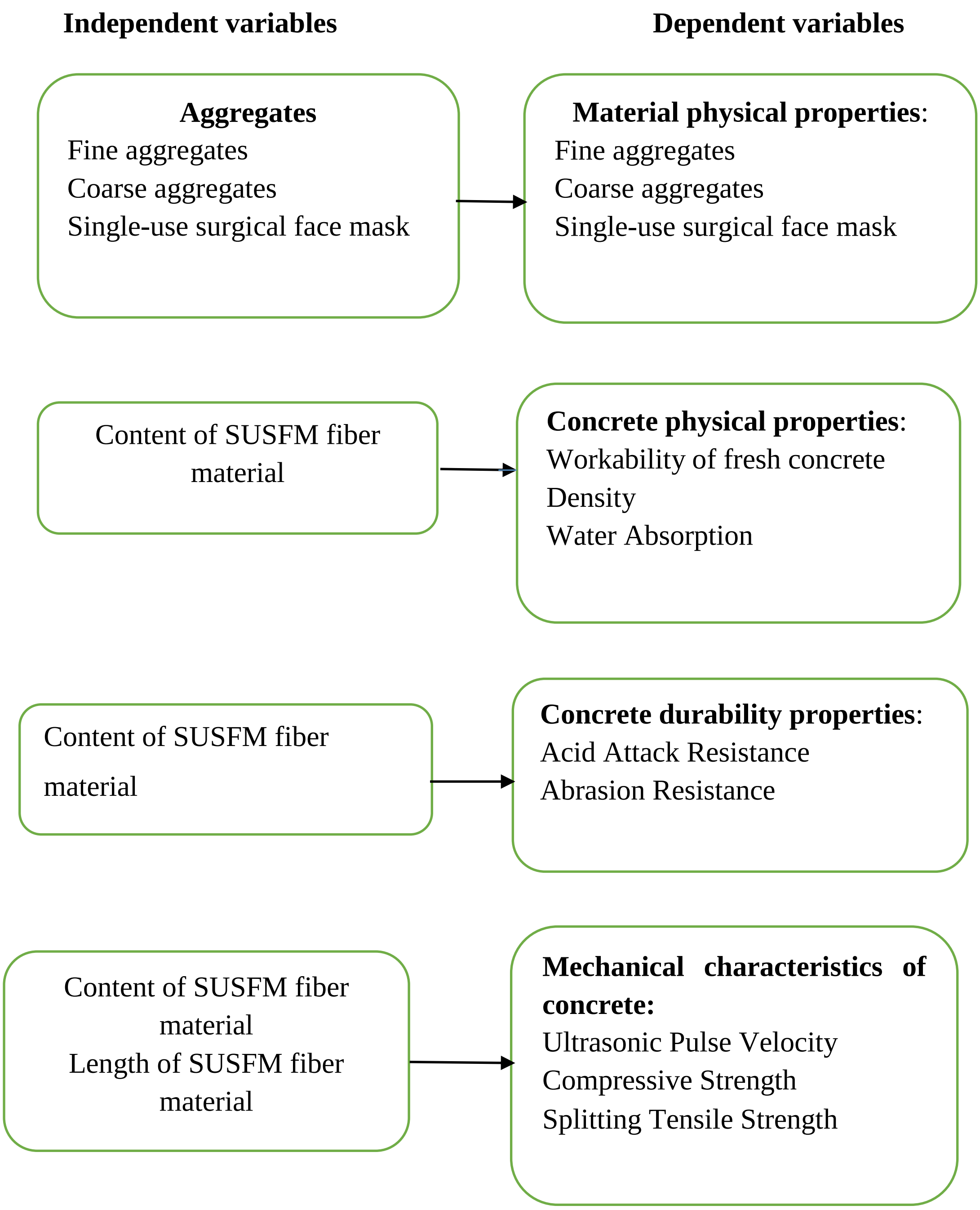

Figure 2.1: Conceptual Framework

CHAPTER THREE

RESEARCH METHODOLOGY

3.1 Introduction

In this section, the materials used and methods adopted have been discussed. The study experiments were conducted in JKUAT Civil Engineering laboratories, Kiambu County, Materials Testing and Research Division Regional laboratories of the Ministry of Transport, Infrastructure, Housing and Urban Developments, Bungoma County, and Kibabii University, Bungoma County. The study was undertaken in six sections, as illustrated in the research design (Figure 3.1).

The study focused on the comparison of the physical characteristics, mechanical properties, and durability of the control and test specimens containing shredded SUSFM fiber material. The contents and lengths of fiber materials were varied to determine their influence on the properties of concrete. The study was executed through laboratory experimentation.

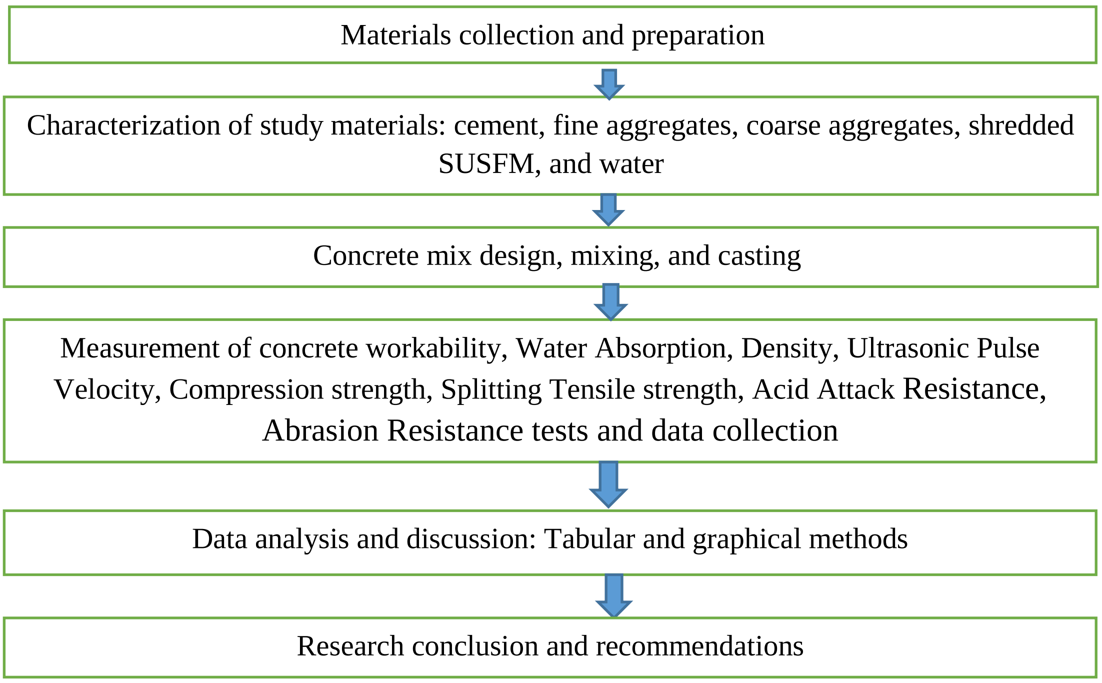

Figure 3.1: Research Design

3.2 Research Materials and Equipment

3.2.1 Ordinary Portland Cement

Ordinary Portland cement of strength class CEM1/42.5N, conforming to Kenyan standards (KS EAS 18-1:2001), was used in all the mixes. Cement was sourced from local hardware stores in Bungoma town. It was stored on a raised platform, away from moisture. The choice of cement was informed by the previous researches by Kilmartin-Lynch et al., (2022) who used Portland cement and Malek et al., (2020) who used Portland cement CEM I, 42.5

3.2.2 Fine Aggregate

The fine aggregate used was river sand sourced from the Malakisi River, Kenya.

3.2.3 Coarse Aggregate

The natural coarse aggregates used in the study were sourced from Nzoia Quarry, Kakamega, Kenya.

3.2.4 Single Use Surgical Face Masks

New SUSFMs were used for the study because the current COVID-19 restrictions didn't allow the adoption of used SUSFM materials in the laboratories. The Promo-Kings 3-ply SUSFMs were sourced from a local pharmaceutical shop in Bungoma, Kenya complying with Kenyan standards KS 2636:2021 (Plate 3.1).

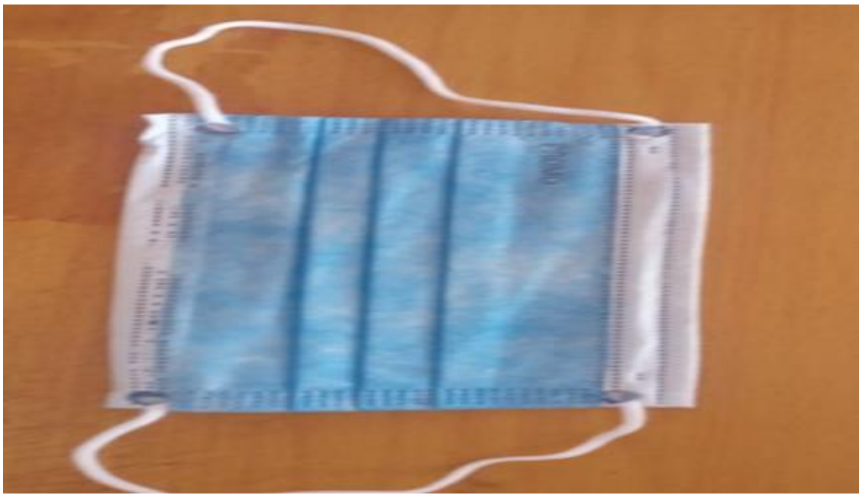

Plate 3.1: Single use surgical face mask

3.2.5 Concrete Plasticizer

Sika plastiment 40KE, sourced from Sika Kenya Ltd., Nairobi, Kenya, with a density of 1.05 kg/m^3, was used as a plasticizer to achieve the desired workability in all concrete mixes except the workability tests. The plasticizer was a low alkaline aqueous modified polycarboxylic ethers (PCE) and Gluconates solution with low chloride ion content of less than 0.1%. The solution do not react with cement compounds and steel in concrete. The plasticizer dosage adopted was 1 kg for every 100 kg of cement material in concrete, in accordance with the manufacturer's specifications.

3.2.6 Mixing Water

The concrete mixing water was ordinary drinking tap water supplied by Nzoia Water Services Company in Bungoma town and used in all mixes and the curing of specimens in the curing tank.

3.2.7 Concrete Mix Design

Mix proportion for C30 grade concrete was determined in accordance with the Department of Environment (D.O.E.). The choice of the concrete class in agreement with Nakov et al., (2017); Sideris and Manita, (2013). After mix design, the batch mix proportions were determined for the casting of the test specimens, (Appendix II).

3.2.8 Key Testing Equipment

Key testing equipment employed were Universal Testing Machine with digital read out unit model no. 00701/A, Hot Air Oven as Biobase BOV-V225F, Ultrasonic Pulse Velocity testing kit as MATEST C372M, weighing balance, micrometer screw gauge, and slump cone.

3.2.9 Naming Nomenclature for Concrete Test Specimens

The specimens were labeled to avoid mismatching and testing on the wrong specimens. In a naming nomenclature such as 20CO15, the first two digits denote the length of single-use surgical face material, in this case 20 mm. The second two letters denote the test prescribed on the specimen, in this case, the compression strength test. Finally, the last two digits denote the dosage of SUSFM material in the concrete, in this case, 1.5%. The dates of casting test specimens were indicated on the specimens to track the concrete specimen's aging.

3.3 Assessing Physical characteristics of Fine Aggregate, Coarse Aggregate and Single Use Surgical Face Masks

3.3.1 Fine Aggregates

The tests performed on the fine aggregates were particle size distribution tests according to BS EN 933-1:2012. In addition, fineness modulus, water absorption, silt content, bulky density, and specific gravity of fine aggregates tests were done to BS standards.

3.3.1.1 Particle Size Distribution of Fine Aggregates

Particle size distribution was done to BS 812-103-1. Fine aggregate samples were dried cooled and then weighed as W_1. Clean dry sieves were nested in order of increasing aperture size from bottom to top. The dried sample was placed on the top coarsest sieve and covered with a fitting lid. The assembly was shaken by mechanical means sufficiently to separate the sample into size fractions by sieve aperture size. The weight of fine aggregate material retained on each sieve size was measured as W_2. The cumulative material retained on the sieves were determined as W_3

The weight of fine aggregate material passing each sieve was calculated as a cumulative percentage of the total sample weight. The cumulative percentage of the weight of the sample passing each of the sieves versus nominal sieve aperture size were plotted on a semi-log chart and compared with the grading envelope specified.

3.3.1.2 Water Absorption of Fine Aggregates

Approximately 500 g of fine aggregates passing 5.0 mm sieve but retained on sieve 0.075 mm sieve was washed in distilled water to remove finer materials. The washed specimens were transferred to shallow tray and fully submerged in water for 24 hours. Water was then drained by decantation. The wet aggregates were allowed to air dry to evaporate surface moisture. The weight of the (SSD) fine aggregates were taken (W_1). The sample was dried in an oven at 110^o for 24 hours. The sample was removed at allowed to cool before weight being measured as W_2

Water absorption was determined using the formula in equation (3.1).

$$\text{Water absorption (\%)} = \frac{100(W1-W2)}{W2} \qquad (3.1)$$

Where,

W_1 is the weight of the SSD aggregate specimen in Kilograms

W_2 is the weight of the dry fine aggregate specimen in Kilograms

3.3.1.3 Fineness Modulus of Fine aggregates

Fineness modulus was carried out to BS 812-103.1 (1985). Fine aggregate was sieved until no more particles could pass through a certain sieve. The Fineness Modulus of fine aggregates was calculated from formula in the equation (3.2).

$$\text{Fineness modulus (F.M) (100\%)} = \frac{\Sigma \text{ cumulative coarser}}{100} \qquad (3.2)$$

3.3.1.4 Fine Aggregate Silt Content

Fine aggregate silt content were done to BS 812 (1990). The procedure is similar to 3.3.1.1. The total fine aggregate material was measured as W_1. The fine aggregate material passing through 0.15 mm sieve and retained on the pan were measured W_2. Silt content is determined by using the formula in the equation (3.3).

$$\text{Silt Content (\%)} = \frac{W2}{W1} \tag{3.3}$$

3.3.1.5 Specific Gravity of Fine Aggregates

Approximately 500 g of fine aggregates passing 5.0 mm sieve but retained on sieve 0.075 mm sieve was washed in distilled water to remove finer materials. The washed specimens were transferred to shallow tray and fully submerged in water for 24 hours. Water was then drained by decantation. The wet aggregates were allowed to air dry to evaporate surface moisture. The weight of Specific Gravity Bottle (SGB) was taken as W_1. The weight of the (SSD) fine aggregates were taken (W_5). The fine aggregates were then placed in the SGB and weight taken as W_2. Water was poured into the contents in the SGB until it was full. Entrapped air was eliminated and the outer surface of SGB was wiped clean and weight taken as W_3. The contents in the SGB was poured unto a tray. The SGB was refilled with distilled water to the same level and its weight taken as W_4.

The procedure was repeated two other samples and specific gravity determined. The average of the three samples were taken as specific gravity of fine aggregates.

The Specific gravity was calculated using the formula in the equation (3.4).

$$\text{Specific gravity of fine aggregates (\%)} = \frac{W5}{W2-(W3-W4)} \tag{3.4}$$

3.3.2 Coarse aggregates

The tests performed on the coarse aggregates were fineness modulus, bulky density and water absorption tests according to BS standards.

3.3.2.1 Water Absorption of Coarse Aggregates

The water absorption of coarse aggregates were tested and analyzed as in 3.3.1.2

3.3.2.2 Fineness Modulus

Fineness modulus of coarse aggregates were tested and analyzed as in 3.3.1.3

3.3.3 Single-Use Surgical Face Masks

3.3.3.1The Physical Properties of the SUSFM

Nose strip and ear loops were cut of the SUSFM. The weight of SUSFM was measured on a weighing scale and recorded as W. The size of the mask material was measured by using a scale ruler as length, A and width, B. The thickness of SUSFM was determined by using a micrometer screw gauge and recorded as T.

SUSFM were cut 5 mm widths using scissors. The shredded SUSFM material were then cut into different lengths of 20 mm, 30 mm, and 40 mm and recorded as L (Plate 3.2).

Plate 3.2: Shredded Single use surgical face mask material

The aspect ratio for the SUSFM fiber material was calculated by Equation (3.5).

$$\text{Aspect ratio} = \frac{L}{\text{Dfiber}} \tag{3.5}$$

Where,

L is the fiber length, and

D_{fibre} is an equivalent diameter.

The equivalent diameter, D_{fibre} is calculated by Equation (3.6).

$$D_{fibre} = 4 * A/\psi \quad (3.6)$$

Where,

A is fiber cross-sectional area, and

ψ is the fiber cross-sectional perimeter.

3.4 Effect of Re-Utilizing Single Use Surgical Face Masks on Physical Characteristics of Concrete

The physical properties of concrete in terms of density, workability, and water absorption were studied. The concrete tests were carried out on three test specimens for each content ranging from 0.5% to 3.0% with an increment of 0.5% of the 20 mm length SUSFM material to achieve reliability. According to Yuan and Jia (2021), the specimen's test result was determined by taking the mean of the values of the three test results. The data was collected from test equipment, tabulated, and represented graphically to compare the impact of SUSFM material on the workability of wet concrete, density, and water absorption capacities of hardened concrete with a reference control specimen of concrete with 0% SUSFM material to BS standards.

3.4.1 Workability Tests on Fresh Concrete

The workability properties of fresh concrete were determined by the slump test to BS EN 12350-2:2019.

The fine and coarse aggregates were batched in saturated dry conditions. In the mixing procedure, the fine aggregate, coarse aggregate, and cement were weighed on a weighing scale and mixed on a dry metallic, non-absorbent pan, manually by use of a spade, till the mix was uniform (Plate 3.3). Mixing water was added to the mix and mixed until uniform. The 20mm length shredded SUSFM fiber material was then gradually added to the concrete mix while mixing to ensure even distribution and avoid clamping together (Plate 3.4). Three specimens were prepared for each of the seven concrete mix dosage regimes incorporating shredded SUSFM material in proportions by weight of cement as 0% (control mix), 0.5%, 1.0%, 1.5%, 2.0%, 2.5%, and 3.0% (Table 3.1). This range is consistent with Malek et al., (2020); Islam and Gupta (2016).

The cone mold was cleaned and dried, and a thin coat of mold oil was applied internally to prevent fresh concrete from sticking to the surface of the mold. The mold was then placed on the base plate centrally and held firmly. Wet concrete was filled in three layers of equal volume. Standard steel rod was used to tamp each layer 25 times to consolidate, and then the top of the mold was troweled level. Surplus concrete around the slump cone was cleaned up. The original height of the cone was measured before carefully lifting off the mold vertically, leaving the unsupported enclosed concrete material to slump to a certain height owing to gravity. The amount by which the concrete test specimen slumped was measured. The procedure was repeated with all the batch mixes and corresponding slumps measured and tabulated. The average slump height for the three samples in each batch was taken as the concrete slump for the batch.

Plate 3.3: Concrete mixing

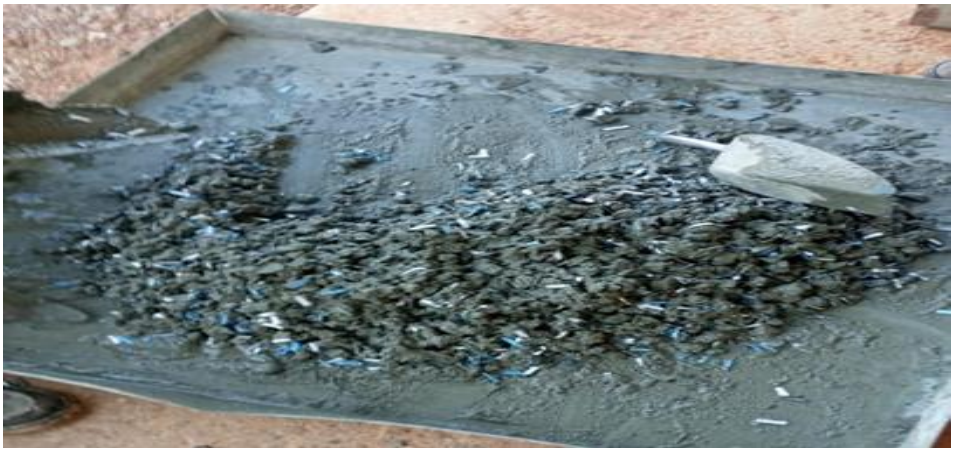

Plate 3.4: Concrete mixed with SUSFM materials

Table 3.1: Mixing plain concrete with various contents of SUSM fiber material

Tests performed	**Length of SUSFM fiber**	**Dosage of SUSFM in concrete**
Workability	20 mm	0%, 0.5%, 1.0%, 1.5%, 2.0%, 2.5%, 3.0%
Density		
Water Absorption		
Compressive Strength	20 mm	0%, 0.5%, 1.0%, 1.5%, 2.0%, 2.5%, 3.0%
Ultrasonic Pulse Velocity		
Splitting Tensile Strength	30 mm	0%, 0.5%, 1.0%, 1.5%, 2.0%, 2.5%, 3.0%
	40 mm	0%, 0.5%, 1.0%, 1.5%, 2.0%, 2.5%, 3.0%
Acid Attack	20 mm	0%, 0.5%, 1.0%, 1.5%, 2.0%, 2.5%, 3.0%
Abrasion Resistance		

3.4.2 Water Absorption Tests on Hardened Concrete

The concrete's capacity to absorb water was determined on specimens according to BS EN 1881-122:2011+A1:2020.

The fine and coarse aggregates were batched in saturated dry conditions. In the mixing procedure, the fine aggregate, coarse aggregate, and cement were weighed on a weighing scale and mixed on a dry metallic, non-absorbent pan, manually by use of a spade, till the mix was uniform. Half of the mixing water was added to the mix and mixed until uniform. Plasticizer, Sika plastiment 40KE was added to the remaining half of the mixing water before adding on the concrete mixture to avoid the cement paste from reacting directly with the plasticizer. Mixing continued until a uniform mix was achieved. The shredded SUSFM fiber material was then gradually added to the concrete mix while mixing to ensure even distribution and avoid clamping together. Three specimens were prepared for each of the seven concrete mix dosage regimes incorporating shredded SUSFM material in proportions by weight of cement as 0% (control mix), 0.5%, 1.0%, 1.5%, 2.0%, 2.5%, and 3.0% (Table 3.1). This range is consistent with Malek et al., (2020).

After curing for 28 days, 150 mm cube test samples were removed from the curing tank and air dried. The specimens that were saturated surface dry (SSD) were weighed on a 10 kg weighing scale as W_1. The surface-dried test specimens were stored for 24 hours in a hot air oven (Biobase, BOV-V225F) set at 105°C. After being taken out of the hot air oven, the samples were allowed to cool in the open air before being weighed as W_2 (Plate 3.5). Water absorption is the decrease in mass of the test specimen as a percentage of the mass of the dry specimen, calculated using Equation (3.7).

$$\text{Water absorption (\%)} = \frac{100(W1-W2)}{W2} \quad (3.7)$$

Where,

W_1 is the weight of the SSD cube specimen in Kilograms

W_2 is the weight of the dry cube specimen in Kilograms

Plate 3.5: Water absorption testing of concrete with SUSFM material

3.4.3 Density Tests on Hardened Concrete

The Density test was performed on hardened concrete to BS EN 12390-7:2019. The concrete mixing is similar procedure used in 3.4.2. 150mm cube test specimens were removed from the curing tank after 28 days and air dried. The saturated surface dry (SSD) specimens were weighed on a 10 kg weighing scale as M. The hardened concrete density, ρ, of the specimen was evaluated using Equation (3.8).

$$\text{Density, } \rho = \frac{M}{V} \ (\text{kg/m}^3) \qquad (3.8)$$

Where,

M is the mass of the as-received cube specimen in the air in kilogram

V is the cube specimen volume calculated from its dimensions in cubic metre

3.5 Effect of Re-Utilizing Single Use Surgical Face Masks on Mechanical Characteristics of Concrete

The compressive strength, ultrasonic pulse velocity, and splitting tensile strength tests were conducted on hardened concrete to establish the effect of SUSFM fibers on the mechanical properties of concrete. The concrete tests were conducted on three test specimens for SUSFM dosages ranging from 0% to 3.0% with an incremental of 0.5% for 20 mm lengths, 30 mm lengths and finally 40 mm lengths of SUSFM materials. The mean of the values of the three tests of each batch was taken as the result of the test. The readings and data collected from test equipment were tabulated and represented graphically to compare the impact of the addition of shredded single use surgical mask material on the compressive strength, ultrasonic pulse velocity and splitting tensile strength characteristics of concrete with reference control specimens of concrete with a nil content of SUSFM material.

3.5.1 Compressive Strength Tests on Hardened Concrete

The capacity of concrete to withstand axial forces is its compressive strength. The tests were conducted using Basic Wizard type compressive strength testing machine with a digital readout unit model No. 00701/A in accordance with BS EN 12390-3:2019 from the Ministry of Transport and Infrastructure, Regional Testing and Research Laboratories in Bungoma. The machine had a load precision of 0.1N.

The concrete mixing is similar procedure used in 3.4.2. Test specimens were removed from the curing tank after 28 days and air dried. The saturated surface dry (SSD) specimens were placed on the bearing surfaces of the testing machine between the platens central to the loading axle, and a uniform rate of loading was applied until the test cube failed. At the maximum load, compressive strength of test specimens were read out. The compressive strength, f_c, of the test specimen was recorded in the test record sheet.

3.5.2 Splitting Tensile Strength Tests on Hardened Concrete

Tensile strength is the capacity of concrete to resist shear forces. The splitting tensile strength test was conducted using Universal testing machine, Basic Wizard type with a digital readout unit 00701/A to BS EN 12390-6:2009. The concrete mixing is similar procedure used in 3.4.2.

The machine had a load precision of 0.1N. The cylindrical steel molds measuring 100 mm in diameter and 200 mm in height were used. Saturated surface dry (SSD) specimens were placed between the loading surface of the test machine, and the load was gradually applied till the cylindrical specimen failed along the vertical diameter at load P (Plate 3.6). This splitting tensile strength, F_{sp}, of the concrete cylindrical specimen was calculated using Equation (3.9).

Splitting tensile strength, $F_{sp} = \frac{2P}{\pi LD}$ (N/mm^2) (3.9)

Where,

P is the load at failure in Newtons.

L is the length of the test specimen in millimeters.

D is the diameter of the test specimen in millimeters.

π is a constant of 3.14.

Plate 3.6: Testing of concrete specimens for splitting tensile strength

3.5.3 Ultrasonic Pulse Velocity Tests on Hardened Concrete

The ultrasonic pulse velocity tests on hardened concrete was conducted after 28 days of specimen curing to BS EN 12504-4:2004. The concrete mixing is similar procedure used in 3.4.2.

The saturated surface dry (SSD) specimens were measured for Ultrasonic Pulse Velocity using the MATEST UPV testing machine model no. C372M (Plate 3.7). The ultrasonic pulse was generated by a pulse generator and transmitted to the concrete surface. The time taken for the pulse to travel through the concrete and be received by the transducer on the opposite side of the concrete specimen was measured. To ensure good contact, a thin film of solid jelly was applied between the interface of the concrete specimen surface and the transducer (Bogas et al., 2013). The time taken for the ultrasonic pulse to pass through the concrete test specimen was measured as T. The pulse velocity was then calculated using Equation (3.10).

$$\text{Ultrasonic Pulse Velocity} = \frac{W}{T}\ (\text{m/s}) \qquad (3.10)$$

Where,

W is the width of the concrete test specimen in metres.

T is the time taken by the pulse to go through the concrete test specimen in seconds.

Plate 3.7: Concrete Ultrasonic Pulse Velocity testing equipment

3.6 Influence of Re-Utilized Single Use Surgical Face Masks Material on Concrete Durability

Concrete testing was conducted to determine the influence of re-utilized SUSFM material on the concrete durability characteristics in terms of resistance to acid attack and abrasion resistance. The concrete tests were conducted on three test specimens for each content of the 20 mm length SUSFM material. The average value of the three tests was taken as the result of the test. The data was collected from test equipment, tabulated, and represented graphically to compare the impact of SUSFM material on the acid attack resistance and abrasion resistance characteristics of concrete with a reference control specimen of plain concrete.

3.6.1 Acid Attack Tests on Hardened Concrete

The concrete's capacity to resist attack by acidic solutions was investigated in terms of compression strength loss and weight loss in test specimens. The concrete mixing was similar to procedure used in 3.4.2.

The hydrochloric acid was sourced from a local laboratory equipment supplier in Bungoma town. The 2% hydrochloric acid was prepared from the 35.4% AR of 1.18 specific gravity concentrated hydrochloric acid. 56.5 cm^3 of 35.4% concentrated hydrochloric acid was mixed with 1 liter of water to produce 2% concentrated hydrochloric acid. 2,260 cm^3 of 35.4% hydrochloric acid was mixed with 37,740 cm^3 of distilled water to produce 40 liters of 2% hydrochloric acid that was used in every 100-liter tank.

After 28 days, the cube test specimens were then taken out of the curing tank and allowed to air dry. The specimens that were saturated surface dry (SSD) were weighed on a 10 kg weighing scale as W_1. The specimens were then submerged in a 2% hydrochloric acid solution in 100-liter plastic tanks for a period of 60 days. The tanks were closed to ensure the acid concentration remained the same throughout the period of testing. After 60 days, the concrete specimens were removed from the tank and air dried. (Plate 3.8) The specimens' residual weight was tested and recorded as W_2. This procedure is in agreement with, Rao et al., (2012). Acid attack resistance was determined by the weight lost using Equation (3.11).

$$\text{Weight loss (WL)} = \frac{100(W1-W2)}{W1} \ (\%) \qquad (3.11)$$

Where,

W_1 is the weight of the sample before it is immersed in the acid in kilograms.

W_2 is the weight of the sample after the acid attack in kilograms.

To determine acid resistance using the compressive strength loss test, the concrete test specimens were removed from the curing tank and air dried. One set of the saturated surface dry (SSD) specimens were placed on the bearing surfaces of the testing machine between the platens central to the loading axle, and a uniform rate of loading was applied until the test cube failed. At the maximum load, compressive strength of test specimens were read out and recorded as compressive strength, FC_1.

Another set of the saturated surface dry specimens was completely submerged in a 2% hydrochloric acid solution in a plastic tank for a period of 60 days. The tanks were covered throughout the testing period to ensure the acid concentration remained the same. After 60 days, the concrete specimens were removed from the acid tank and air dried. The specimens were placed on the bearing surfaces of the testing machine between the platens central to the loading axle, and a uniform rate of loading was applied until the test cube failed. At the maximum load, compressive strength of test specimens were read out and recorded as residual compressive strength, FC_2. Acid attack resistance was determined by the compressive strength lost using Equation (3.12).

$$\text{Compressive Strength Loss (CSL)} = \frac{100(FC1-FC2)}{FC1}\ (\%) \qquad (3.12)$$

Where,

FC_1 is the compressive strength before acid attack in N/mm^2.

FC_2 is the residual compressive strength in N/mm^2.

(a) **(b)**

Plate 3.8: (a) Acid attack test samples in the acid curing tank, (b) Samples after 60 days of acid attack exposure

3.6.2 Abrasion Tests on Hardened Concrete

The concrete abrasion was investigated in terms of weight loss as a result of concrete degradation. The concrete mixing was similar to procedure used in 3.4.2. The degradation is a result of friction and wear. After 28 days of curing, the saturated surface dry (SSD) specimens were dusted and weighed as W_1. The samples were then set on the wooden table and securely clamped in place before being tested. The to-and-fro brushing made one stroke. Wire brushing was done on the upper surface of the specimen for 50 strokes. The specimens were dusted and weighed on a weighing scale, W_2. This procedure is in agreement with Arasa et al., (2021). The abrasion resistance was determined by the weight loss of test samples, using Equation (3.13)

$$\text{Weight loss (WL)} = \frac{100(W1-W2)}{W1}(\%) \tag{3.13}$$

Where,

W_1 is the weight of the sample before abrasion in kilograms.

W_2 is the weight of the sample after abrasion in kilograms.

CHAPTER FOUR

RESULTS AND DISCUSSION

4.1 Physical Characteristics of Fine Aggregates, Coarse Aggregates, and Single Use Surgical Face Masks

4.1.1 Physical Properties of Fine Aggregates

Table 4.1 shows the physical properties of the fine aggregate used in the study. The fineness modulus was 2.8, which was between the acceptable limits of 2.3 - 3.1. The silt content was 2.1%, less than the maximum allowable of 4%. Higher silt content affects the fine aggregate bonding with the cementious materials in the concrete. The specific gravity of the fine aggregate was 2.7, higher than the acceptable minimum of 2.6. Lower specific gravity shows the presence of deleterious materials and affects concrete negatively. Water absorption was 2.2%, which was less than the maximum allowable of 2.3%, hence suitable for use in concrete. Lower absorption means less porous material, while higher water absorption means more water is required for the production of concrete with acceptable workability.

Table 4.2 and Figure 4.1 show the fine aggregate particle size distribution and the grading curve, respectively. 20 g of fine aggregate passed through a sieve of 0.15 mm, representing 2.2%. There was 40.3 % passing through a 0.6 mm sieve. There was no loss of fine aggregate materials, hence within the acceptable limits of 0.3%. This indicates suitable fine aggregate for concrete. The results indicate that the fine aggregate was within the lower and upper limits.

Table 4.1: Properties of Fine Aggregate

Property	Tested value	Limit
Particle Size Distribution	The grading curve lies between the lower limit and upper limit	Between the lower limit and upper limit, BS EN 1260: 2002
Fineness Modulus	2.8	2.3 - 3.1, ASTM C33
Silt Content	2.1%	Maximum 4% , BS 882
Bulk Density	1510 kg/m^3	1327-1684 kg/m^3, BS EN 1097-3:1998
Specific Gravity	2.7	Minimum 2.6, BS 812-102:1995
Water Absorption	2.2%	Maximum 2.3%, BS 813-2:1995

Table 4.2: Fine aggregate particle size distribution

Sieve size	Retained material weight W_2 (g)	Cum. retained material weight, W_3 (g)	% Cumulative retained material	% Passing	Lower limit	Upper limit
5.0	0	0	0	100	89	100
2.36	63	63	6.8	93.2	60	100
1.0	219	282	30.3	69.7	30	100
0.6	274	556	59.7	40.3	15	100
0.3	268	824	88.5	11.5	5	70
0.15	86	910	97.8	2.2	0	15
Pan	20	930				

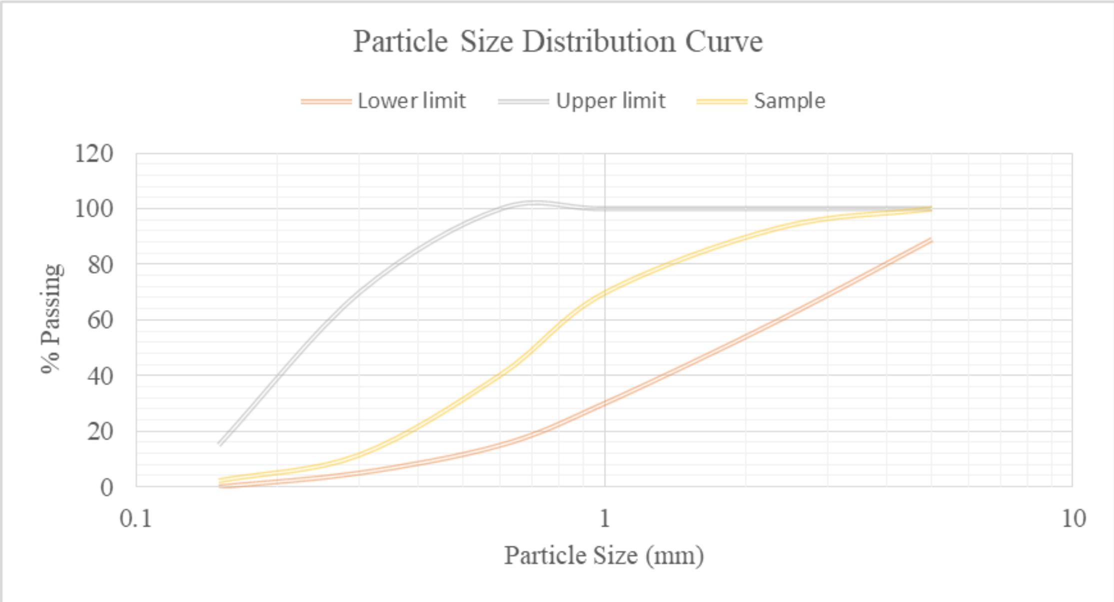

Figure 4.1: Fine aggregate particle size distribution curve

4.1.2 Physical Properties of Coarse Aggregates

Table 4.3 shows the physical properties of the coarse aggregate used in the study. The fineness modulus was 3.5, and the bulky density was 1398 kg/m^3. The water absorption was recorded at 1.92 %, less than the maximum allowable of 2.3%. Lower absorption means less porous material while higher water absorption means more water is required to produce concrete with acceptable workability.

Table 4.3: Properties of Coarse Aggregate

Property	Tested value	Limit
Fineness modulus	3.5	3.5 – 6.5 BS EN 933-8
Bulk density	1398 kg/m^3	1200 -1750 kg/m^3 BS EN 1097-3:1998
Water absorption	1.92%	Maximum 2.3% BS 813-2:1995

4.1.3 Physical Properties of Single Use Surgical Face Masks

Table 4.4 below shows the physical properties of single use surgical face masks used in the study. The masks contained three layers, with the outer layer made from cotton and polyester material, the middle layer made from polypropylene material, and the inner layer made from cotton and polyester material, according to KS 2636:2016, for surgical face masks. The mask material was shredded into rectangular fiber materials, 5 mm wide lengths ranging from 20 mm, 30 mm, and 40 mm. The aspect ratio of SUSFM fiber material ranged between 29 and 58, which agrees with Wang et al., (2010), who used fibers with aspect ratios ranging from 20 to 60.

Table 4.4: Properties of Single-use Surgical Face Masks

Physical Properties	**Description**
Size of SUSFM	172.5 mm by 97.0 mm
Width of shredded SUSFM fibers	5 mm
Length of shredded SUSFM fibers, L	20 mm, 30 mm, 40 mm
Thickness, T	0.35 mm
Aspect Ratio	20 mm – 29 30 mm - 43 40 mm - 58
Density	0.166 kg/m^3
Weight, W	3.5 g
Shape	Rectangular

4.2 Effect of Reutilizing Single-Use Surgical Face Masks on Physical Characteristics of Concrete

4.2.1 Workability of Fresh Concrete

The results of workability are shown in Table 4.5 and Figure 4.2. The concrete slump decreased from 51 mm in the control specimen to 45 mm, 11 mm, 3 mm, and 0 mm for 0.5%, 1.0%, 1.5%, and 2.0%, respectively. Dosages from 2.0% to 3.0% registered a 0 mm slump. These represent a reduction of the slump by 11.8% at 0.5% SUSFM material dosage, 78.4% at 1.0% SUSFM material dosage, 94.1% for 1.5% SUSFM material dosage, and 100% for dosages of 2.0%, 2.5%, and 3.0% SUSFM material. These results agrees with Hidaya et al., (2017), where the workability was reduced by 33%, 48.9%, and 62.2% at 1%, 2%, and 3% fiber content, respectively. Malek et al., (2020) reported the same trend, where the addition of plastic fibers to concrete resulted in a decrease in workability from 22.9% at a 0.5% fiber dosage to 62.9% at a 1.5% fiber dosage. The reduction in workability of concrete with reference to the control specimen was attributed to the increased SUSFM material added to the mix, which lumped on each other, reducing the concrete's fluidity. Further, loss of workability may be a result of increased adhesion within the concrete matrix and SUSFM material, holding other ingredients together and impeding easy flow.

When the SUSFM material is added beyond 1.0%, its workability is zero, indicating that the concrete mix is not workable. This trend is consistent with what Mohod (2015) who reported that workability reduces with increase in PP fibers, but beyond 1% PP fiber dosage, concrete was stiff and difficult to compact. This phenomenon can be connected to the fact that fibers lumped on each other and increased material surface area absorbing the available free water in the concrete matrix, which aids in improving workability. The mix with high SUSFM material required more compaction effort to achieve proper compaction. Mixes beyond 1.0% require the addition of a plasticizer to improve workability.

Table 4.5: Workability of fresh concrete blended with 20 mm length of SUSFM material

Sample No.	SUSFM content (%)	Slump (mm)
20WO00	0	51
20WO05	0.5	45
20WO10	1.0	11
20WO15	1.5	3
20WO20	2.0	0
20WO25	2.5	0
20WO30	3.0	0

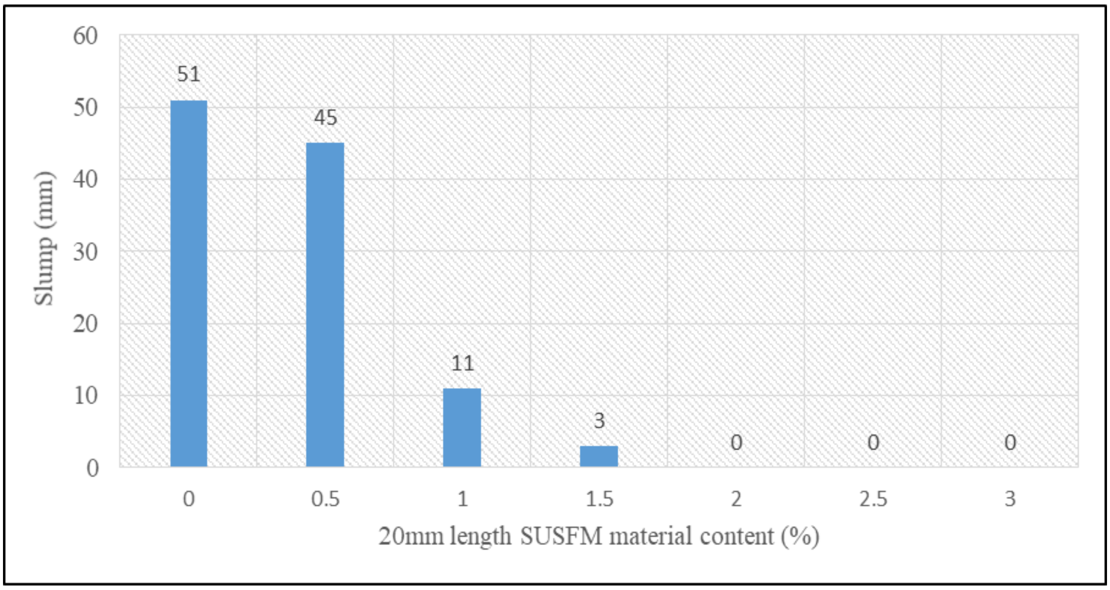

Figure 4.2: Workability of fresh concrete blended with SUSFM material

4.2.2 Water Absorption of Hardened concrete

The water absorption results of the test concrete are shown in Table 4.6 and Figure 4.3. The results show that the water absorption of concrete mixed with SUSFM material increased gradually compared to the control sample. Water absorption of hardened concrete increased by 16.9% at 0.5% fiber dosage, 40.3% at 1.0 fiber, 53.6% at 1.5% dosage, 60.7% at 2.0% dosage, 64.4% at 2.5% dosage and 70.8% at 3.0% content of added SUSFM fiber material. In general, the water absorption of concrete increased with the increase of SUSFM material. Yuan & Jia (2021) and Noor et al., (2017) observed similar results. However, Mohod (2015), reported improved workability at 0.5% polypropylene fibers in concrete while the workability dropped beyond 1.0% of PP fibers in concrete.

The increased water absorption of concrete may be attributed to the increased amount of SUSFM fiber material, with the innermost layer made from non-woven absorbent material with higher water absorption properties than other concrete constituents. Further, the increased water absorption could be as a result of the presence of inter-tape voids between adjacent polypropylene material plies. These inter-tape voids may be created because of incomplete material consolidation hence providing a route for water ingress into the concrete composite material. In addition, at a constant water cement ratio, the water absorption tends to reduce with a small margin beyond 2.0% dosage of SUSFM material. This trend was associated with the fact that at lower SUSFM fiber dosages, the fibers are better distributed in the concrete matrix, while at higher SUSFM volumes, the fiber dispersion becomes non-uniform and clumps on each other, causing a balling effect, hence reducing the rate of water absorption in the concrete blend.

Table 4.6: Water Absorption of concrete blended with 20 mm length of SUSFM material

Sample No.	SUSFM content (%)	Water Absorption (%)
20WA00	0	2.95
20WA05	0.5	3.45
20WA10	1.0	4.14
20WA15	1.5	4.53
20WA20	2.0	4.74
20WA25	2.5	4.85
20WA30	3.0	5.04

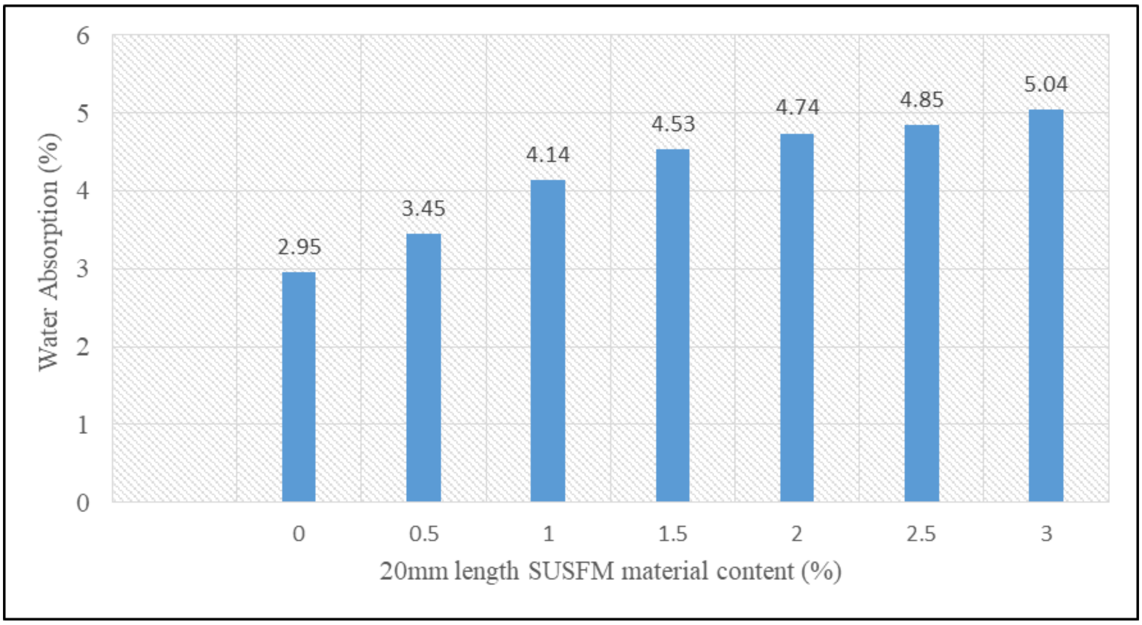

Figure 4.3: Water absorption of concrete blended with SUSFM material

4.2.3 Density of Hardened Concrete

The results in Table 4.7 and Figure 4.4 show the density of hardened concrete blended with SUSFM material. When SUSFM was introduced to concrete at 0.5% dosage the density reduce by 2% to 2412 kg/m^3. Further when the dosage was 1.0% density reduced by 5.4% to 2328 kg/m^3. Density of the blend material reduced by 5.2% to 2332 kg/m^3 at 1.5% dosage, 7.0% to 2289 kg/m^3 at 2.0%, 7.6% to 2275 at 2.5% and finally, 7.7% to 2272 kg/m^3 at 3.0%. Concrete density decreased between 1.5% and 7.7% at dosages between 0.5% and 3.0% of the SUSFM fiber material content. The results show that the concrete density progressively decreases with an increase in the SUSFM material added to the concrete. These results are consistent with Taherkhani (2014) who reported that density of concrete with PET fibers reduced by 1.0% at 0.5% PET fiber dosage and 2.0% at 1.0% PET fiber dosage. Reduction of concrete dead weight indicates a reduction in earthquake forces on a structure by the same rate (Yasar et al., 2003). Since density is a function of weight of concrete constituent materials, the reduced concrete density may be attributed to the increased quantities of added SUSFM material, which is lightweight compared to other concrete components. Further, the light SUSFM material occupies the volume that would otherwise be occupied by heavier concrete components since the fibers are added to affixed volume.

Table 4.7: Density of concrete blended with 20 mm length of SUSFM material

Sample No.	SUSFM content (%)	Density (kg/m^3)
20DE00	0	2461
20DE05	0.5	2412
20DE10	1.0	2328
20DE15	1.5	2332
20DE20	2.0	2289
20DE25	2.5	2275
20DE30	3.0	2272

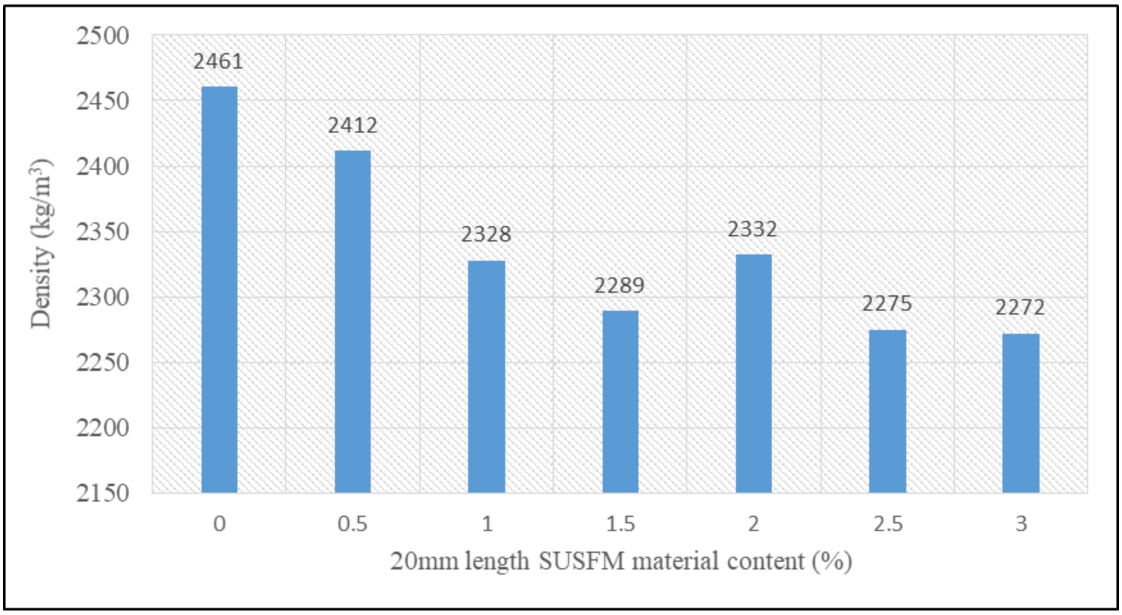

Figure 4.4: Density of concrete blended with SUSFM material

4.3 Effect of Re-Utilizing Single Use Surgical Face Masks on Mechanical Characteristics of Concrete

4.3.1 Compressive Strength of Hardened Concrete

Table 4.8 and Figure 4.5 shows the effect of the addition of 20 mm long shredded SUSFM material in concrete. The compressive strength for control specimen was 50.1 N/mm^2 which reduced by 11.6% to 44.3 N/mm^2 at 0.5% SUSFM dosage. Further, the compressive strength reduced by 22.1% to 39.0 N/mm^2 at 1.0% SUSFM fiber to lowest of 49.9% at 25.1 N/mm^2 a 3.0% SUSFM fiber material dosage. The least decrease of compressive strength was reported at 0.5% of 20 mm length SUSFM dosage which gave 44.3 N/mm^2 strength representing a decrease of 11.6%. This trend registers lower percentage compressive strength reduction compared to what was reported by Taherkhani (2014) who reported that 20 mm length PET fibers reduced compressive strength by 21.0% at 0.5% dosage rate and 36.1% at 1.0% PET fiber dosage. SUSFM dosages less than 2.0% gives compressive strength more the prescribed characteristic strength of 30 N/mm^2. This indicates that concrete with SUSFM less than 2.0% dosage can be utilized in construction. This trend however is contrary to what was reported by Kilmartin lynch et al., (2021) who reported increased compressive strength with addition shredded nitrile gloves in concrete.

Table 4.8: Compressive Strength of concrete blended with 20 mm length SUSFM material

Sample No.	SUSFM content (%)	Compressive strength (N/mm^2)
20CO00	0	50.1
20CO05	0.5	44.3
20CO10	1.0	39.0
20CO15	1.5	32.8
20CO20	2.0	31.3
20CO25	2.5	25.4
20CO30	3.0	25.1

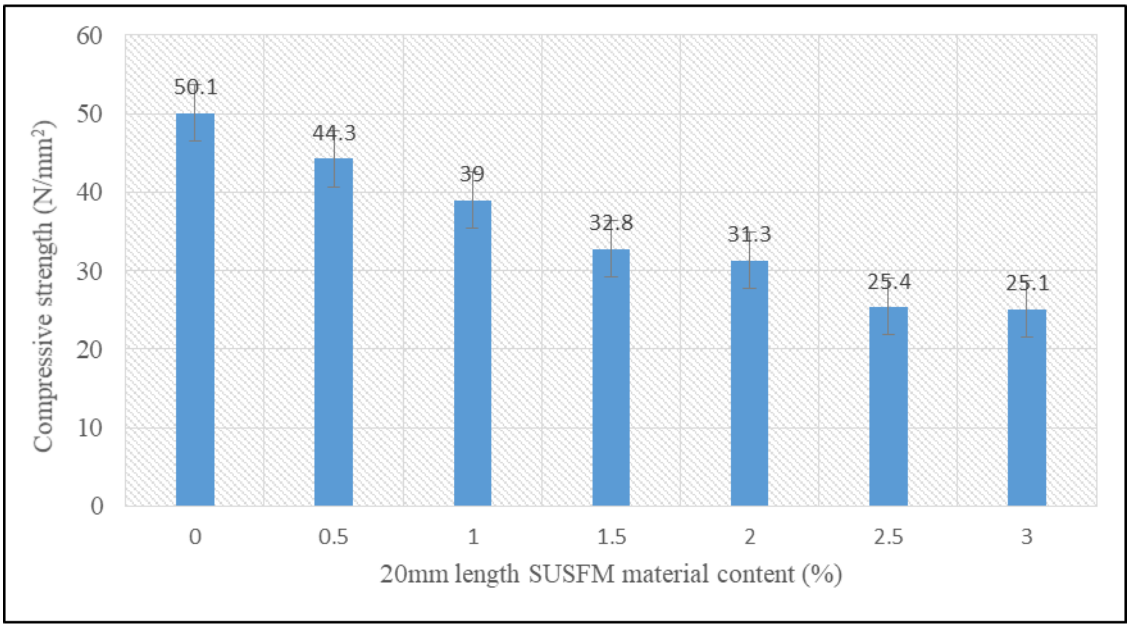

Figure 4.5: Compressive strength of concrete with 20 mm length SUSFM material

The results for compressive strength in Table 4.9 and Figure 4.6 show the effect of the addition of 30 mm long shredded SUSFM material in concrete. The results indicated a systematic decrease in the compressive strength of concrete with an increased amount of shredded 30 mm long SUSFM material. The control sample reported 50.1 N/mm^2 reducing by 10.4% to 44.9 N/mm^2 at 0.5% and reducing gradually to 26.6 N/mm^2 at a 2.5% SUSFM material dosage. The least decrease in compressive strength was registered at 44.9 N/mm^2 when 0.5% of 30 mm long SUSFM material was added representing a 10.4% decrease.

Table 4.9: Compressive Strength of concrete blended with 30 mm length SUSFM material

Sample No.	SUSFM content (%)	Compressive strength (N/mm^2)
30CO00	0	50.1
30CO05	0.5	44.9
30CO10	1.0	37.5
30CO15	1.5	34.9
30CO20	2.0	31.4
30CO25	2.5	26.6
30CO30	3.0	28.3

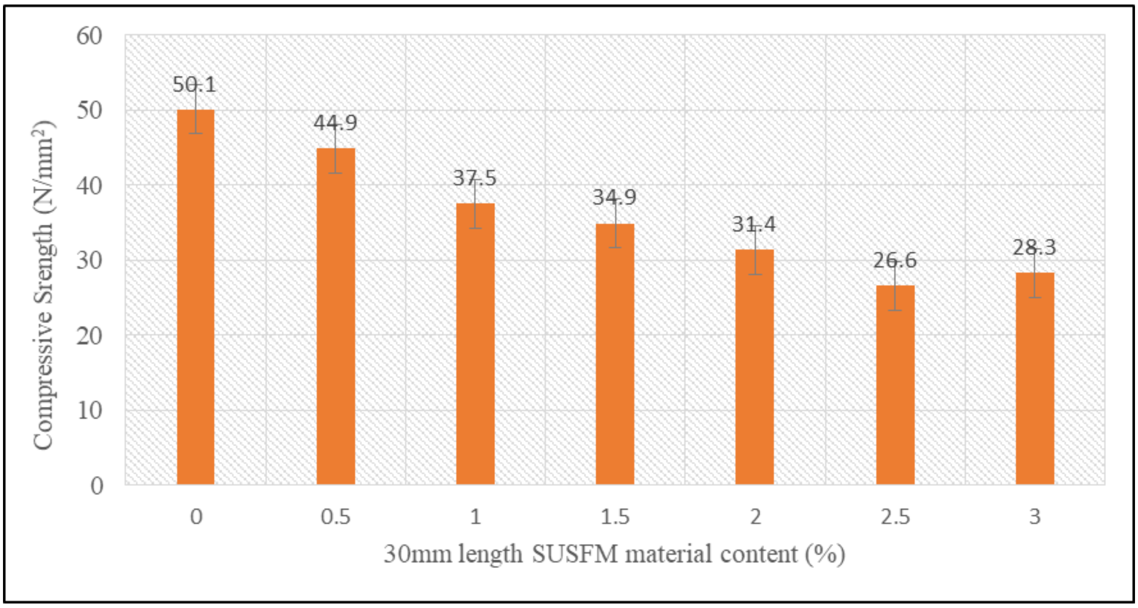

Figure 4.6: Compressive strength of concrete with 30 mm length SUSFM material

Table 4.10 and Figure 4.7 illustrate the behavior of the concrete's compressive strength when 40 mm long shredded SUSFM material was added to the concrete. The control strength was 50.1 N/mm^2, decreasing by 20.8% to 39.7 N/mm^2 at a 0.5% dosage. Increasing the SUSFM material in concrete caused compressive strength to further decline by 27.1% at 1.0% to a minimum of 24.0 N/mm^2 at a 2.5% dosage of SUSFM fiber material. The least decrease in compressive strength of concrete blended with 40 mm long SUSFM fiber material was registered at 0.5% dosage with a compressive strength of 39.7 N/mm^2.

Table 4.10: Compressive Strength of concrete blended with 40 mm length SUSFM material

Sample No.	SUSFM content (%)	Compressive strength (N/mm^2)
40CO00	0	50.1
40CO05	0.5	39.7
40CO10	1.0	36.5
40CO15	1.5	34.0
40CO20	2.0	27.2
40CO25	2.5	24.0
40CO30	3.0	28.0

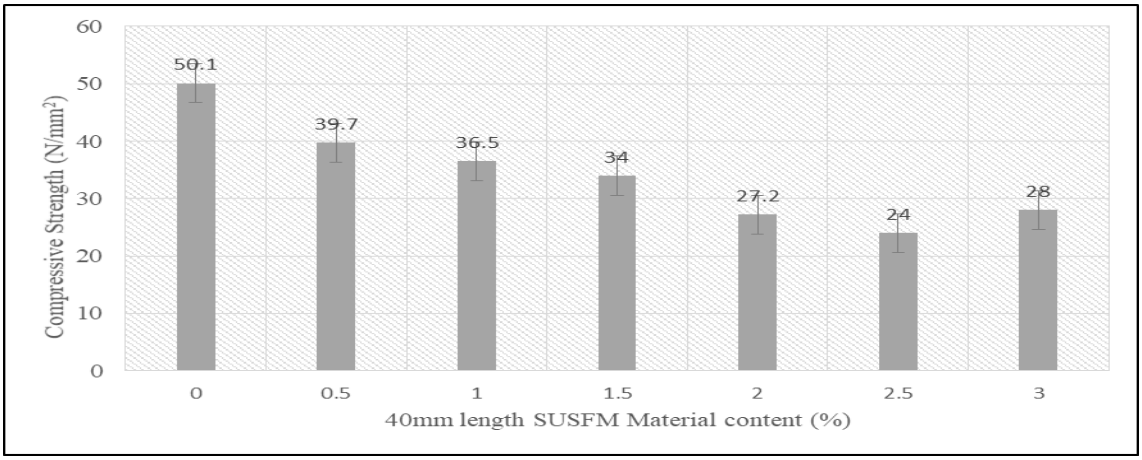

Figure 4.7: Compressive strength of concrete with 40 mm length SUSFM material

The comparative effect of different volumes and lengths of SUSFM fiber material on the compressive strength of concrete is illustrated in Table 4.11 and Figure 4.8. The control specimen recorded 50.1 N/mm^2 of compressive strength. At 0.5% SUSFM fiber dosage, 30 mm length fibers recorded the highest strength of 44.9 N/mm^2, a decline from the control sample by 10.4%. At 1.0% SUSFM fiber dosage, 20 mm length gave the highest strength of 39.0 N/mm^2. The highest compressive strength for the 1.5% SUSFM material dosage was recorded at 34.9 N/mm^2 for the 30 mm length fiber material. The lowest recorded compressive strength among the different lengths of fiber material was 24.0 N/mm^2 at 2.0% of the 40 mm length fiber material.

For 20 mm length of SUSFM material, the highest compressive strength of 44.3 N/mm^2 was recorded at a 0.5% SUSFM material dosage. This value, however, is 11.6% lower than the control specimen. In addition, the highest compressive strength for 30 mm fiber material was 44.9 N/mm^2 at a 0.5% dosage higher than that registered for 20 mm by 1.3%. Further, the highest for 40 mm length fiber material was 39.7 N/mm^2. This value recorded was 11.6% lower than that registered by 30 mm long fibers. Dosages ranging from 0.5% to 2.0% recorded strengths were greater than the designed characteristics strength of 30 N/mm^2. At 2.5% and 3.0% dosages, the strength fell outside acceptable design strength by more than 15.3% and 16.3%, respectively.

For 30 mm length fibers, the dosages from 0.5% to 2.0% were higher than the design characteristic strength. At 2.5%, the strength was 11.3% lower than the characteristic strength, while at 3.0%, the strength was 5.7% lower than the characteristic strength. However, the strength registered falls within the concrete compressive strength growth range. Concrete compressive strength increases with age, up to 15% of the 28 day strength. For 40 mm length fibers, the dosages from 0.5% to 1.5% were greater than the design characteristic strength. At 2.0% dosage, the strength was 27.2 N.mm^2, 9.3% lower than the characteristic strength, and at 3.0% dosage, the strength was 6.6% lower than the characteristic strength. The strength registered fell within the concrete compressive strength growth range. Concrete compressive strength increases with age up to 15% of the 28 day strength. However, at 2.5% dosage, the strength was 24 N/mm^2 representing 20.0% lower than the characteristic strength.

This strength falls outside the concrete compressive strength growth range as reported by (Abdelgader et al., 2019).

From the findings, 0.5% of 30 mm long SUSFM material was the optimum SUSFM material dosage to concrete to yield the least negative impact in terms of compressive strength. These results agree with Islam and Gupta, (2016), who concluded that increasing the amount of polypropylene fiber material in concrete decreases its compressive strength. Similarly, when expanded polystyrene beads were added to concrete, the compressive strength decreased, as evidenced by (Salahaldeen & Al-Hadithi, 2022). Further the results agrees with Hongbo et al., (2020) and Tavakoli et al., (2019). These results slightly differs with what Mohod, (2015) who reported that compressive strength improved at 0.5% polypropylene dosage but reduced beyond 1.5% dosage. In addition, (Nili & Afroughsabet, 2010) reported marginal increase in compressive strength at 0.5% PP fiber volume in concrete compared to plain concrete. The reduction in the compressive strength of concrete can be connected to the increase in SUSFM blend material in concrete, which has a low specific gravity compared to coarse aggregate, a key strength determinant, in the concrete matrix. Further, the lower compressive strength than the control sample recorded may be a result of the weak interfacial bonds between the SUSFM fiber material and the concrete binder material. In addition, higher amounts of SUSFM fiber material in concrete may limit the contact surface of water and cement matrix and therefore affecting the cement hydration process and hence weakening the concrete matrix against formation of cracks. The figures 4.5, 4.6, and 4.7 indicate the compression strength decreased marginally from a dosage of 2.0% SUSFM material. These trends were attributed to the fact that at lower SUSFM fiber dosages, there was improved hydration products filling up pore spaces (Ji et al., 1997), while when the SUSFM fiber volume increases, there was reduction in hydration due to non-uniform fiber dispersion and clumping near the coarse aggregates, hence marginally reducing the filling up of pores.

Table 4.11: Compressive Strength of concrete blended with 20 mm, 30 mm, and 40 mm lengths of SUSFM material

Sample No.	SUSFM content (%)	Compressive strength for 20 mm SUSFM (N/mm^2)	Compressive strength for 30 mm SUSFM (N/mm^2)	Compressive strength for 40 mm SUSFM (N/mm^2)
CO00	0	50.1	50.1	39.7
CO05	0.5	44.3	44.9	36.5
CO10	1.0	39.0	37.5	34.0
CO15	1.5	32.8	34.9	27.2
CO20	2.0	31.3	31.4	24.0
CO25	2.5	25.4	26.6	28.0
CO30	3.0	25.1	28.3	29.7

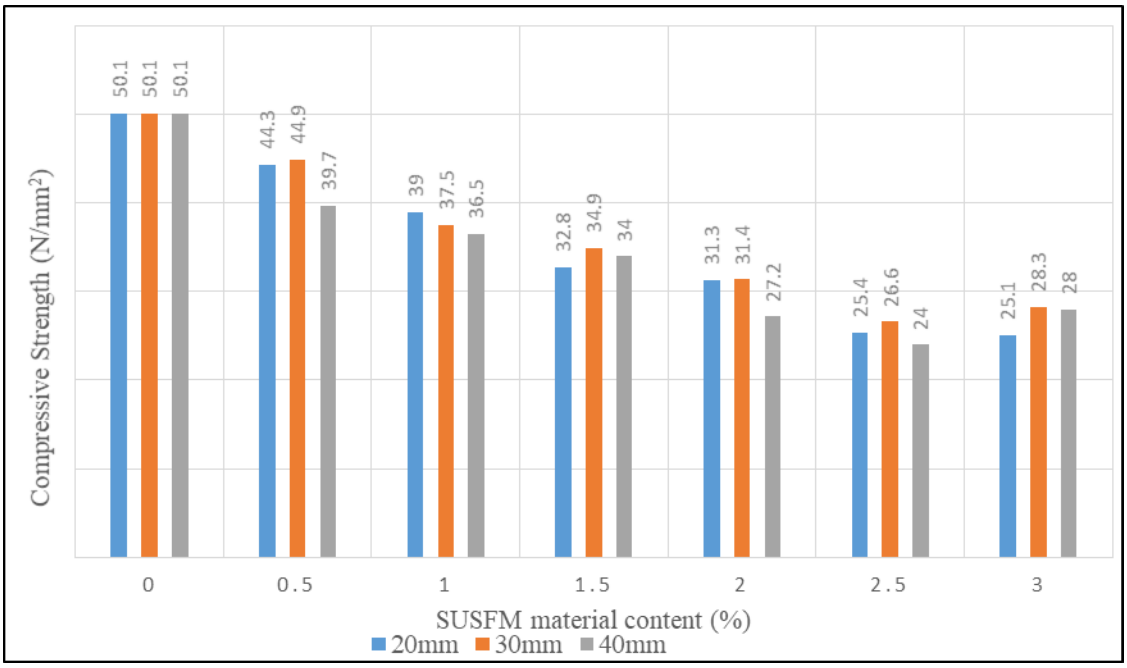

Figure 4.8: Comparative illustration of compressive strength of concrete with different volumes and lengths of SUSFM material

4.3.2 Splitting Tensile Strength of Hardened Concrete

In testing for split tensile strength, a total of 57 cylindrical test specimens were used. The test specimens with no SUSFM material content failed suddenly and did split into separate parts, while those with SUSFM fiber materials failed without separating. Table 4.12 and Figure 4.9 shows the results of adding 20 mm long SUSFM material to concrete. The control specimen recorded 3.3 N/mm^2. Addition of SUSFM material at 0.5% caused a decline in splitting tensile strength by 9.1% to 3.0 N/mm^2. Addition of more SUSFM material gradually reduced the splitting tensile strength to lowest 2.5 N/mm^2 at a 2.0% dosage, representing a 24.2% decrease before slightly increasing to 2.7 N/mm^2 at 3.0% dosage representing 18.2% decline in strength.

Table 4.12: Splitting Tensile Strength of concrete blended with 20 mm length SUSFM material

Sample No.	SUSFM content (%)	Splitting Tensile Strength (N/mm^2)
20TE00	0	3.3
20TE05	0.5	3.0
20TE10	1.0	2.7
20TE15	1.5	2.6
20TE20	2.0	2.5
20TE25	2.5	2.7
20TE30	3.0	2.7

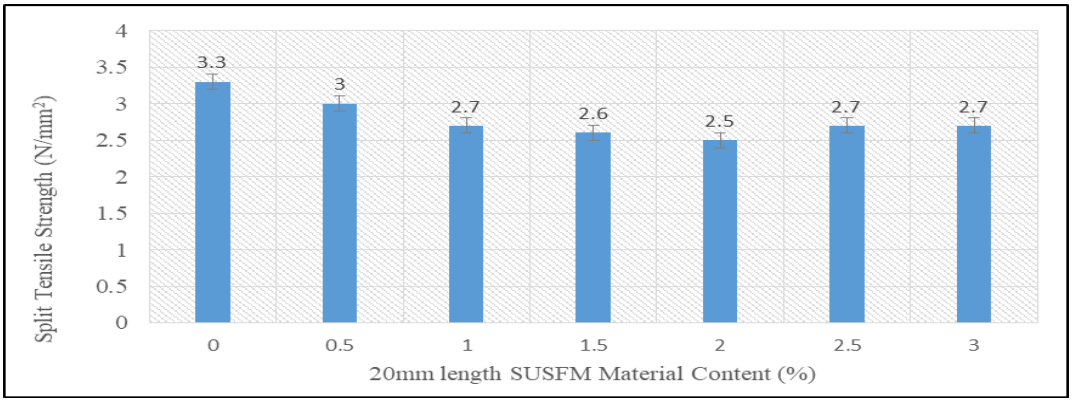

Figure 4.9: Splitting tensile strength of concrete with 20 mm length SUSFM material

However, with the addition of 30 mm long SUSFM material, the split tensile strength increased from 3.3 N/mm^2 in the control sample to 3.8 N/mm^2 at 0.5% SUSFM fiber, and 3.4 N/mm^2 at 1.0%, as shown in Table 4.13 and Figure 4.10. Thereafter, a further increase in SUSFM fiber material reduces the splitting tensile strength of concrete. The lowest split tensile strength of 2.4 N/mm^2 was witnessed at 3.0% of 30 mm long SUSFM material, an equivalent of 27.3% drop in strength.

Table 4.13: Splitting Tensile Strength of concrete blended with 30 mm length SUSFM material

Sample No.	SUSFM content (%)	Splitting Tensile Strength (N/mm^2)
30TE00	0	3.3
30TE05	0.5	3.8
30TE10	1.0	3.4
30TE15	1.5	2.7
30TE20	2.0	2.9
30TE25	2.5	2.8
30TE30	3.0	2.4

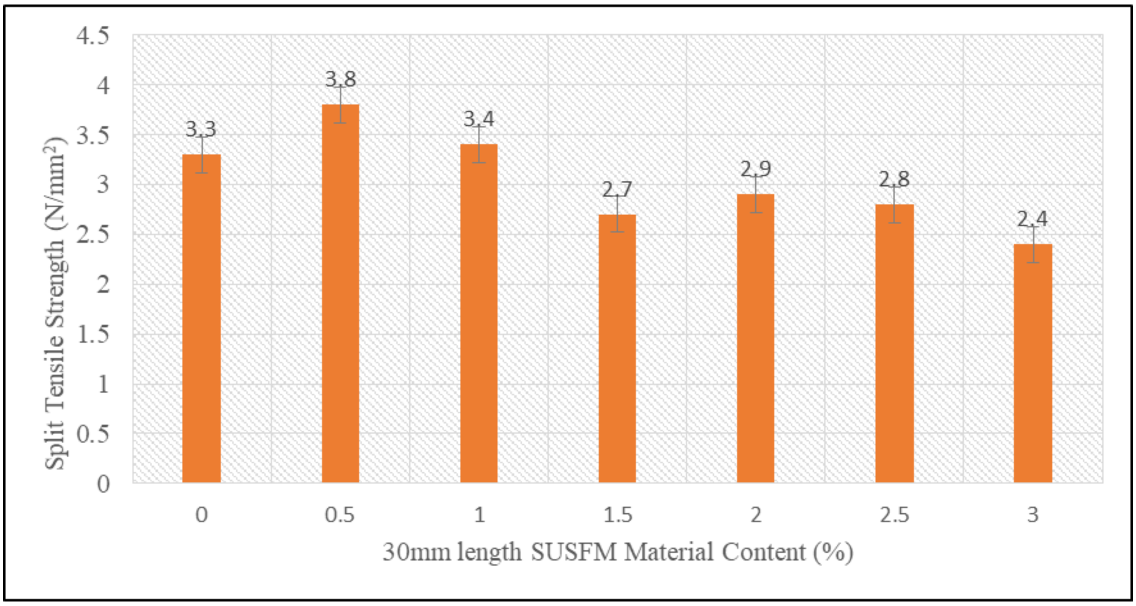

Figure 4.10: Splitting tensile strength of concrete with 30 mm length SUSFM material

Table 4.14 and Figure 4.11 shows the results of addition of 40mm length SUSFM material in concrete.it was observed that adding 0.5% of 40 mm long SUSFM material yields similar splitting tensile strength to the control sample at 3.3 N/mm^2. The strength slightly drops by 3.0% to 3.2 N/mm^2 at 1.0% dosage of 40 mm length SUSFM fiber material. However, further increasing the 40 mm long shredded SUSFM in concrete resulted in decreased split tensile strength compared to the control specimen. The lowest split tensile strength was 2.6 N/mm^2 registered with 3.0% of 40 mm length SUSFM material representing a 21.2% decrease.

Table 4.14: Splitting Tensile Strength of concrete blended with 40 mm length SUSFM material

Sample No.	SUSFM content (%)	Splitting Tensile Strength (N/mm^2)
40TE00	0	3.3
40TE05	0.5	3.3
40TE10	1.0	3.2
40TE15	1.5	2.6
40TE20	2.0	2.7
40TE25	2.5	3.0
40TE30	3.0	2.6

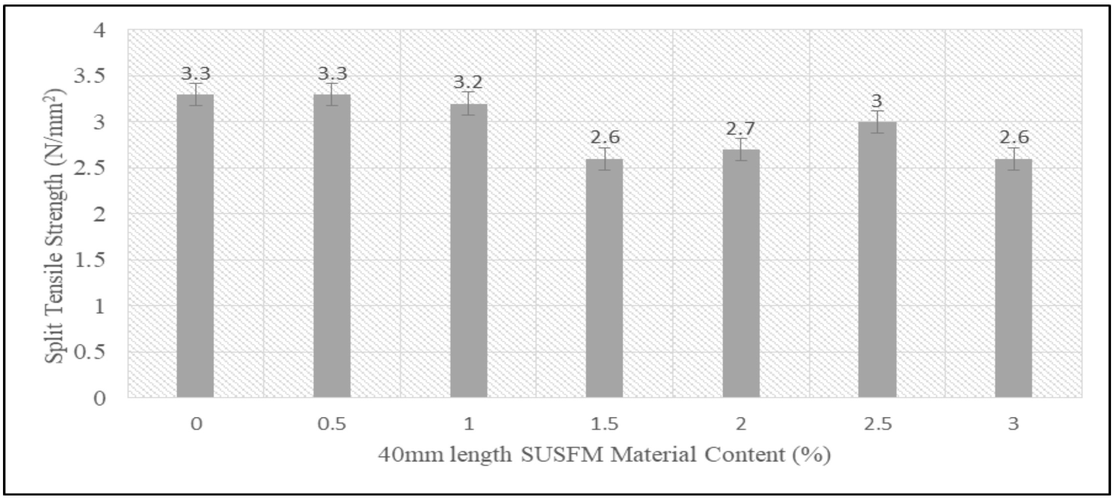

Figure 4.11: Splitting tensile strength of concrete with 40 mm length SUSFM material

A comparison of the effect of 20 mm, 30 mm, and 40 mm lengths of SUSFM material on concrete splitting tensile strength is represented in Table 4.15 and Figure 4.12. The control specimen recorded 3.3 N/mm^2 of split tensile strength. At 0.5% SUSFM fiber dosage, 30 mm length fibers recorded the highest strength of 3.8 N/mm^2, an increase of 15.2% compared to control sample. At 0.5% SUSFM fiber dosage, 20 mm length gave the highest strength of 3.0 N/mm^2 but lower than the control sample's strength of 3.3 N/mm^2 representing a decline of 9.1%. For 40mm long SUSM fibers, the highest split tensile strength was recorded as 3.3 N/mm^2 at 0.5% and 1.0% dosages. These values are similar to the values obtained for plain concrete strength.

For 20 mm length of SUSFM material, the highest split tensile strength of 3.0 N/mm^2 was recorded at a 0.5% SUSFM material dosage. This value, however, is 9.1% lower than the control specimen. In addition, the highest split tensile strength for 30 mm fiber material was 3.8 N/mm^2 at a 0.5% dosage higher than that registered for 20 mm by 26.7%. Further, the highest for 40 mm length fiber material was 3.3 N/mm^2. This value recorded was 13.2% lower than that registered by 30 mm long fibers.

All dosages ranging from 0.5% to 3.0% recorded lower split tensile strengths than the control sample for 20 mm SUSFM material fibers. However, the strengths registered were greater than design strength of 2.56 N/mm^2. For 30 mm SUSFM material fibers, 0.5% and 1.0% added SUSFM material registered split tensile strength greater than the control sample. Dosages more than 1.5% to 2.5% recorded lower split tensile strengths than the control sample but greater than design strength of 2.56 N/mm^2. At 3.0% dosage, the split tensile strength was lower than the design strength. For 40 mm SUSFM material fibers, 0.5% and 1.0% dosages registered split tensile strength similar to the control sample. Dosages more than 1.5% to 3.0% recorded lower split tensile strengths than the control sample. However, the strengths were greater than design strength of 2.56 N/mm^2.

The specimens with 0.5% and 1.0% of 30 mm long SUSFM material, and 0.5% of 40 mm length SUSFM fiber material, registered improved split tensile strength compared to the control specimen. The highest recorded split tensile strength among the different lengths of fiber material was 3.8 N/mm^2 at 0.5% of the 30 mm length fiber material. These results showed that the optimum mix giving the highest concrete splitting tensile strength was 0.5% of 30 mm long SUSFM material fibers in concrete in agreement with Yuan and Jia, (2021) who reported that optimum dosage for macro fibers between 20 mm to 70 mm long was between 0.5 to 1.0%. Further, the results obtained were in consistence with Islam and Gupta, (2016), who reported that the splitting tensile strength was greater than that of the control specimen when polypropylene fibers were blended with normal concrete up to a dosage of 0.25%. Doses greater than 0.25% registered decreased splitting tensile strength with reference to the control specimen. This also affirms the results that were obtained by (Hidaya et al., 2017).

This improvement in the splitting tensile strength may be a result of micro-cracks developing in the concrete matrix being arrested by the SUSFM fibers in the vicinity, thus preventing them from propagating. These may have caused the cracks to meander, therefore demanding more energy for the cracks to propagate and hence increasing the ultimate tensile load. Beyond 1.5% dosage, the test specimens registered reduced splitting tensile strength. This could be as a result of increased SUSFM fiber material in concrete, causing an insufficient binder matrix around the fibers to transfer stresses from the concrete to the fibers through bonding. Comparing different SUSFM material length regimes, the split tensile strength increased with an increase in the length of SUSFM material up to the optimum length of 30 mm. This observation may be attributed to longer fibers forming bridges for cracks to traverse in the matrix because of greater adhesion and friction between the fibers and concrete matrix. On the other hand, the splitting tensile strength marginally reduced beyond 1.5% SUSFM material dosage for the 20 mm, 30 mm, and 40 mm length SUSFM fiber material.

The figures 4.5, 4.6, and 4.7 indicate the tendency of the graphs to flatten from 1.5% SUSFM material dosages. This phenomenon could be associated to the fact that the range of fiber distribution is proportional to the volume of SUSFM fiber. Therefore, at lower volumes of SUSFM fibers, the dispersion is uniform and, hence, well distributed at the interfacial transition zone between the fibers and the cement matrix.

At higher volumes of SUSFM materials, the dispersion is non-uniform, clumping near the coarse aggregates (Qin et al., 2019). This reduces the capacity to transfer stresses in the concrete matrix, resulting in a marginal reduction in the strength properties of concrete.

Table 4.15: Splitting Tensile Strength of concrete blended with 20 mm, 30 mm, and 40 mm lengths of SUSFM materials

Sample No.	SUSFM content (%)	Splitting Tensile Strength for 20 mm SUSFM (N/mm^2)	Splitting Tensile Strength for 30 mm SUSFM (N/mm^2)	Splitting Tensile Strength for 40 mm SUSFM (N/mm^2)
TE00	0	3.3	3.3	3.3
TE05	0.5	3.0	3.8	3.3
TE10	1.0	2.7	3.4	3.2
TE15	1.5	2.6	2.7	2.6
TE20	2.0	2.5	2.9	2.7
TE25	2.5	2.7	2.8	3.0
TE30	3.0	2.7	2.4	2.6

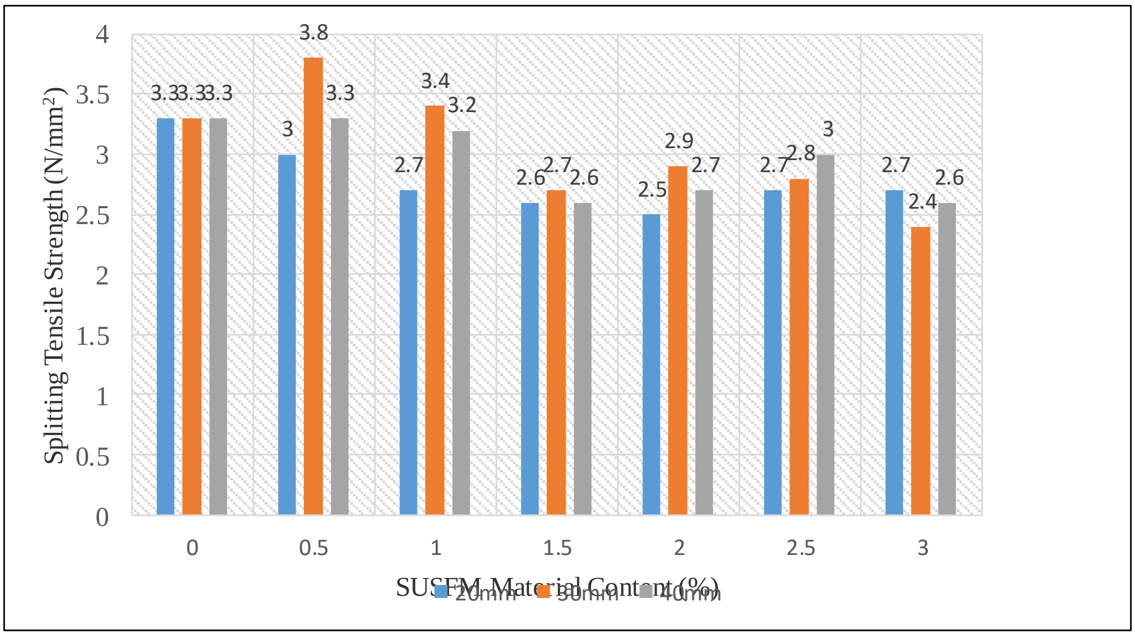

Figure 4.12: Comparative illustration of splitting tensile strength of concrete with different volumes and lengths of SUSFM material

4.3.3 Strength of Hardened Concrete (Ultrasonic Pulse Velocity)

The results of the UPV test for concrete with added 20 mm long SUSFM material are represented in Table 4.16 and Figure 4.13. It was observed that the UPV value for the control specimen was 4436 m/s. For concrete with 20 mm long SUSFM material, UPV values increased by 1.4% at 1.0% dosage to 4496 m/s, after which the values dropped off at 1.5% dosage to 4367 m/s and progressively decreased to the lowest 4011 m/s at 3.0% dosage, representing a 9.6% decrease.

Table 4.16: Ultrasonic Pulse Velocity of concrete blended with 20 mm length SUSFM material

Sample No.	SUSFM content (%)	Ultrasonic Pulse Velocity (m/s)
20UP00	0	4436
20UP05	0.5	4320
20UP10	1.0	4496
20UP15	1.5	4367
20UP20	2.0	4201
20UP25	2.5	4199
20UP30	3.0	4011

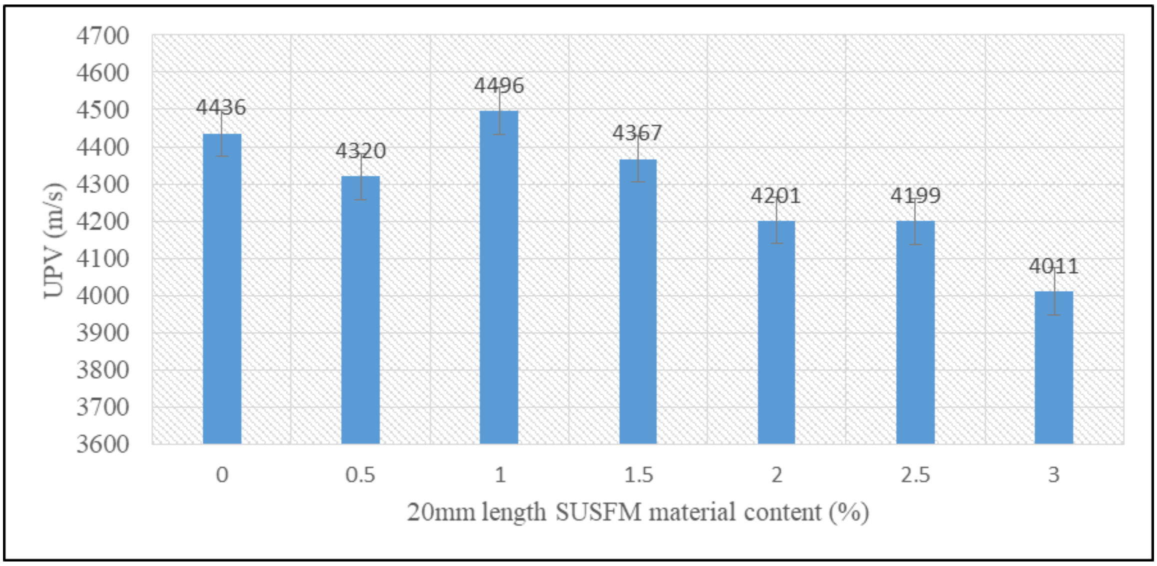

Figure 4.13: Ultrasonic Pulse Velocity of concrete with 20 mm length SUSFM material

The results of the UPV test for concrete with added 30 mm long SUSFM material are represented in Table 4.17 and Figure 4.14. It was observed that the UPV value increased from the control specimen value of 4436 m/s to 4487 m/s at 0.5% dosage representing a 1.1% increase. There was a further increase of 2.0% at 1.0% dosage to 4523 m/s and an increase of 0.3% at 1.5% to 4448 m/s. When the content of SUSFM material increased beyond 2.0%, the UPV values gradually dropped from 4271 m/s to lowest of 4152 m/s at 3.0% dosage.

Table 4.17: Ultrasonic Pulse Velocity of concrete blended with 30 mm length SUSFM materials

Sample No.	SUSFM content (%)	Ultrasonic Pulse Velocity (m/s)
30UP00	0	4436
30UP05	0.5	4487
30UP10	1.0	4523
30UP15	1.5	4448
30UP20	2.0	4271
30UP25	2.5	4353
30UP30	3.0	4152

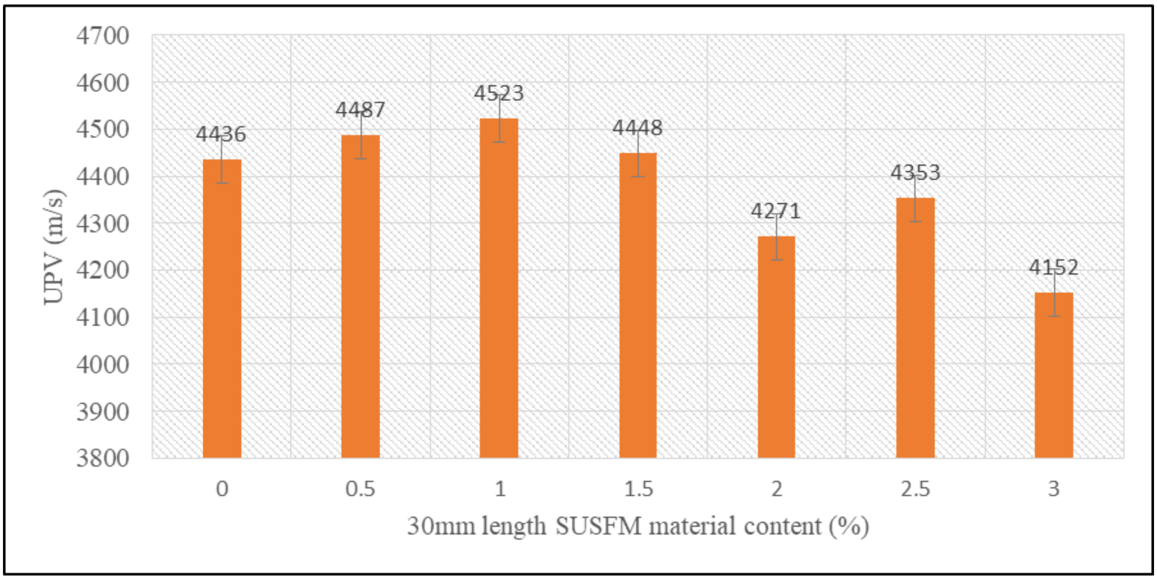

Figure 4.14: Ultrasonic Pulse Velocity of concrete with 30 mm length SUSFM material

Table 4.18 and Figure 4.15 shows the UPV results for concrete blended with 40 mm long SUSFM material. Concrete UPV values increased by from control value of 4436 m/s to 4509 m/s an equivalent of 1.7% at 0.5% dosage before starting to reduce progressively to the lowest of 4026 m/s at 3.0% SUSFM material dosage.

Table 4.18: Ultrasonic Pulse Velocity of concrete blended with 40 mm length SUSFM materials

Sample No.	SUSFM content (%)	Ultrasonic Pulse Velocity (m/s)
40UP00	0	4436
40UP05	0.5	4509
40UP10	1.0	4434
40UP15	1.5	4316
40UP20	2.0	4278
40UP25	2.5	4222
40UP30	3.0	4026

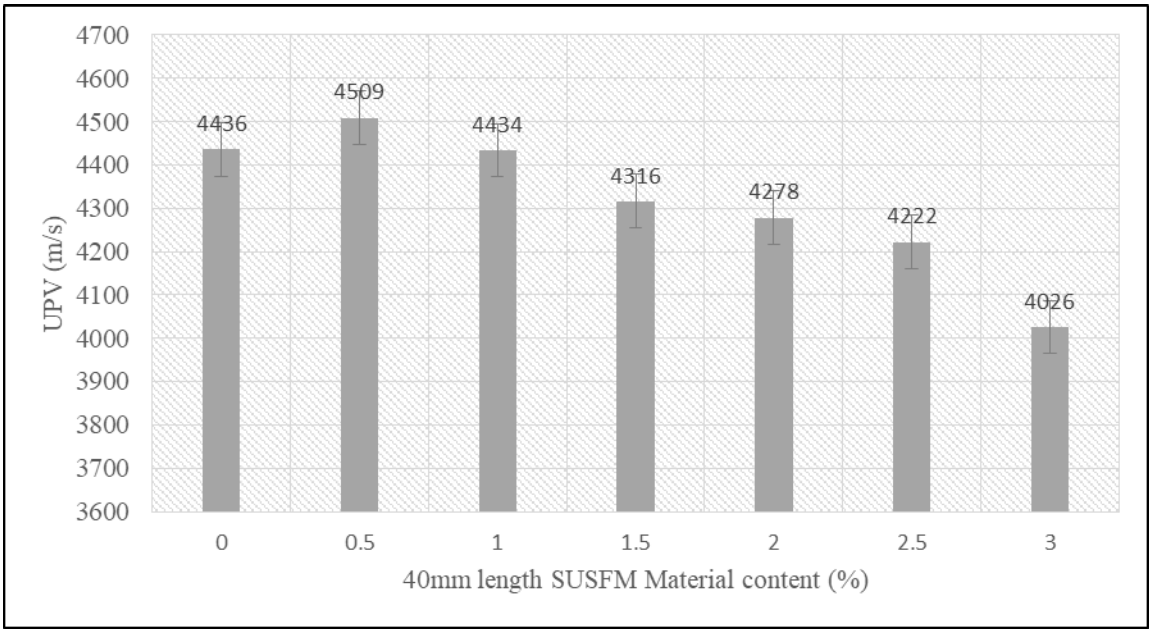

Figure 4.15: Ultrasonic Pulse Velocity of concrete with 40 mm length SUSFM material

Table 4.19 and Figure 4.16 shows a comparative illustration of the UPV of the concrete with 20 mm, 30 mm, and 40 mm lengths of SUSFM material. The UPV values for concrete with 20 mm long SUSFM material ranged between 4320 m/s and 4011 m/s. For all the dosages the UPV values were less than the control sample. However, all the values are above 4000 m/s registering “Good’’ quality concrete.

Blend concrete with 30 mm lengths of SUSFM material had values of 4487 m/s at 0.5% dosage and 4523 m/s at 1.0% dosage, and 4448 m/s at 1.5% dosage that were higher than the control sample. Beyond 2.0% the UPV values decreased from the control sample by 3.7% at 4271 m/s, at 2.5% at 4353 m/s representing 1.8%, and at 3.0% giving a UPV value of 4152 m/s. The UPV values for concrete with 30 mm long SUSFM material ranged between 4487 m/s and 4152 m/s indicating “Good’’ quality concrete. The values recorded for 30 mm SUSFM material were greater compared to the same dosage with 20 mm lengths.

For 40 mm SUSFM materials, the UPV values improved to 4509 m/s at 0.5% dosage before dropping off at 1.0% to the lowest 4026 m/s at 3.0% dosage. The UPV values for concrete with 40 mm long SUSFM material ranged between 4509 m/s and 4026 m/s indicating “Good’’ quality concrete.

It was observed that all the concrete blend with SUSFM fiber material recorded above 4000 m/s UPV values indicating “good” quality concrete (Al-Hadithi & Hilal, 2016), while concrete with an ultrasonic pulse velocity above 4500 m/s is considered “excellent” quality (Simsek et al., 2019).

The highest recorded UPV value was at 4523 m/s for 30 mm length SUSFM fibers at 1.0% dosage in concrete. Therefore, the optimum dosage to yield the highest improved concrete quality (UPV) was reported as 1.0% of the 30 mm length of SUSFM material. The optimum dosage resulted into “excellent” quality concrete at UPV value of 4523 m/s. These observation was in agreement with Yuan and Jia (2021) who reported that optimum dosage for PP macro fibers between 20 mm to 70 mm long was between 0.5 to 1.0%. These results are in consistence with those reported by Islam and Shahjalal (2021) where UPV increased at 10% PP fiber replacement and decreased with higher replacement ratios. This increased ultrasonic pulse velocity at lower contents of SUSFM fiber material indicates concrete with no voids or cracks. This was as a result of SUSFM fibers limiting the initiation and development of micro-cracks in the concrete matrix. Further, the surface of SUSFM fiber material provided frictional resistance between concrete constituents hence minimizing voids in the concrete mix. However, decrease in concrete UPV values with increase in the SUSFM material content compared to the control specimen may be attributed to a reduction in bonding between the concrete matrix and the additional SUSFM fiber materials because of increase surface area for cementious material coating.

Table 4.19: Ultrasonic Pulse Velocity of concrete blended with 20 mm, 30 mm, and 40 mm lengths of SUSFM materials

Sample No.	SUSFM content (%)	Ultrasonic Pulse Velocity for 20 mm SUSFM (N/mm^2)	Ultrasonic Pulse Velocity for 30 mm SUSFM (N/mm^2)	Ultrasonic Pulse Velocity for 40 mm SUSFM (N/mm^2)
UP00	0	4436	4436	4436
UP05	0.5	4320	4487	4509
UP10	1.0	4496	4523	4434
UP15	1.5	4367	4448	4316
UP20	2.0	4201	4271	4278
UP25	2.5	4199	4353	4222
UP30	3.0	4011	4152	4026

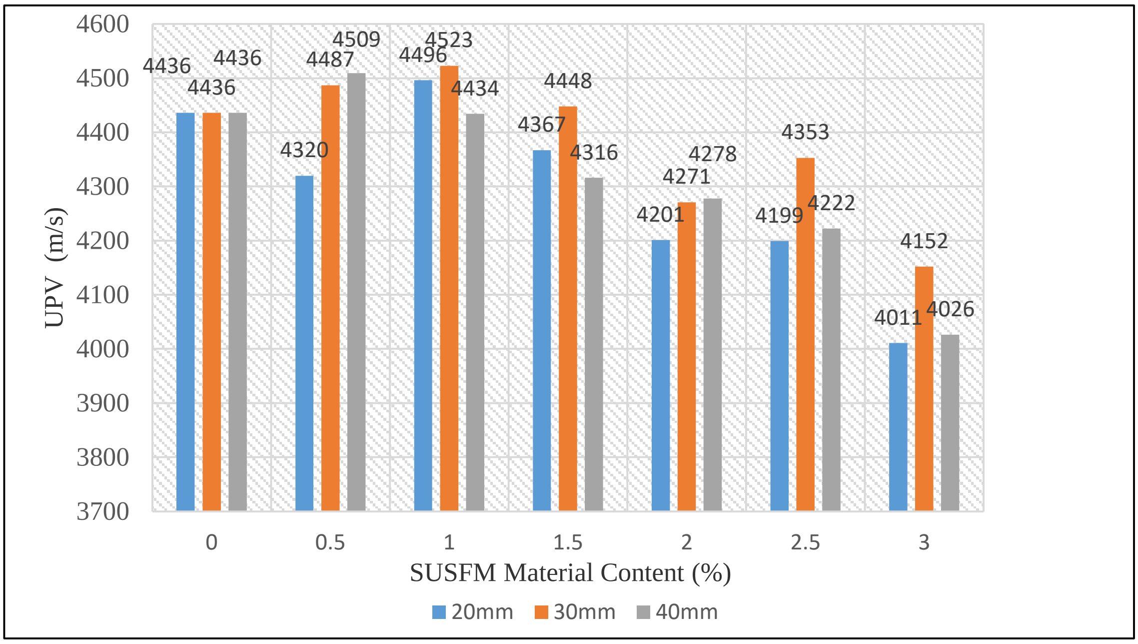

Figure 4.16: Comparative illustration of Ultrasonic Pulse Velocity of concrete with different volumes and lengths of SUSFM material

4.4 Influence of Reutilized Single-Use Surgical Face Mask Material on Concrete Durability

4.4.1 Acid Attack Resistance of Hardened Concrete

Compressive strength loss and weight loss were used in evaluating the acid attack resistance as represented in Figures 4.20 and 4.17. The results of the acid attack show that when concrete with SUSFM material is exposed to acidic conditions, the residual compressive strength decreases below the original compressive strength. The loss of compressive strength gradually increased with an increase in SUSFM fiber material content compared to control samples. The loss of compressive strength for the control sample was 9.0%. A compressive strength loss of 20.5% was recorded for the 0.5% SUSFM fiber content, gradually increasing to 38.3% for the 2.0% content, before slightly falling off to 30.7% and 32.3% at the 2.5% and 3.0% SUSFM fiber material contents, respectively. The minimum effect on compressive strength loss was observed to be 20.5% at 0.5% SUSFM fiber material content.

The results of weight loss indicated a control specimen's weight loss of 0.54%. The weight loss increased to 1.04% at 2.0% before slightly falling off to 0.8% and 0.46% at 2.5% and 3.0% SUSFM material content, respectively. The minimum effect on concrete weight loss was observed to be 0.82 at 1.0%. The increase in percentage weight loss and loss of compressive strength were attributed to the degradation of concrete that was provoked by the acid attack. Since concrete is an alkaline substance, aggressive hydrochloric acid penetrates the concrete substance and reacts with the calcium compounds contained therein to form soluble calcium salts. Leaching of these soluble salts reduces concrete volume, resulting in a reduction in the cohesion of the paste.

On the other hand, there was reduced weight loss and compressive strength at SUSFM dosages beyond 2.0%. Reduced loss of strength was attributed to reduced binder material relative to other concrete constituents as the SUSFM material increases in the concrete mix. Since Acid attack in mainly on cementious matrix, the severity of acid attack reduces as there was less binder material surface area for acid attack hence reduced production of soluble salts per volume of concrete.

Table 4.20: Compressive Strength before and after Acid attack of concrete blended with 20 mm length SUSFM materials

Sample No.	SUSFM content (%)	Residual Compressive strength (N/mm^2)	Compressive strength before Chemical attack (N/mm^2)
20CA00	0	46.5	50.1
20CA05	0.5	35.2	44.3
20CA10	1.0	30.8	39.0
20CA15	1.5	22.3	32.8
20CA20	2.0	19.3	31.3
20CA25	2.5	17.6	25.4
20CA30	3.0	17.2	25.1

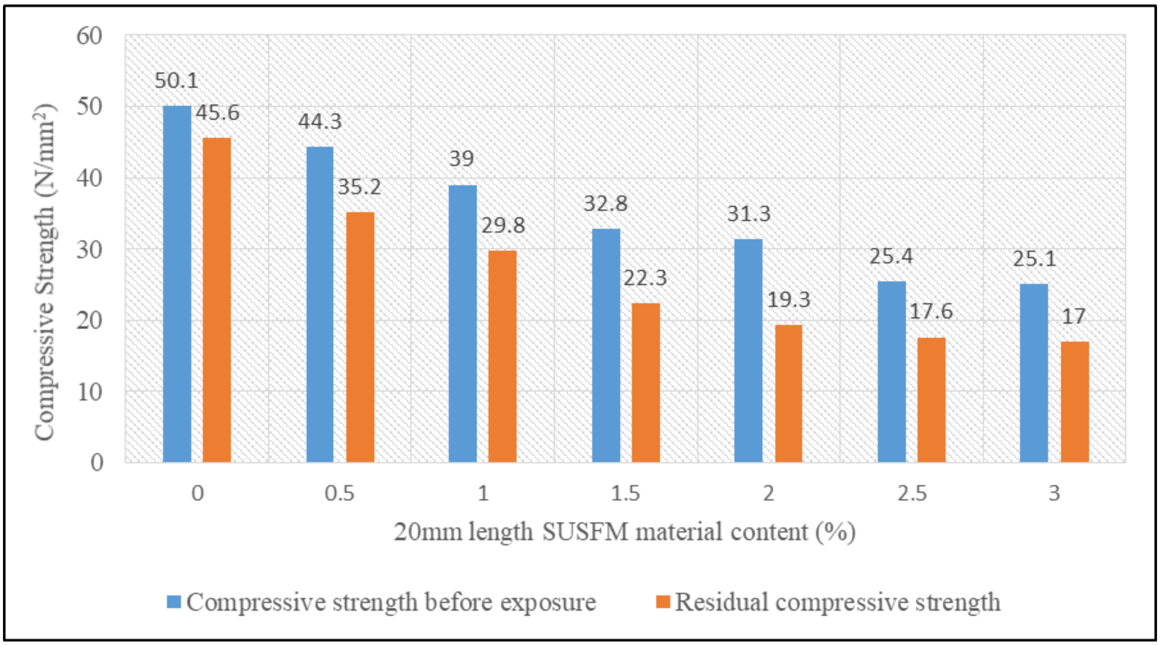

Figure 4.17: Compressive strength of concrete blended with SUSFM material before exposure and residual compressive strength after the acid attack

Table 4.21: Compressive Strength Loss of concrete blended with 20 mm length SUSFM materials

Sample No.	**SUSFM content (%)**	**Compressive Strength Loss, CSL (%)**
20CA00	0	7.2
20CA05	0.5	20.5
20CA10	1.0	21.0
20CA15	1.5	32.0
20CA20	2.0	38.3
20CA25	2.5	30.7
20CA30	3.0	31.5

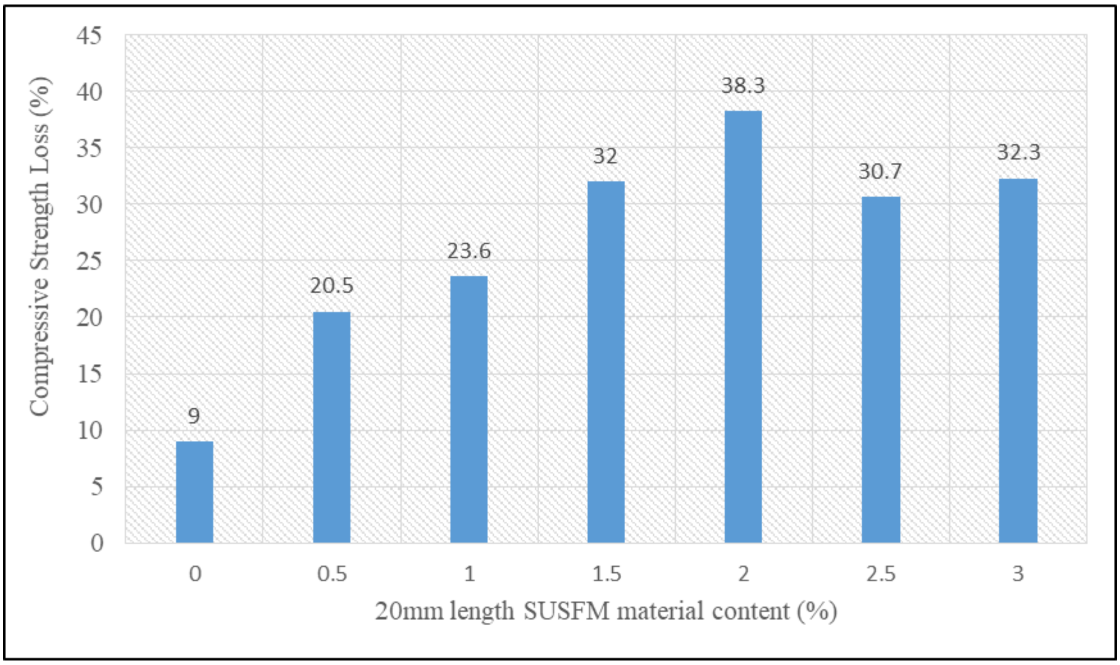

Figure 4.18: Compressive strength loss of concrete blended with SUSFM material after acid attack

Table 4.22: Weights Loss after Acid attack of concrete blended with 20 mm length SUSFM materials

Sample No.	**SUSFM content (%)**	**Average Weight Loss (%)**
20CA00	0	0.54
20CA05	0.5	0.83
20CA10	1.0	0.82
20CA15	1.5	0.95
20CA20	2.0	1.04
20CA25	2.5	0.80
20CA30	3.0	0.46

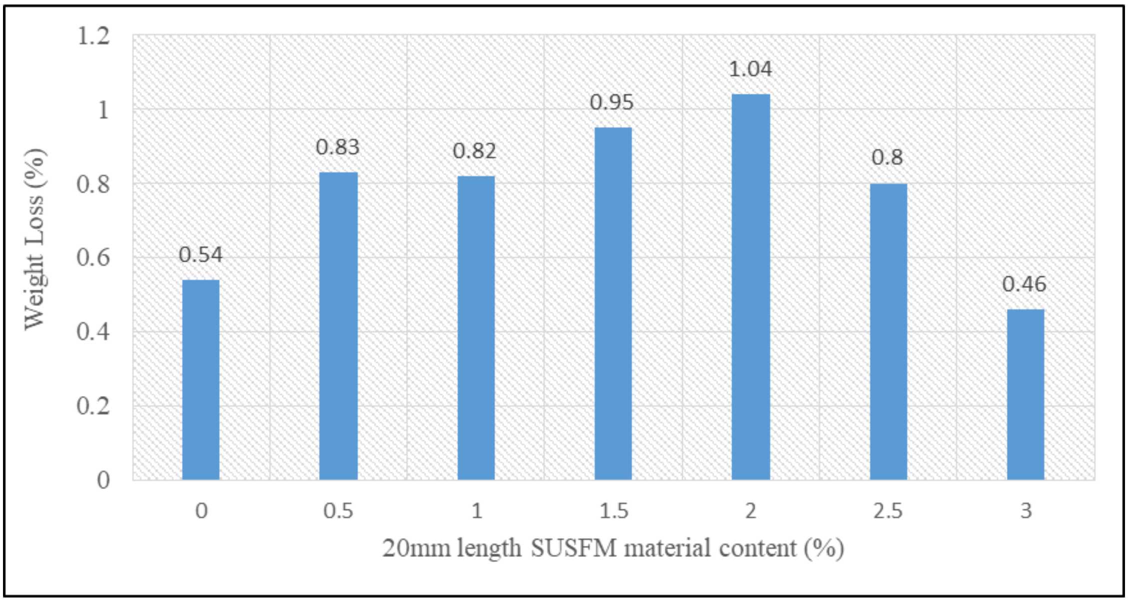

Figure 4.19: Weight loss of concrete blended with SUSFM material after acid attack

4.4.2 Abrasion Resistance of Hardened Concrete

Figure 4.19 shows the results of abrasion test on concrete blended with SUSFM fiber material. From the results, 0.05% abraded material was registered for the control concrete specimen. The percentage of abraded material decreased steadily from the control sample to a minimum value of 0.043% at 1.0% and 1.5% for SUSFM material content. A slight increase of 0.044% was reported at 2.0% and 2.5% mix regimes, while an increase of 0.045% was reported at 3.0% SUSFM fiber material content. These results were in agreement with Alaskar et al., (2021), who concluded that the highest abrasion resistance was achieved at 1.25% of the polypropylene fiber mixed in concrete. Further, Abu-Saleem et al., (2021) reported similar results with PET fiber material in concrete. The optimum SUSFM material content was 1.0% and 1.5%, which gave the highest abrasion resistance with the lowest percentage of abraded material at 0.043%. This reduction in percentage abraded material can be attributed to the bridging effect of the SUSFM fiber material and the strong bonding between the concrete matrix and the SUSFM material, resulting in a higher energy absorption capacity. Beyond 2% SUSFM material content, the percentage abraded material increases. This may be associated with the increased SUSFM fiber material in concrete that leads to development of weaker bonds between the concrete matrix and SUSFM fiber material. The slight increase in abraded material from the concrete blend could be associated with increased fiber content beyond 2.0%, the entrapped air voids in concrete increase reducing workability causing concrete finishing problems where fibers are exposed to the surface of concrete. These exposed fibers are worn out by frictional forces

Table 4.23: Abrasion of concrete blended with 20 mm length SUSFM materials

Sample No.	SUSFM content (%)	Abrasion (%)
20AB00	0	0.050
20AB05	0.5	0.047
20AB10	1.0	0.043
20AB15	1.5	0.043
20AB20	2.0	0.044
20AB25	2.5	0.044
20AB30	3.0	0.045

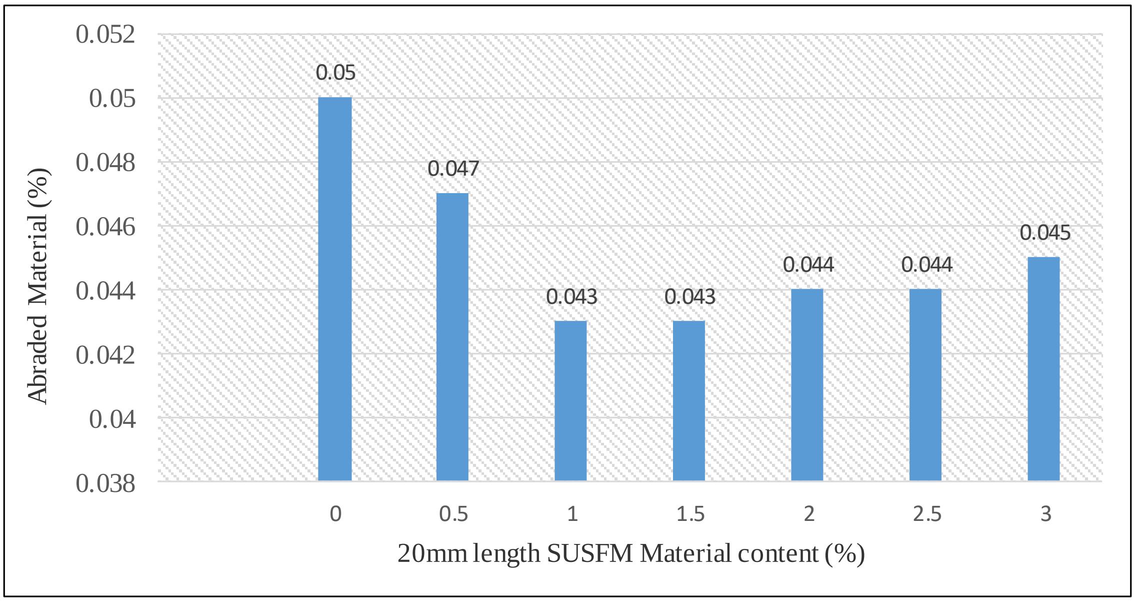

Figure 4.20: Abrasion of concrete blended with SUSFM material

CHAPTER FIVE

CONCLUSIONS AND RECOMMENDATIONS

5.1 Conclusions

i. The fine aggregate had modulus of fineness 2.8, silt content of 2.1% and specific gravity of 2.7 and the grading curves lies between the specified lower and upper limit. Coarse aggregate had water absorption of 1.92% which was less than maximum allowable of 2.3% and fineness modulus of 3.5 within the limits of 3.5-6.5. The single use surgical face mask material shredded into fibers with aspect ratios of 29, 43 and 58 was within the description of macro fibers with aspect ratios ranging between 20 mm to 60 mm. Fine aggregates, coarse aggregates and single use surgical face mask materials were suitable for use in concrete.

ii. The addition of SUSFM material to concrete reduced its density by between 1.5% and 7.7%. Workability of concrete reduced by 11.8% at 0.5% SUSFM dosage. Water absorption of concrete with SUSFM material increased from 16.9% to 70.8%. Therefore, SUSFM can be used in concrete at a 0.5% dosage without the need for plasticizer. Higher volumes may need plasticizer to aid workability.

iii. Mixing SUSFM fiber materials into concrete reduces the compressive strength of the concrete. The minimum loss was registered at a 0.5% dosage of 30 mm SUSFM length with a compressive strength of 44.9 N/mm^2 representing a 10.4% loss. However, despite the decrease in compressive strength, the strength was more than the designed characteristic strength.

    SUSFM fiber material improved the splitting tensile strength of concrete by 15.2% from 3.3 N.mm^2 to 3.8 N/mm^2 at 0.5% for 30 mm lengths. The optimum dosage of 1.0% for the 30 mm length of SUSFM fiber material incorporated in concrete marginally improved ultrasonic pulse velocity by 2.0% to UPV value of 4523 m/s from plain concrete UPV value of 4436 m/s.

SUSFM fiber material can be used in concrete to improve the splitting tensile strength of concrete by 15.2% from 3.3 $N.mm^2$ to 3.8 N/mm^2 at 0.5% for 30 mm lengths. 30 mm long SUSFM at 0.5% dosage can be used in concrete to improve split tensile strength of concrete.

iv. When SUSFM fiber materials are added to concrete and subjected to acid attack, their compressive strength loss increases from 7.2% at 0.5% dosage to high of 38.3% at 2.0%. 20 mm long SUSFM fiber materials with an aspect ratio of 29 improved abrasion resistance in concrete at 1.0% or 1.5% dosages. 20 mm SUSFM at dosage of 1.0% can be used in concrete to improve abrasion resistance of concrete.

5.2 Recommendations

5.2.1 Recommendation from study

From the findings, it is recommended that 0.5% of 30 mm long SUSFM fiber material can be added to concrete to improve split tensile strength and the UPV of concrete, while 1.0% of 20 mm long SUSFM fibers be used in concrete to improve its abrasion resistance. This is a low-carbon strategy for the safe disposal of SUSFM material generated mostly from the COVID-19 pandemic to reduce the environmental pollution threat by breaking the landfill's lifecycle.

5.2.2 Recommendation for Further Studies

It was observed from the study that shorter fibers at lower dosages improved concrete characteristics. It is therefore recommended that further research be done on the influence of SUSFM fiber materials that are shorter and at lower dosages than the sizes and dosages used in the study on concrete performance.

REFERENCES

Abbasi, S. A., Khalil, A. B., & Arslam, M. (2020). Extensive use of face masks during Covid-19 pandemic: (Micro) plastic pollution and potential health concerns in Arabian Peninsula. *Saudi Journal of Biological Sciences, 27*(12), 3181-3186.

Abdelgader, H. S., Wilde, K., El-Baden, A. S., Kurpinska, M., Moaf, F. O., & Rajab, A. M. (2019). Self-compacting grout to produce two-stage concrete. *Conference: International RILEM Symposium. Germany: Dresden*.

Abu-Saleem, M., Zhuge, Y., Hassanli, R., Ellis, M., Rahman, M., & Levett, P. (2021). Evaluation of concrete performance with different types of recycled plastic waste for kerbs application, *Construction and Building Materials*, *293*,123477.

Akshayaa, L., Brundha, M. P., & Ezhilarasan, D. (2020). Recent types and functions of face masks. *European Journal of Molecular & Clinical Medicine*, *07*(01), 1182-1188.

Alaskar, A., Alabduljabbar, H., Mohamed, A. M., Alrshoudif, F., & Alyousef, R. (2021). Abrasion and skid resistance of concrete containing waste polypropylene fibres and palm oil fuel ash as pavement material. *Construction and Building Materials*, *282,* 122681.

Al-Hadithi, A. I., & Hilal, N. N. (2016). The possibility of enhancing some properties of self- compacting concrete by adding waste plastic fibers. *Journal of Building Engineering, 8,* 20-28.

Ali, M., Wang, W., Chaudhry, N., & Geng, Y. (2017). Hospital waste management in developing countries: a mini review. *Waste Management Resources*, *35*(6), 581-592.

Arasa, F. O., Onchiri, R., & Abiero-Gariy, Z. C. (2021). Experimental investigation on the compressive strength and durability performance of modified Dry-stack hollow sandcrete blocks. *Open Access Library Journal*, *8*(12), 1-13.

Balogh, A., Farkas, B., Faragó, K., Farkas, A., Wagner, I., Vanassche, I., Verreck, G., Naggy, Z., & Marosi, G. (2015). Melt-blown and electrospun drug-loaded polymer fiber mats for dissolution enhancement: A comparative study. *Journal of Pharmaceutical Sciences*, *104*(5), 1767–1776.

Bheel, N., Awoyera, P., Aluko, O., Mahro, S., Viloria, A., & Serria, C. A. S. (2020). Sustainable composite development: Novel use of human hair as fiber in concrete. *Case Studies in Construction Materials, 13,* e00412.

Blazy, J., & Blazy, R. (2021). Polypropylene fiber reinforcement concrete and its application in creating architectural forms of public spaces. *Case Studies in Construction Materials, 14,* e00549.

Boroujeni, M., Saberian, M., & Li, J. (2021). Environmental impacts of COVID-19 on Victoria, Australia, witnessed two waves of corona virus. *Environmental Science and Pollution Research, 28,* 14182–14191.

British Standard Institution; BS EN 12350-2 (2019). *Testing Fresh Concrete: Slump Test.* London: BSI.

British Standard Institution; BS EN 12390-3 (2019). *Testing Hardened Concrete. Compressive strength test of test specimens*. London: BSI.

British Standard Institution; BS EN 12390-6 (2009). *Testing of Hardened Concrete. Tensile splitting strength of test specimens*. London: BSI.

British Standard Institution; BS EN 12390-7 (2019). *Testing of Hardened Concrete. Density of hardened concrete*. London: BSI.

British Standard Institution; BS EN 12504-4 (2004). *Testing concrete: Determination of Ultrasonic Pulse Velocity*. London: BSI.

British Standard Institution BS EN 12620:2002+A1 (2008). *Aggregates for concrete*. London: BSI.

British Standard Institution; BS EN 1881-122:2011+A1 (2020). *Testing concrete. Methods for determination of water absorption*. London: BSI.

Bogas, J. A, Gomes, M. G., & Gomes, A. (2013). Compressive strength evaluation of structural lightweight concrete by non-destructive ultrasonic pulse velocity method. *Ultrasonic*, *53*(5), 962-972.

Chandan, A, & Sharma, A. (2023). Sub-grade characteristics of flexible pavements incorporation shredded face masks in clayed soil. *Journal of Mining and Environment (JME)*, *14*(3), 789-797.

Dhawan, R., Bisht, B. M. S., Kumar, R., Kumar, S., & Dhawan, S. K. (2019). Recycling of plastic waste into tiles with reduced flammability and improved tensile strength. *Process Safety and Environment protection, 124*, 299-307.

Fadare, O. O., & Okoffo, E. D. (2020). Covid-19 Face Masks: A Potential source of microplastic fibers in the environment. *Science of the Total Environment, 737*, 140279.

Gupta, S., & Sharma, A. (2018). Human hair as a fiber material in reinforced concrete. *International Conference on Advances in Construction Materials and Structures.* India: Rooke, Uttarakhand.

Gupta, T., Sharma, R. K., & Chaudhary, S. (2015). Influence of waste tyre fibers on strength, abrasion resistance and carbonation of concrete. *Scientia Iranica, Transactions A: Civil Engineering, 22*(4), 1481-1489.

Hamzavi, I. H., Lyons, A. B., Kohli, I., Narla, S., Parks-Miller, A., Gelfand, J. M., Lim, H. W., & Ozog, D. (2020). Ultraviolet germicidal irradiation: possible method for respirator disinfection to facilitate reuse during COVID-19 pandemic. *Journal of American Academy of Dermatology*, *82*(6), 1511–1512.

Hidaya, N., Mutuku, R. N., & Mwero, J. N. (2017). Physical and mechanical experimental investigation of concrete incorporated with polyethylene terephthalate (PET) fibres. *European International Journal of Science and Technology, 6*(8), 31-41.

Hongbo, Z., Haiyun, Z., & Hongxiang, G. (2020). Characteristics of Ductility enhancement of concrete by macro polypropylene fiber. *Results in Materials, 100087*.

Iffat, S. (2015). Relation between density and compressive strength of hardened concrete. *Concrete Research Letters*, *6*(4), 182-189.

Islam, G. M. S., & Gupta, S. D. (2016). Evaluating plastic shrinkage and permeability of polypropylene fiber reinforced concrete. *International Journal of Sustainable Built Environment*, *5*(2), 345-354.

Islam, M. J., & Shajalal, M. (2021). Effect of polypropylene plastic on concrete properties as partial replacement of stone and brick aggregates. *Case Studies in Construction Materials*, *15*, e00627.

Ji, X., Chan, S. Y. N., & Feng, N. (1997). Fractal model for simulating the space-filling process of cement hydrates and fractal dimensions of pore structure of cement-based materials. *Cement and Concrete Research*, *27*(11), 1691-1699.

Kashinath, N., & Gupta, A. (2015). To study the effect of age on compressive strength of various RCC members using the rebound hammer test. *International Journal of Pure & Applied Research in Engineering and Technology, 3*(8), 208-218.

Kilmartin-Lynch, S., Saberian, M., Li, J., & Roychan, R. (2021). Preliminary evaluation of the feasibility of using polypropylene fibres from covid-19 single use face masks to improve mechanical properties of concrete. *Journal of Cleaner Production, 296*, 126460.

Kilmartin-Lynch, S., Roychan, R., Saberian, M., Li, J., Zhang, G., & Setunge, S. (2022). A sustainable approach on the utilization of COVID-19 plastic based isolation gowns in structural concrete. *Case Studies in Construction Materials, 1*, e01408.

Kim, M., Lee, B., Kim, H., Kim, S., & Kim, K. (2017). Crack properties of press concrete for varying types of fiber reinforcement. *Advanced Composites Letters, 26*(3), 68-72.

Kurup, A. R., & Kumar, K. S. (2017). Novel fibrous concrete mixture made from recycled PVC fibres from electronic waste. *Journal of Hazardous, Toxic, and Radioactive Waste, 21*(2), 04016020

Konin, A. (2011). Effect of plastic waste content on physico-mechanical properties of flexible pavement. *International Journal of Civil and Structural Engineering, 2*(1), 0976-4399

Li, N., Jin, Z., Long, G., Chen, L., Fu, Q., Yu, Y., Zhang, X., & Xiang, C. (2021). Impact resistance of steel fiber-reinforced self-compacting concrete (SCC) at high strain rates. *Journal of Building Engineering, 38*, 102212.

Liu, Y., Wang, L., Cao, K., & Sun, L. (2021). Review on durability of polypropylene Fibre-Reinforced concrete. *Advances in Civil Engineering*, 6652077.

Madhavi, T. C., Raju, L. S., & Mathur, D. (2014). Polypropylene fiber reinforced concrete - A Review. *International Journal of Emerging Technology and Advanced Engineering*, *4*(4), 114-119.

Malagavelli, V., & Paturu, N. R. (2011). Strength characteristics of concrete using solid waste an experimental investigation. *International Journal of Earth Sciences and Engineering, 04*(06), 937-940.

Malek, M., Jackowski, M., Lasica, W., & Kadela, M. (2020). Characteristics of recycled polypropylene fibres as an addition to concrete fabrication based on Portland cement. *Materials, 13*(8), 1827.

Meddah, M. S., & Bencheikh, M. (2009). Properties of concrete reinforced with different kinds of industrial waste fiber materials. *Construction and Building Materials, 23*(10), 3196-3205.

Memon, I. A., Jhatial, A. A., Muhammad S. S., & Zahid, T. L. (2018). Influence of fiber length on behavior of polypropylene fiber reinforced cement concrete. *Civil Engineering Journal, 4*(9), 2124-2131.

Merin, K., Elson, J., & Bybin, P. (2014). A Study on the influence of mineral admixtures in cementitious system containing chemical admixtures. *International Journal of Engineering Research and Development, 10*(3), 76-82.

Mohammadhosseini, H., Awal, A. S. M., & Yatim, J. B. M. (2017). The impact resistance and mechanical properties of concrete reinforced with waste poly-propylene carpet fibers. *Construction and Building Materials, 143*, 147-157.

Mohod, M. V. (2015). Performance of polypropylene fiber reinforced concrete. *Journal of Mechanical and Civil Engineering, 12*(1), 28-36.

Naaman, A. E. (2003). Engineered steel fibers with optimal properties for reinforcement of cement composites. *Journal of Advanced Concrete Technology*, *1*(3), 241–252.

Nakov, D., Markovski, G., Arangjelovski, T., & Mark, T. L. (2017). Experimental and analytical analysis of creep of steel fibre reinforced concrete. *Periodica Polytechnic Civil Engineering, 11184*.

NEMA, Kenya (2020). The *National guidelines for the management of COVID-19 waste* (pp. 4-9).

Neville, A. M. (2000). *Properties of Concrete* (4th ed.). England: Longman.

Nili, M., & Afroughsabet, V. (2010). The effects of silica fume and polypropylene fibers on the impact resistance and mechanical properties of concrete. *Construction and Building Materials, 24*(6), 927-933.

Nibudey, R. N., Nagarnaik, P. B., Parbat, D. K., & Pande, A. M. (2014). Compressive strength and sorptivity properties of PET fiber reinforced concrete. *International Journal of Advances in Engineering and Technology*, *7*(4), 1206-1216.

Noor, N. M., Xiang-ONG, J., Noh, H. M., Abdul Hamid, N. A., Kuzaiman, S., & Ali, A. (2010). Compressive strength, flexural strength and water absorption of concrete containing palm oil kernel shell. *Materials Science and Engineering, 271*, 012073.

Nzediegwu, C., & Chang, S. X. (2020). Improper solid waste management increases potential for COVID-19 spread in developing countries. *Resources, Conservation and Recycling, 161*, 104947.

Pakravan, H. R., & Ozbakkaloglu, T. (2019). Synthetic fibers for cementious composites: a critical and in-depth review of recent advances. *Construction and Building Materials, 207*, 491-518

Pandya, J. M., & Purochit B. M. (2014). Experimental study on the mechanical properties of concrete incorporating PET fibers. *International Journal for Scientific Research & Development*, *2*(09), 43-45

Prata, J. C., Silvia, A. L. P., Walker, T. R., Duarte, A. C., & Rocha-Santos, T. (2020). COVID-19 pandemic repercussions on the use and management of plastics. *Environmental Science & Technology, 54*(13), 7760-7765.

Qasim, M. F., Abbas, Z. K., & Abed, S.K. (2021). Producing green concrete with plastic waste and nano silica sand. *Engineering, Technology & Applied Science Research*, *11*(6), 7932-7937.

Qin, Y., Wu, H., & Zheng, Y., Wang, W., & Yi, Z. (2019). Microscopic texture of polypropylene Fibre- Reinforced concrete with x-ray computed tomography. *Advances in Civil* E*ngineering, 2019, 2386590.*

Rao, H. S., Somasekharaiah, H. M., & Ghorpade V. G. (2012). Residual compressive strength of fly ash based glass fiber reinforced high performance concrete subjected to acid attack. *International Journal of Engineering, Science and Technology*, *4*(1), 71-80.

Ravinkumar, A. G., & Manjunath, M. (2015). Investigation on the waste plastic fiber reinforced concrete using manufactured sand as fine aggregate. *International Journal of Innovative Technology and Exploring Engineering*, *5*(1), 21-23.

Reju, R., & Jacob, G. J. (2012). Investigations on the chemical durability properties of Ultra High Performance Fiber Reinforced Concrete. *2012 International Conference on Green Technologies* (pp. 181-185). India: Trivandrum.

Saberian, M., Li J., Kilmartin, S., & Boroujeni, M. (2021). Repurposing of Covid-19 single use face masks for pavement base/subbase. *Science of Total Environment*, *769*, 145527.

Salahaldeen, A. S., & Al-Hadithi, A. I. (2022). The effect of adding Expanded Polystyrene Beads (EPS) on hardened properties of concrete. *Engineering, Technology & Applied Science Research, 12*(6), 9692-9696.

Salunke, S. P. (2017). Comparative study of fiber reinforced concrete and nominal concrete. *International Journal for Scientific Research & Development, 5*(10), 102-105.

Sharma, P., & Jha, A. K. (2019). An experimental investigation of fiber reinforced concrete using waste polymer fiber. *International Journal of Scientific Research in Civil Engineering, 3*(1), 23-28.

Semanda, J., Mutuku, R. N., & Kaluli, J. W. (2014). The effect of cement-waste mixes on the physical and strength properties of floor tiles. *European International Journal of Science and Technology, 3*(9), 32-43.

Senathirajah, K., Attwood, S., Bhagwat, G., Carbery, M., Wilson, S., & Palanisami, T. (2021). Estimation of the mass of microplastics ingested - A pivotal first step towards human health risk assessment. *Journal of Hazardous Materials, 404*, 124004.

Sideris, K. K., & Manita, P. (2013). Residual mechanical characteristics and spalling resistance of fibre reinforced self compacting concretes exposed to elevated temperatures. *Construction and Building Materials, 41*, 296-302.

Silva, A. L. P., Prata, J. C., Walker, T. R., Duarte, A. C., Ouyang, W., Barcelo, D., & Rocha Santos, T. (2021). Increased pollution due to COVID-19 Pandemic: challenges and recommendations. *Chemical Engineering Journal, 405*, 126683.

Simsek, B., Uygunoglu, T., Korucu, H., & Kocakerim, M. M. (2019). 11-Performance of Diocyl Terephthalate concrete. *Woodhead Publishing* *in Civil and Structural Engineering- Use of Recycled Plastics in Eco-Efficient Concrete,* 249-267.

Taherkhani, H. (2014). An investigation on the properties of the concrete containing waste PET fibers. *International Journal of Science and Engineering Investigations, 3*(27), 37-43.

Tavakoli, H. R., Omran, O. L., Shiade, M. F., & Kutanei, S. S. (2019). Prediction of combined effects of fibers and nano silica on mechanical properties of self compacting concrete using artificial neural network. *Latin American Journal of Solids and Structures, 11*, 1906-1923.

Vodounon, N., Kanali, C., & Mwero, J. (2018). Compressive and flexural strengths of cement stabilized earth bricks reinforced with treated and untreated pineapple leaves fibers. *Open Journal of Composite Materials, 8*(4), 145-160.

Wang, G., Li, J., Saberian, M., Rahat, H. H., Massarra, C., Buckhalter, C., Farrington J., Collins T., & Johnson, J. (2022). Use of COVID -19 Single-Use face masks to improve the rutting resistance of asphalt pavement. *Science of Total Environment, 826*, 154118.

Wang, Z. L., Wu, J., & Wang, J. G. (2010). Experimental and numerical analysis on effect of fiber aspect ratio on mechanical properties of SRFC. *Construction and Building Materials*, *24*(4), 559-565.

Xiang, Y., Song, Q., & Gu, W. (2020). Decontamination of surgical face masks and N95 respirators by dry heat pasteurization for one hour at 70°C. *American Journal of Infection Control, 48*(8), 880–882.

Xu, H., Shao, Z., Wang, Z., Cai, L., Li, Z., Jin, H., & Chen, T. (2020). Experimental study on mechanical properties of fiber reinforced concrete: Effect of cellulose fiber, polyvinyl alcohol fiber and polyolefin fiber. *Construction and Building Materials, 261*, 120610.

Yasar, E., Atis, C. D., Kilic, A., & Gulsen, H. (2003). Strength properties of lightweight concrete made with basaltic pumice and fly ash. *Materials Letters*, *57*(15), 2267-2270.

Yuan, Z., & Jia, Y. (2021). Mechanical properties and microstructure of glass fiber and polypropylene fiber reinforced concrete: An experimental study. *Construction and Building Materials, 266*, 121048.

Zhang, S. P., & Zong, L. (2014). Evaluation of relationship between water absorption and durability of concrete materials. *Advances in Material Science and Engineering*, *2014,* 650373.

Zhu, J., Saberian, M., Perera S. T. A. M., Roychand, R., Li, J., & Wang, G. (2022). Reusing COVID-19 disposable nitrile gloves to improve the mechanical properties of expansive clay subgrade: an innovative medical waste solution. *Journal of Cleaner Production*, *375*, 134086.

APPENDICES

Appendix I: Fine and Coarse Aggregates

Table 1-1: Particle size distribution of Fine aggregates sample 1 (930g)

Sieve size	Retained material weight (g)	Cum. retained material weight (g)	% Cumulative retained material	% Passing	Lower limit	Upper limit
5.0	0	0	0	100	89	100
2.36	72	72	7.7	92.3	60	100
1.0	231	303	32.6	67.4	30	100
0.6	281	584	62.8	37.2	15	100
0.3	252	836	89.9	10.1	5	70
0.15	76	912	98.1	1.9	0	15
Pan	16	928				

Table 1-2: Particle size distribution of Fine aggregates sample 2 (952g)

Sieve size	Retained material weight (g)	Cum. retained material weight (g)	% Cumulative retained material	% Passing	Lower limit	Upper limit
5.0	0	0	0	100	89	100
2.36	59	59	6.2	93.8	60	100
1.0	216	275	28.9	71.1	30	100
0.6	278	553	58.1	41.9	15	100
0.3	284	837	87.9	12.1	5	70
0.15	93	930	97.7	2.3	0	15
Pan	21	951				

Table 1-3: Particle size distribution of Fine aggregates sample 3 (912g)

Sieve size	Retained material weight (g)	Cumulative retained material weight (g)	% cumulative retained material	% passing	Lower limit	Upper limit
5.0	0	0	0	100	89	100
2.36	58	58	6.4	93.6	60	100
1.0	211	269	29.5	70.5	30	100
0.6	262	531	58.2	41.8	15	100
0.3	269	800	87.7	12.3	5	70
0.15	90	890	97.6	2.4	0	15
Pan	22	912				

Table 1-4: Fineness Modulus (FM) of fine aggregates

Sample	Cumulative coarse (g)	Modulus Fineness
1	290.5	2.9
2	278.8	2.8
3	279.4	2.8
Average FM		2.8

Table 1-5: Bulk Density of fine aggregates

Sample	Container weight W_1 (g)	Container +sand weight, W_2 (g)	Container+ water, W_3 (g)	Sand weight, W_4 (g)	Water weight, W_5 (g)	Bulk density (kg/m^3)
1	2997	6966	5622	3969	2625	1512
2	2997	6963	5622	3966	2625	1511
3	2997	6955	5622	3958	2625	1508
Average Bulky Density						1510

Table 1-6: Silt Content of fine aggregates

Sample	Sample weight (g)	Fine content (g)	Silt content (%)
1	930	16	1.7
2	952	21	2.2
3	912	22	2.4
Average Silt Content			2.1

Table 1-7: Specific gravity of fine aggregates

Sample	Weight of SGB, W_1 (g)	Weight of SGB + sand, W_2 (g)	Weight of SGB + sand + water, W_3 (g)	Weight of SGB + distilled water, W_4 (g)	Weight of sand, W_5 (g)	Specific gravity
1	681.9	1182.0	1965.0	1654.0	500	2.65
2	681.9	1181.6	1966.4	1654.0	500	2.67
3	681.9	1181.5	1966.0	1654.0	500	2.66
Average Specific Gravity						2.66

Table 1-8: Water Absorption of fine aggregates

Sample	Mass of fine aggregate material, W_1 (g)	Mass of fine aggregate oven dry, W_2 (g)	Water absorption (%)
1	992	970	2.3
2	978	958	2.1
3	979	957	2.3
Average Water Absorption			2.2

Table 1-9: Particle size distribution of coarse aggregate sample 1 (1037g)

Sieve size	Retained material weight (g)	Cum. Retained material weight (g)	% Cum. Retained material	% passing
28	0	0	0	100
20	20	20	1.9	98.1
14	502	522	50.3	49.7
10	469	991	95.6	4.4
6.3	33	1024	98.7	1.3
4.75	3	1027	99.0	
Pan	10	1037		

Table 1-10: Particle size distribution of coarse aggregate Sample 2 (1001g)

Sieve size	Retained material weight (g)	Cum. Retained material weight (g)	% Cum. Retained material	% passing
28	0	0	0	100
20	57	57	5.7	94.3
14	469	526	52.7	47.3
10	438	964	96.5	3.5
6.3	25	989	99.0	1.0
4.75	2	991	99.2	0.8
Pan	8	999		

Table 1-11: Particle size distribution of coarse aggregate Sample 3 (1001g)

Sieve size	Retained material weight (g)	Cum. Retained material weight (g)	% Cum. Retained material	% passing
28	0	0	0	100
20	39	39	3.9	96.1
14	450	489	48.9	51.1
10	473	962	96.1	3.9
6.3	29	991	99.0	1.0
4.75	1	992	99.1	0.9
Pan	9	1001		

Table 1-12: Fineness Modulus of coarse aggregate

Sample	Cumulative coarse (g)	Modulus Fineness
1	345.5	3.46
2	353.1	3.53
3	347.0	3.47
Average Fineness Modulus		3.5

Table 1-13: Flakiness Index of coarse aggregate

Sample	Total pass material weight (g)	Flakiness Index (FI)
1	135	13.62
2	191	19.33
3	168	16.41
Average Flakiness Index		16.45

Table 1-14: Water Absorption of coarse aggregate

Sample	Mass of coarse aggregate material, W_1 (g)	Mass of coarse aggregate oven dry, W_2 (g)	Water absorption (%)
1	995	974	2.16
2	995	977	1.84
3	977	960	1.77
Average Water Absorption			1.92

Table 1-15: Bulk Density of coarse aggregate

Sample	Container weight, W_1 (g)	Container +coarse aggregate weight, W_2 (g)	Container + water weight, W_3 (g)	Coarse aggregate weight, W_4 (g)	Water weight, W_5 (g)	Bulk density (kg/m^3)
1	2997	6717	5622	3720	2625	1417.1
2	2997	6663	5622	3666	2625	1396.6
3	2997	6620	5622	3623	2625	1380.2
Average Bulky Density						1398

Appendix II: Concrete Mix Design

Concrete Mix Design

Characteristic strength = 30 N/mm^2

Target strength, $F_m = F_c + KS$

F_c = specific characteristic strength

KS = the margin

$KS = s\,k$

Where,

s = standard deviation

k = constant

Constant, k is derived from the normal distribution curves of concrete strength which reduces as defective increases

k for 1% defective = 2.33

k for 2.5% defective = 1.96

k for 5.0% defective = 1.64

k for 10.0% defective = 1.28

Mix design based on 2.5% proportion of defective level

Therefore k = 1.96

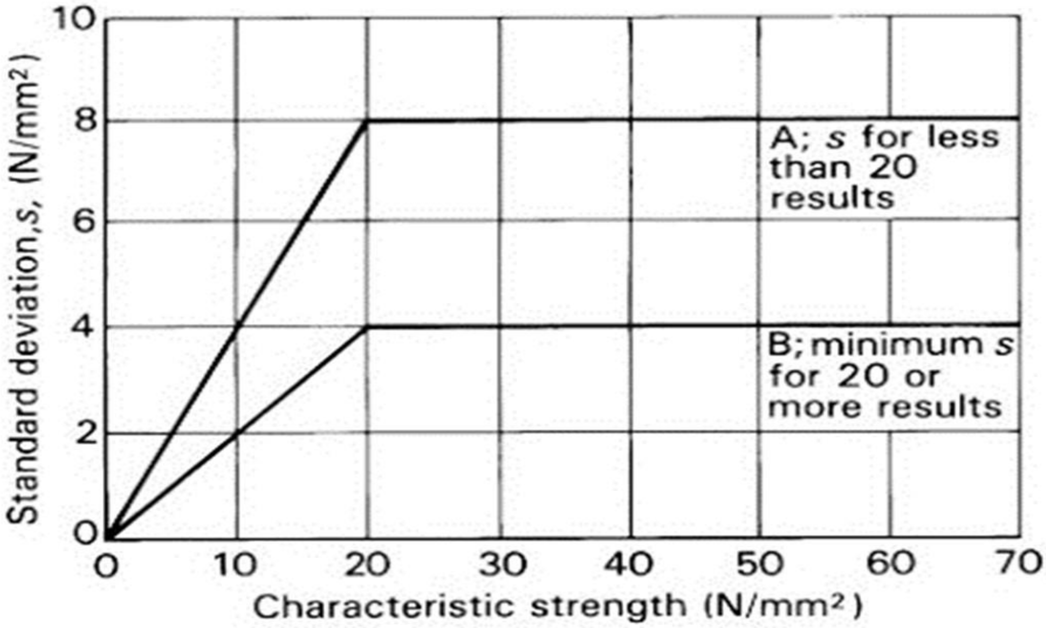

Figure 2-1: Relationship between standard deviation and characteristic strength

From Figure 2-1, the characteristic strength of 30N/mm^2 and for less than 20 results, the standard deviation, s = 8 N/mm^2

Therefore, $KS = s\ k$

$= 8 \times 1.96$

$= 15.68$

Hence target mean strength, F_m $= F_c + KS$

$= 30 + 15.68$

$= 45.68$

$= 46$ N/mm^2

Water cement ratio

From Table 2-1 below, the crushed coarse aggregate of maximum size 20 mm, cement class 42.5, the approximate compressive strength corresponding to free water cement ratio of 0.5 at 28 days = 49 N/mm^2.

Table 2-1: Approximate compressive strength (N/mm²) of concrete mixes made with

Cement strength class	Type of coarse aggregate	Compressive strengths (N/mm²) Age (days) 3	7	28	91
42.5	Uncrushed	22	30	42	49
	Crushed	27	36	49	56
52.5	Uncrushed	29	37	48	54
	Crushed	34	43	55	61

Throughout this publication concrete strength is expressed in the units N/mm^2.
1 N/mm^2 = 1 MN/m^2 = 1 MPa. (N = newton; Pa = pascal.)

free water/cement ratio of 0.5

Determined free water cement ratio from Figure 2-2. Using strength value 49 N/mm^2 and plotting a curve from that point parallel to the printed curve till intersection with horizontal line passing through ordinate indicating the target strength. This gave free water cement ratio of 0.52.

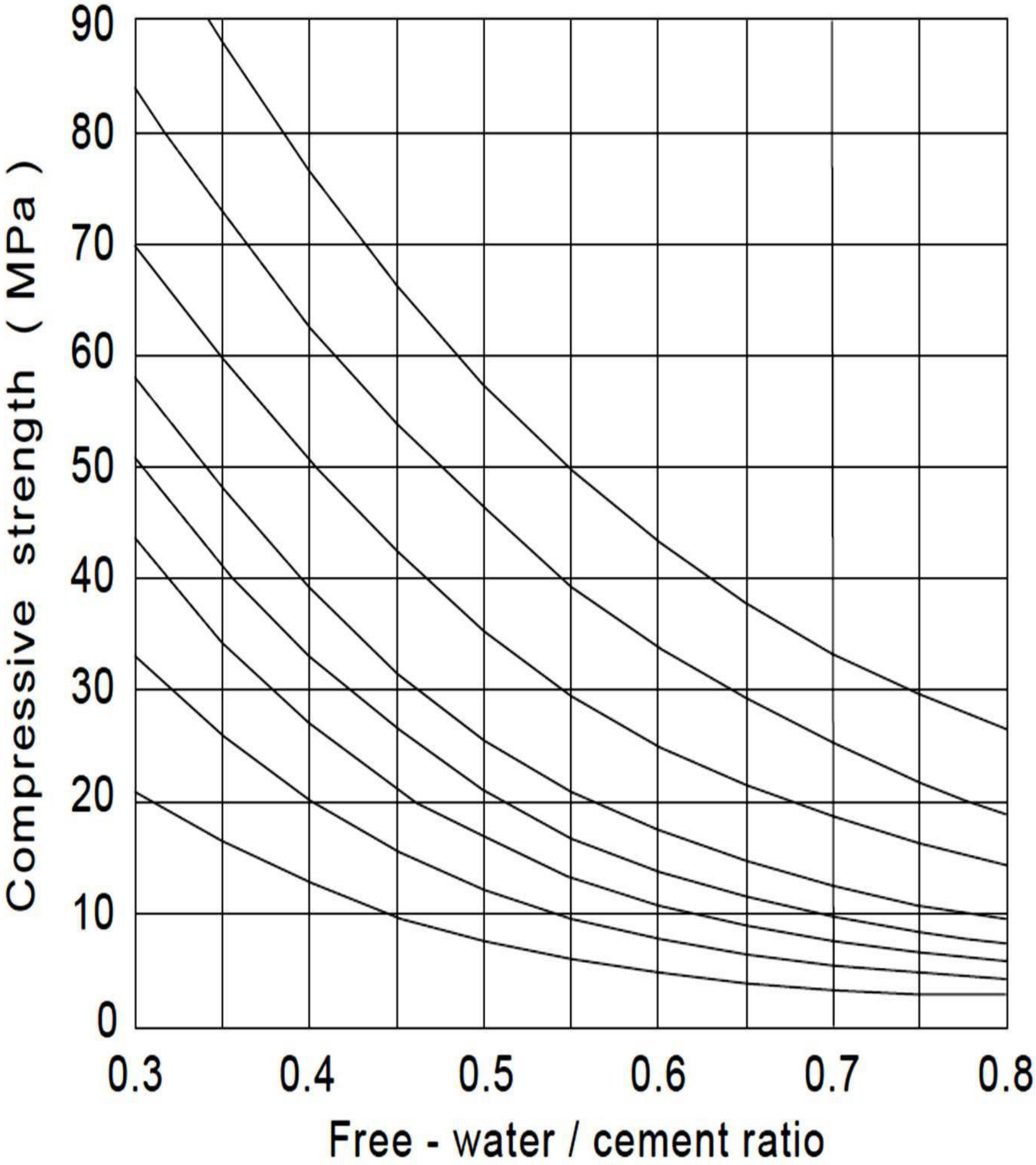

Figure 2-2: Relationship between compressive strength and free-water/cement ratio

Using table 2-2 below, free water content with 20 mm maximum size of crushed coarse aggregate with slump of 30-60 mm, the free water content was found to be 210 kg/m^3

Table 2-2: Approximate free-water contents (kg/m³) required to give various levels of workability

Slump (mm)		0–10	10–30	30–60	60–180
Vebe time (s)		>12	6–12	3–6	0–3
Maximum size of aggregate (mm)	Type of aggregate				
10	Uncrushed	150	180	205	225
	Crushed	180	205	230	250
20	Uncrushed	135	160	180	195
	Crushed	170	190	210	225
40	Uncrushed	115	140	160	175
	Crushed	155	175	190	205

Cement content

Cement content = free water content/ free WC ratio

= 210/0.52

= 404 kg

Aggregate content

Using Figure 2-3, with water content of 210 kg/m^3, and specific gravity of 2.7, the wet density was found to be 2400 kg/m^3

Total aggregate content = wet density – water content- cement content

= 2400 – 210 - 404

= 1786 kg/m^3

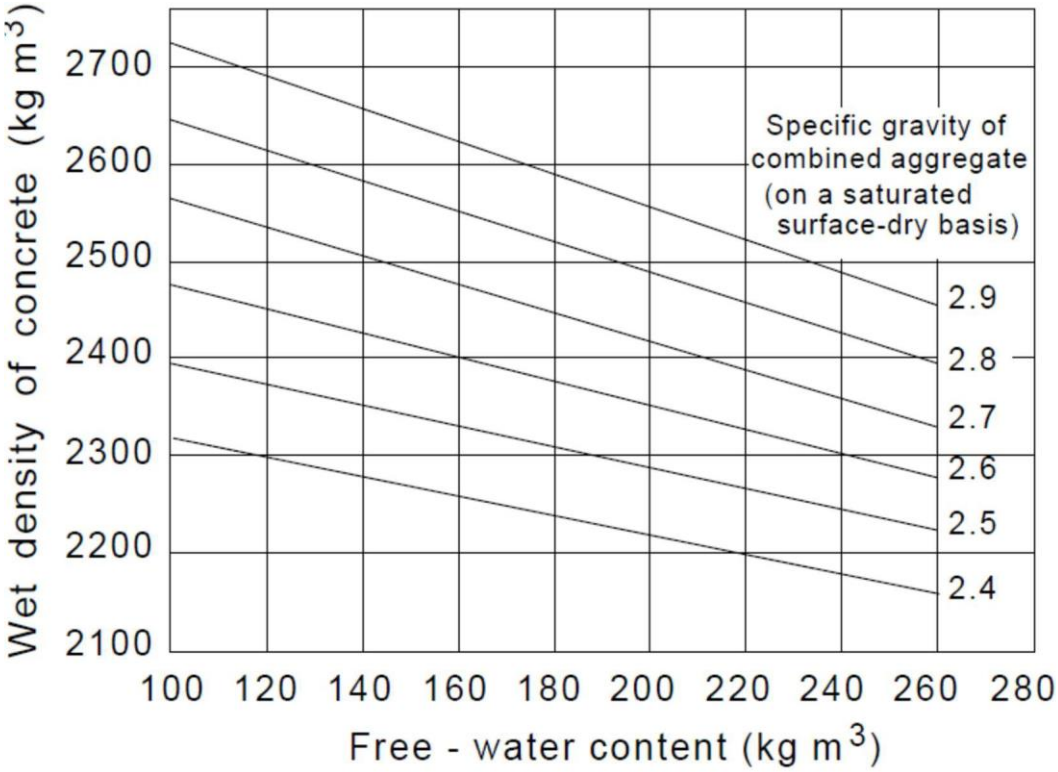

Figure 2 Wet density of fully compacted concrete

Figure 2-3: Estimated wet density of fully compacted concrete

Proportion of fine aggregates was determined using the water cement ratio of 0.52, % passing 600 mm micron sieve of 40.3%, slump of 30-60 mm, 20 mm maximum coarse aggregate, and Figure 2-4. The fine aggregate proportion was determined as 38% of the total aggregates in content.

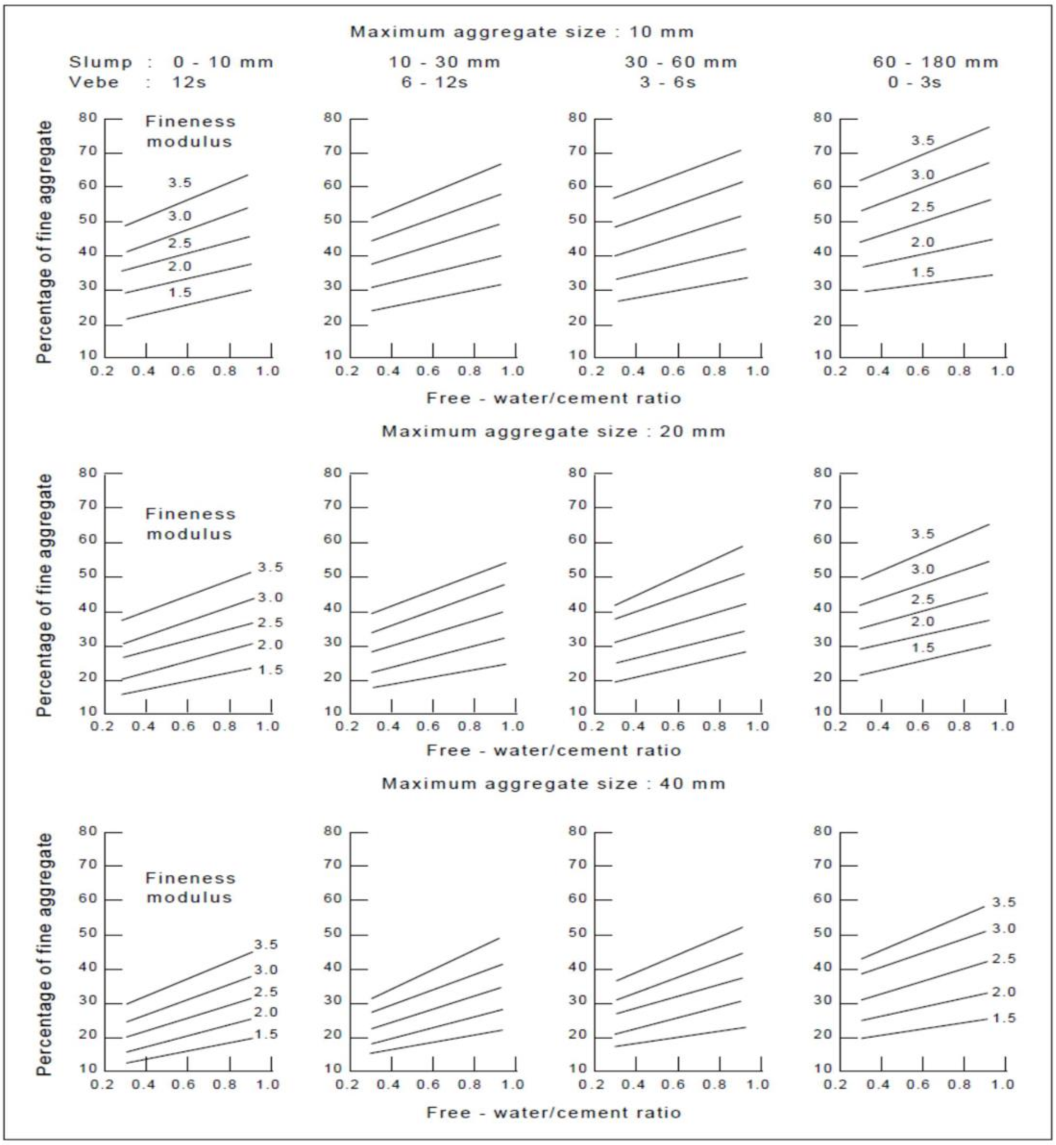

Figure 3 Proportions of fine aggregate determined from Fineness Modulus

Figure 2-4: Recommended proportion of fine aggregate according to percentage passing a 600micron sieve for maximum aggregate size of 10 mm, 20 mm and 40 mm.

Fine aggregate content = Total aggregate content x % proportion of fine aggregates

= 1786*38/100

= 679 kg

Coarse aggregates content = 2400 – 210 – 404 - 679

=1107 kg

In proportion of 20 mm: 10mm of 2:1

20mm aggregates = 738 kg

10mm aggregates = 369 kg

Proportions

Per 1.0 m^3 concrete

Cement = 404 kg

Water =210 kg

Fine aggregate = 679 kg

Coarse aggregate = 1,107 kg

Table 2-3: Design Mix proportion per cubic metre of concrete

Batch ID	Cement (kg)	Water (kg)	Fine Aggregate (kg)	Coarse Aggregate (kg)	SUSFM fibers
00	404	210	679	1107	0 %
05	404	210	679	1107	0.5%
10	404	210	679	1107	1.0%
15	404	210	679	1107	1.5%
20	404	210	679	1107	2.0%
25	404	210	679	1107	2.5%
30	404	210	679	1107	3.0%

Appendix III: Test Results

Table 3-1: Workability test results

Sample No.	SUSFM content (% cement weight)	Sample	Slump (mm)	Average Slump (mm)
20WO00	0	1	55	51
		2	49	
		3	50	
20WO05	0.5	1	43	45
		2	47	
		3	45	
20WO10	1.0	1	10	11
		2	15	
		3	8	
20WO15	1.5	1	4	3
		2	0	
		3	5	
20WO20	2.0	1	0	0
		2	0	
		3	0	
20WO25	2.5	1	0	0
		2	0	
		3	0	
20WO30	3.0	1	0	0
		2	0	
		3	0	

Table 3-2: Density test results

Sample No.	SUSFM content (% cement weight)	Sample	Weight (g)	Density (kg/m^3)	Average Density (kg/m^3)
20DE00	0	1	8311	2463	2461
		2	8314	2468	
		3	8279	2453	
20DE05	0.5	1	8288	2456	2412
		2	8094	2398	
		3	8037	2381	
20DE10	1.0	1	7869	2332	2328
		2	7847	2325	
		3	7852	2327	
20DE15	1.5	1	7948	2355	2332
		2	7802	2312	
		3	7862	2329	
20DE20	2.0	1	7667	2272	2289
		2	7731	2291	
		3	7779	2305	
20DE25	2.5	1	7643	2265	2275
		2	7722	2288	
		3	7667	2272	
20DE30	3.0	1	7934	2351	
		2	7698	2281	
		3	7634	2262	2272

Table 3-3: Water Absorption test results

Sample No.	SUSFM content (% cement weight)	Sample	SSD weight (g)	Oven Dry weight (g)	Water Absorption (%)	Average water absorption (%)
20WA00	0	1	7962	7733	2.96	2.95
		2	8048	7816	2.97	
		3	8031	7803	2.92	
20WA05	0.5	1	7957	7688	3.42	3.45
		2	7923	7657	3.48	
		3	7951	7686	3.45	
20WA10	1.0	1	7701	7377	4.39	4.14
		2	7740	7440	4.03	
		3	7858	7555	4.01	
20WA15	1.5	1	7787	7450	4.52	4.53
		2	7715	7378	4.57	
		3	7759	7424	4.51	
20WA20	2.0	1	7711	7521	3.86	4.74
		2	7685	7330	4.84	
		3	7765	7421	4.64	
20WA25	2.5	1	7762	7406	4.81	4.85
		2	7681	7326	4.85	
		3	7745	7383	4.90	
20WA30	3.0	1	7726	7350	5.12	5.04
		2	7692	7332	4.91	
		3	7753	7378	5.08	

Table 3-4: Compressive strength test results

Sample No.	SUSFM content (% cement weight)	Sample	Compressive strength f_c (N/mm^2)	Average compressive strength f_c (N/mm^2)
20CO00	0	1	49.3	50.1
		2	50.3	
		3	50.6	
20CO05	0.5	1	43.2	44.3
		2	46.5	
		3	43.3	
20CO10	1.0	1	40.6	39.0
		2	38.4	
		3	38.0	
20CO15	1.5	1	32.2	32.8
		2	32.8	
		3	33.3	
20CO20	2.0	1	30.7	31.3
		2	32.0	
		3	31.2	
20CO25	2.5	1	25.1	25.4
		2	24.7	
		3	26.3	
20CO30	3.0	1	24.7	25.1
		2	24.8	
		3	25.8	
30CO05	0.5	1	45.0	44.9
		2	44.8	
		3	37.1	
30CO10	1.0	1	37.5	37.5
		2	37.4	
		3	32.0	
30CO15	1.5	1	34.4	34.9
		2	35.2	
		3	35.1	
30CO20	2.0	1	31.9	31.4
		2	30.1	
		3	32.1	
30CO25	2.5	1	25.6	26.6
		2	27.2	
		3	26.9	
30CO30	3.0	1	28.1	28.3
		2	28.5	
		3	28.4	
40CO05	0.5	1	38.0	39.7
		2	39.4	
		3	41.8	
40CO10	1.0	1	36.8	36.5
		2	36.2	
		3	36.5	
40CO15	1.5	1	33.2	34.0
		2	33.8	
		3	34.9	
40CO20	2.0	1	27.4	27.2
		2	27.2	
		3	26.9	
40CO25	2.5	1	22.3	24.0
		2	24.0	
		3	25.6	
40CO30	3.0	1	28.9	28.0
		2	28.0	
		3	27.2	

Table 3-5: Ultrasonic Pulse Velocity test Results

Sample No.	SUSFM content (% cement weight)	Sample	Time (s)	Ultrasonic Pulse Velocity (m/s)	Average Ultrasonic Pulse velocity (m/s)
20UP00	0	1	33.7	4451	4436
		2	34.9	4298	
		3	32.9	4559	
20UP05	0.5	1	35.1	4274	4320
		2	35.0	4286	
		3	34.1	4399	
20UP10	1.0	1	33.5	4478	4496
		2	33.5	4478	
		3	33.1	4532	
20UP15	1.5	1	35.8	4190	4367
		2	34.3	4373	
		3	34.4	4360	
20UP20	2.0	1	35.9	4178	4201
		2	34.5	4348	
		3	36.8	4076	
20UP25	2.5	1	36.7	4087	4199
		2	35.4	4237	
		3	35.1	4274	
20UP30	3.0	1	37.1	4043	4011
		2	35.3	4249	
		3	37.7	3979	
30UP05	0.5	1	34.0	4415	4487
		2	35.0	4286	
		3	32.9	4559	
30UP10	1.0	1	32.8	4573	4523
		2	33.2	4518	
		3	33.5	4478	
30UP15	1.5	1	34.5	4348	4448
		2	33.4	4491	
		3	33.3	4505	
30UP20	2.0	1	34.4	4360	4271
		2	35.1	4274	
		3	35.9	4178	
30UP25	2.5	1	35.4	4237	4353
		2	34.0	4412	
		3	34.0	4412	
30UP30	3.0	1	36.8	4076	4152
		2	35.4	4237	
		3	36.2	4144	
40UP05	0.5	1	33.5	4478	4509
		2	33.4	4491	
		3	32.9	4559	
40UP10	1.0	1	34.0	4412	4434
		2	33.4	4491	
		3	34.1	4399	
40UP15	1.5	1	35.5	4225	4316
		2	34.8	4310	
		3	34.0	4412	
40UP20	2.0	1	34.7	4323	4278
		2	35.5	4225	
		3	35.0	4286	
40UP25	2.5	1	36.3	4132	4222
		2	35.2	4261	
		3	35.1	4272	
40UP30	3.0	1	36.6	4098	4026
		2	38.1	3937	
		3	37.1	4043	

Table 3-6: Splitting Tensile Strength test Results

Sample No.	SUSFM content (% cement weight)	Sample	Splitting Tensile force (N)	Splitting Tensile strength (N/mm^2)	Average Splitting tensile strength (N/mm^2)
20TE00	0	1	102.1	3.3	3.3
		2	100.4	3.2	
		3	104.1	3.3	
20TE05	0.5	1	95.7	3.0	3.0
		2	96.8	3.1	
		3	91.7	2.9	
20TE10	1.0	1	84.1	2.7	2.7
		2	81.7	2.6	
		3	83.8	2.7	
20TE15	1.5	1	80.6	2.6	2.6
		2	80.0	2.5	
		3	81.8	2.6	
20TE20	2.0	1	79.7	2.5	2.5
		2	80.4	2.5	
		3	81.2	2.6	
20TE25	2.5	1	86.7	2.8	2.7
		2	83.8	2.7	
		3	86.8	2.7	
20TE30	3.0	1	86.6	2.8	2.7
		2	83.6	2.7	
		3	79.6	2.5	
30TE05	0.5	1	122.9	3.9	3.8
		2	113.1	3.6	
		3	118.4	3.8	
30TE10	1.0	1	108.2	3.4	3.4
		2	108.4	3.4	
		3	86.0	2.7	
30TE15	1.5	1	79.8	2.5	2.7
		2	87.2	2.8	
		3	85.4	2.7	
30TE20	2.0	1	94.4	3.0	2.9
		2	86.4	2.8	
		3	91.7	2.9	
30TE25	2.5	1	88.8	2.8	2.8
		2	87.4	2.8	
		3	92.0	2.9	
30TE30	3.0	1	76.8	2.4	2.4
		2	74.4	2.3	
		3	77.4	2.5	
40TE05	0.5	1	108.7	3.5	3.3
		2	100.4	3.1	
		3	106.9	3.4	
40TE10	1.0	1	99.5	3.2	3.2
		2	102.7	3.2	
		3	97.7	3.1	
40TE15	1.5	1	83.1	2.6	2.6
		2	81.6	2.5	
		3	81.2	2.6	
40TE20	2.0	1	94.1	3.0	2.7
		2	89.3	2.8	
		3	91.3	2.9	
40TE25	2.5	1	96.8	3.1	3.0
		2	89.9	2.9	
		3	90.6	2.9	
40TE30	3.0	1	84.1	2.7	2.6
		2	84.6	2.7	
		3	80.0	2.5	

Table 3-7: Weights Loss after Acid attack test results

Sample No.	SUSFM content (% cement weight)	Sample	Weight before chemical attack, W_1 (g)	Residual Weight after chemical attack, W_2 (g)	Weight Loss (%)	Average Weight Loss (%)
20CA00	0	1	8052	8004	0.60	0.54
		2	7988	7945	0.54	
		3	8031	7992	0.49	
20CA05	0.5	1	8067	7985	1.02	0.83
		2	7947	7874	0.92	
		3	7996	7951	0.56	
20CA10	1.0	1	7907	7824	1.05	0.82
		2	7921	7863	0.73	
		3	7924	7871	0.67	
20CA15	1.5	1	7886	7800	1.09	0.95
		2	7830	7758	0.92	
		3	7876	7809	0.85	
20CA20	2.0	1	7783	7707	0.98	1.04
		2	7684	7600	1.09	
		3	7684	7656	0.35	
20CA25	2.5	1	7762	7704	0.75	0.80
		2	7640	7575	0.85	
		3	7757	7695	0.80	
20CA30	3.0	1	7843	7811	0.40	0.46
		2	7853	7725	0.36	
		3	7852	7803	0.62	

Table 3-8: Compressive Strength Loss after Acid attack test results

Sample No.	SUSFM content (% cement weight)	Sample	Residual Compressive strength (N/mm^2)	Average Residual compressive strength (N/mm^2)	Average compressive before Chemical attack (N/mm^2)	Compressive Strength Loss, CSL (%)
20CA00	0	1	43.8	46.5	50.1	7.2
		2	46.9			
		3	46.0			
20CA05	0.5	1	36.5	35.2	44.3	20.5
		2	34.6			
		3	34.5			
20CA10	1.0	1	29.2	30.8	39.0	21.0
		2	33.8			
		3	29.4			
20CA15	1.5	1	21.1	22.3	32.8	32.0
		2	22.6			
		3	23.3			
20CA20	2.0	1	18.6	19.3	31.3	38.3
		2	19.8			
		3	19.4			
20CA25	2.5	1	16.1	17.6	25.4	30.7
		2	18.6			
		3	18.0			
20CA30	3.0	1	17.1	17.2	25.1	31.5
		2	16.6			
		3	17.2			

Table 3-9: Abrasion test results

Sample No.	SUSFM content (% cement weight)	Sample	Weight before abrasion (g)	Weight after abrasion (g)	Weight loss (%)	Abrasion (%)	Average abrasion (%)
20AB00	0	1	7983	7977	6	0.075	0.050
		2	7939	7935	4	0.050	
		3	8062	8058	4	0.050	
20AB05	0.5	1	7887	7883	4	0.051	0.047
		2	7852	7848	4	0.051	
		3	7958	7954	3	0.038	
20AB10	1.0	1	7883	7880	3	0.038	0.043
		2	7751	7747	4	0.052	
		3	7846	7843	3	0.038	
20AB15	1.5	1	7839	7835	4	0.051	0.043
		2	7732	7729	3	0.039	
		3	7899	7896	3	0.038	
20AB20	2.0	1	7646	7642	4	0.052	0.044
		2	7552	7549	3	0.040	
		3	7657	7654	3	0.039	
20AB25	2.5	1	7585	7581	4	0.053	0.044
		2	7476	7473	3	0.040	
		3	7425	7422	3	0.040	
20AB30	3.0	1	7437	7433	4	0.054	0.045
		2	7427	7424	3	0.040	
		3	7460	7457	3	0.040	

Appendix IV: Approval Documents

JKU/2/84

JOMO KENYATTA UNIVERSITY
OF
AGRICULTURE AND TECHNOLOGY
Sustainable Materials Research & Technology Centre
SMARTEC

P.O BOX 62000-00200, NAIROBI KENYA. • Tel: (067)52181/2/3/4 • Fax: (067)52164 •E-mail: smartec@jkuat.ac.ke

DATE: 22nd September, 2021 **REF:** ENC331-1106/2020

The Chief Engineer, Materials Testing and Research Division,
Ministry of Transport and Infrastructure Development
P. O. Box 11876-00400
Nairobi.

Thro'
Regional Materials Officer,
Bungoma Region.

Dear Sir/Madam,

SUBJECT: RESEARCH MATERIALS TESTING BY WATAKO JULIUS MALOBA ENC331-1106/2020

The above subject refers.

Mr. Watako Julius Maloba of Registration Number ENC331-1106/2020 is a student at Jomo Kenyatta University of Agriculture and Technology (JKUAT) currently undertaking his studies in Master of Science in Construction Engineering and Management.

He successfully completed his course work (First year of study) and passed. He is currently in his second year undertaking his research work on, ***Feasibility of Reutilizing Single-Use Surgical Face Mask to Improve Physical and Mechanical Properties of Concrete.***

Kindly assist him to carry out his research experiments in your laboratories.

For any clarification, kindly contact the undersigned.

Yours Faithfully,

Dr. Eric Charles Cherutyot, Ph.D,
Ag. Director SMARTEC

Approved

MINISTRY OF TRANSPORT, INFRASTRUCTURE, HOUSING & URBAN DEVELOPMENT
STATE DEPARTMENT OF INFRASTRUCTURE
MATERIALS TESTING AND RESEARCH DIVISION
29 SEP 2021
REGIONAL MATERIALS OFFICER (BUNGOMA)
P.O. Box 763-50200, BUNGOMA
RECEIVED

JKUAT is ISO 9001:2015 and ISO 14001:2015 Certified
Setting Trends in Higher Education, Research, Innovation and Entrepreneurship

KIBABII UNIVERSITY
(KIBU)
0?-NOV 2021
Sign.......
Estates Department

KIBABII UNIVERSITY

(Knowledge for Development)

Tel. 020 - 2028660 / 0708-085934 / 0734 831729
P.O. Box 1699-50200
Bungoma

Email: enquiries@kibu.ac.ke
administration@kibu.ac.ke
Website: http://www.kibu.ac.ke

OFFICE OF THE REGISTRAR (ADMINISTRATION & HR)

Ref: PF. No. 0105/87

Date: 2nd November, 2021

Mr. Julius Maloba
Kibabii University,
P.O. Box 1699 – 50200,
BUNGOMA.

Dear Mr. Maloba,

RE: REQUEST FOR PERMISSION TO CARRY OUT RESEARCH STUDIES

The above subject matter refers.

We acknowledge receipt of your letter dated **22nd October, 2021** requesting for permission to use university premises to carry out research studies.

We wish to inform you that your request has been granted.

Thank you.

Dr. Charles Wasike, PhD
For: REGISTRAR (ADMINISTRATION & HUMAN RESOURCE)

Copy to:

- Vice Chancellor
- Deputy Vice Chancellor (AFD)

} – To note in File

Kibabii University ISO 9001:2015 Certified
Knowledge for Development